Protein engineering of a *Pseudomonas fluorescens* esterase
Alteration of substrate specificity and stereoselectivity

I n a u g u r a l d i s s e r t a t i o n

zur

Erlangung des akademischen Grades

doctor rerum naturalium (Dr. rer. nat.)

an der Mathematisch-Naturwissenschaftlichen Fakultät

der

Ernst-Moritz-Arndt-Universität Greifswald

vorgelegt von
Anna Schließmann
geboren am 01.03.1981
in Husum

Greifswald, im Mai 2010

Dekan:	Prof. Dr. Klaus Fesser
1. Gutachter:	Prof. Dr. Uwe T. Bornscheuer
2. Gutachter:	Prof. Dr. Karl-Erich Jaeger
Tag der Promotion:	27.07.2010

„Today is your day!
Your mountain is waiting.
So… get on your way.”

- Theodore Seuss Geisel

Table of contents

1.

Abbreviations

A. dest.	Distilled water
Amp	Ampicillin
APS	Ammonium persulfate
bp	Base pairs
BSA	Bovine serum albumin
c	Conversion
CAS	Cassette
cm	Centimetre
Da	Dalton
DMSO	Dimethylsulfoxide
DNA	Deoxyribonucleic acid
dNTP	Deoxyribonucleoside triphosphate
E	Enantioselectivity
E. coli	*Escherichia coli*
ee	Enantiomeric excess
epPCR	Error prone PCR
g	Gram
GC	Gas Chromatography
H	Hour
HPLC	High pressure liquid chromatography
kb	Kilobase
k_{cat}	Turnover number
kDa	KiloDalton
K_M	Michaelis constant
l	Liter
LB	Lysogeny Broth
M	Mole per liter
mA	Milliampere
MES	2-(N-Morpholino)ethane sulfonic acid
mg	Milligram
min	Minute
ml	Milliliter
mM	Millimole per liter
mmol	Millimole
MS	Mass spectrometry
MTP	Microtiter plate
n.d.	Not determined
nm	Nanometer
OD	Optical density
oligo	oligonucleotide
PAGE	Polyacrylamide gel electrophoresis
PCR	Polymerase chain reaction
PFE I	*Pseudomonas fluorescens* esterase I
pG	pGaston (plasmid)
pNPA	*p*-Nitrophenyl acetate
pNPB	*p*-Nitrophenyl butyrate
pNPC	*p*-Nitrophenyl caprylate
pNPL	*p*-Nitrophenyl laurate
Rha	Rhamnose
RM	Roti Mark Standard ®
s	Second
SDS	Sodium dodecyl sulphate
TEMED	N, N, N‘,N‘-Tetramethylethylendiamine
TLC	Thin-layer chromatography
T_M	Melting temperature
Tris	Tris-(hydroxymethyl)-aminomethane
UV	Ultraviolet
V	Volt
wt	Wild type
℃	Degree Celsius
µg	Microgram
µl	Microliter
%(w/v)	Masspercent
%(v/v)	Volumepercent

Additionally the conventional abbreviations for amino acids and nucleotides are used.

1. Introduction

1.1. Enantioselectivity

Molecules which lack an internal plane of symmetry are called chiral molecules; they cannot be superimposed with their mirror images. Asymmetric centers (e.g. a carbon atom with four different substituents) are the most common causes for chirality in a molecule (see Figure 1-1), but there is also axial chirality (e.g. allenes), planar chirality (e.g. *(E)*-cyclooctene), and inherent chirality (e.g. calixarenes, fullerenes). The two isomers of a chiral molecule rotate the plane of polarized light by the same amount (they are said to be optically active), but in opposite direction; they are called enantiomers. In achiral environments, their chemical behaviour is identical; however, they react differently in the presence of other chiral compounds, such as enzymes. The Cahn Ingold Prelog rule is widely used for the designation of enantiomers. It assigns the four substituents of the chiral center a priority based on the atomic number. When the lowest priority substituent is rotated behind the chiral center, and the priority of the remaining substituents decreases in clockwise direction, the enantiomer is labelled *R*, if it decreases in counterclockwise direction, the enantiomer is labelled *S* [1, 2].

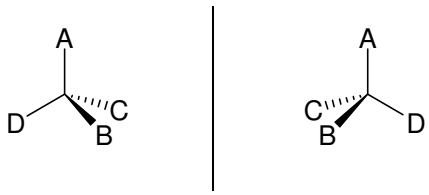

Figure 1-1: Example for a chiral center (A-D are different substituents)

As many pharmaceutically active compounds are chiral and will thus act differently in the chiral environment of a living cell, it is very important to supply optically pure compounds. A prominent example for the different biological activities of enantiomers is Thalidomide. Between 1957 and 1961 it was sold under the name Contergan® as anti-depressant and to alleviate the morning sickness of pregnant women. The intake of Thalidomide during a pregnancy leads to children born with deformities, therefore the drug was forbidden (it is now in use as drug against leprosy, but no longer administered to pregnant women). It is thought that the (*R*)-enantiomer is responsible for the deformities, but administration of the pure (*S*)-enantiomer is no alternative, as racemization occurs *in vivo* [3]. In 1992, the Food and Drug Administration (FDA) of the United States issued a statement, that in the case of chiral drug candidates both enantiomers have to be tested individually for activity and side effects [4].

Chen *et al.* [5] developed simple equations to calculate the enantioselectivity (the ability of a catalyst to distinguish between the enantiomers, defined as the ratio of the reaction rates (v_{max}/K_M) of the enantiomers) based on the optical purity of substrate or product and on the conversion. Two of these three values are needed for the calculation; in most cases the optical purity (enantiomeric excess) of substrate and product can be determined with the highest accuracy.

$$E = \frac{\ln\left[\frac{1-ee_S}{1+(ee_S/ee_P)}\right]}{\ln\left[\frac{1+ee_S}{1+(ee_S/ee_P)}\right]} \qquad c = \frac{ee_S}{ee_S+ee_P} \qquad E = \frac{\ln[(1-c)(1-ee_S)]}{\ln[(1-c)(1+ee_S)]}$$

Figure 1-2: Equations developed by Chen *et al.* [5] for the calculation of enantioselectivity; E is the enantioselectivity, ee_S is the enantiomeric excess of the substrate, ee_P is the enantiomeric excess of the product, c stands for conversion

A completely unselective reaction will have E=1. The enantioselectivity should be above 50 to be useful on preparative scale, E>100 is desirable because it allows the isolation of optically pure substrate and product at 50% conversion. At E≥100, small changes in enantiomeric excess result in drastic changes of E, so in this work E values are only reported for E<100. If the calculated E is above 100, the value is reported as E>100.

1.2. Biocatalysis

The use of enzymes as biological catalysts is called biocatalysis. The enzymes may be purified, or crude lyophilisate or whole cells may be employed, depending on the conditions that have to be met. While purified enzymes guarantee the absence of unwanted activities, the stability often suffers, and cofactors may be lost during the purification, which in itself is often time-consuming and expensive. The stability may be increased through immobilization [6, 7]; this also facilitates the separation of enzyme and products and thus the re-use of the valuable catalyst. Whole cells offer the advantage of *in vivo* cofactor regeneration (which is especially interesting if the reaction in question is a reduction or an oxidation), but it must be ensured that both substrate and product can pass through the cellular membrane, are not toxic to the cells and cannot be modified by other enzymes present in the cell. Additionally, the downstream processing can be more demanding if part of the product remains within the cell. Crude lyophilisate still contains protein stabilizing components and there is no necessity to transport substrate and product through a membrane. However, unwanted enzymes from the host cell are still present and may lead to undesired side-reactions, lowering the yield.

In the early days of biotechnology, wild type bacterial or fungal strains as well as extracts from animal tissue or plants were the primary source of enzymes. However, there are some problems associated with this practice: the concentration of the protein of interest is often low, making the process expensive. Additionally, the composition of enzymes may vary between batches, making quality control an important issue – a prominent example is the pig liver esterase, an extract from pig liver which consists of several isoenzymes with different enantiopreferences and substrate specificities [8, 9]. For the pharmaceutical and food industry, products of animal origin harbour the risk of infections or allergic reactions, as well as preventing the product from being *kosher* or *halal*. Due to the progress in molecular biology and microbiology, many industrially relevant enzymes have been cloned and expressed recombinantly in host organisms such as *E. coli*, *P. pastoris*, *Bacillus* species and *Aspergillus* species. Many strains have been specifically engineered for the overproduction of foreign proteins: they are often nuclease-, recombination- and protease-deficient (e.g. *E. coli* BL21) and support specialized expression systems (e.g. DE3 strains harboring a genomic copy of the T7 RNA polymerase). Some strains contain plasmids encoding rare tRNAs (e.g. *E. coli* BL21 CodonPlus™ from Stratagene, *E. coli* Rosetta™ from Novagen), others have gene-knockouts which allow the formation of disulfide bonds within the cytoplasm (e.g. *E. coli* Origami™ from Novagen), or combinations of the above (e.g. *E. coli* Rosettagami™ from Novagen). Special strains for the overexpression of toxic proteins are also available (e.g. *E. coli* C41 or C43 from Lucigen).

Enzymes display several properties which make them viable alternatives to chemical catalysts:

- they are often regio-, chemo- and stereospecific
- they may save reaction steps compared to organic synthesis (for example by eliminating the need for protection groups)
- they require reaction media which are often “greener” than those used in chemical catalysis (for example less organic solvents, lower temperatures)
- properties may be improved through protein engineering (for example substrate selectivity, thermostability, pH profile)

As many applications in the pharmaceutical industry and fine chemistry require optically pure building blocks, there is a high demand for selective catalysts. Many enzymes already possess excellent selectivity and activity against the desired substrates; additionally, a lot of research is dedicated to finding and optimizing enzymes for new processes. The decision whether to employ a chemical or a biological catalyst depends on the process parameters – how pure the product must be, how cost-effective the production of the catalyst is, whether the catalyst can be recycled and how high the costs for the down-stream processing would be. Consumer preferences can also play a role – while some may demand a process which

is friendly to the environment (possibly favoring biocatalysis), other consumers insist on products created without the use of gene technology (favoring the chemical process).
In addition to high-value, optically pure products, some bulk chemicals are also produced enzymatically, a prominent example being the production of acrylamide (>100 000 t/a) using a nitrile hydratase.

1.3. Sources of suitable biocatalysts

1.3.1. Isolation of new enzymes

In the past, scientists searched for new enzymatic activities by screening environmental samples or strain collections by enrichment cultures. If a desired activity is found, the corresponding gene may be cloned for improvement and overexpression. The disadvantage of this technique is that only a small percentage (estimates vary between 0,001% and 1%) of microorganisms is able to grow under laboratory conditions. Recently, efforts have been made to access the biodiversity of microorganisms which cannot be cultured. In the metagenomic approach, the complete DNA of an environmental sample is isolated and digested into large fragments, which are cloned into a suitable plasmid and transformed into host expression cells. The resulting library can then be screened for the desired activity, with the advantage that the gene of interest is already cloned and can be expressed recombinantly. Some enzymes will still be missed, though, as not all enzymes can easily be expressed. Another approach is the sequence-based discovery. As the size and number of sequence databases [10, 11] available to the public increase constantly, the search for homologous enzymes is greatly facilitated. It is possible to search sequences of entire proteins as well as just structural motifs or consensus sequences to discover proteins of the same class which possibly possess different properties. Unlike in the metagenome approach, it is not possible to find completely new protein families using the sequence based approach.

1.3.2. Protein engineering

As most industrial applications feature non-natural conditions of solvent, substrate concentration, pH, or temperature as well as non-natural substrates, wild type enzymes do not always perform well. Also, the enantioselectivity towards natural and non-natural substrates is not always high enough for an efficient process. In some cases, the reaction conditions can be modified to alleviate the problem; this general approach is referred to as process engineering. Examples of factors to be optimized in an ester hydrolysis are temperature [12], solvent [13], acyl donor [14] and alcohol leaving group [15].
Alternatively, many techniques for protein engineering have been developed and successfully employed [16]. While some methods rely on physico-chemical or post-

translational modifications like the exchange of metal ions [17] or immobilization [7], the majority of methods target the gene. These approaches may be classified into three categories – a data-driven, rational strategy called rational protein design, a random approach called directed evolution, or a combination of these two, dubbed focused directed evolution or semi-rational design (Figure 1-3).

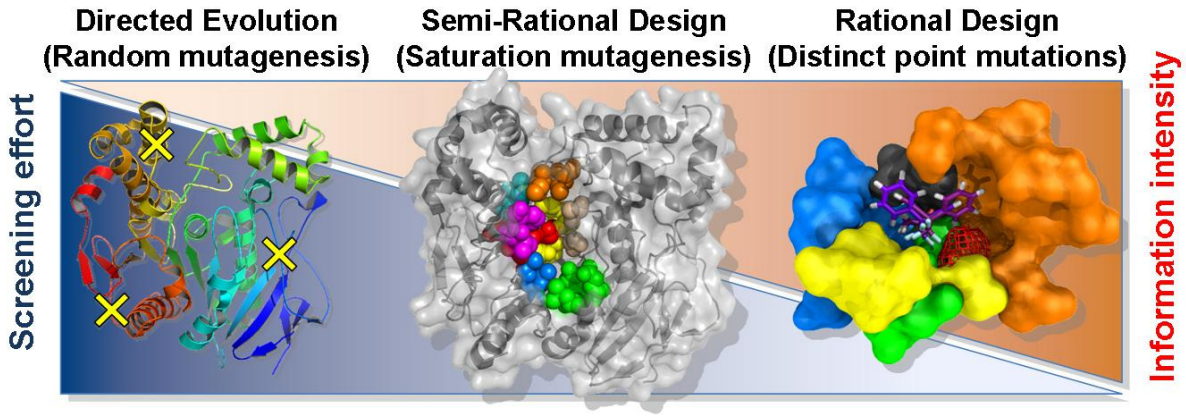

Figure 1-3: Overview of approaches to the generation of improved protein variants

1.3.3. Rational protein design

If an enzyme is to be improved *via* rational protein design, its reaction mechanism has to be known and its structure should be solved (sometimes it is also possible to work with a homology model). The more data about the protein is known, the higher the chances of success are. Predictions are made which amino acids are likely to influence the enantioselectivity or substrate recognition, for instance, and beneficial amino acid exchanges are proposed. Often the necessary data is obtained through a simulation of the transition state which is essential to catalysis. The substrate is modelled into the active site and the energy of the substrate-enzyme-complex is minimized. After a molecular dynamics simulation, residues which interact with the substrate can be identified. These residues are then subjected to site-directed mutagenesis.

Typically not more than a handful of mutants is generated, resulting in low screening effort. A major issue of rational protein design is the need for precise data. The more is known about a certain protein family, the more likely it is to correctly predict beneficial mutations which do not interfere with protein stability. Using new databases such as 3DM [10, 18, 19] can help overcome the problem of incorrect folding by identifying “allowed” amino acid substitutions for a certain position; in this context allowed amino acids are those which are found at the position in question in homologous proteins of the same family; they are less likely to disrupt correct protein folding.

Frequently the mutants generated *via* rational protein design are subjected to directed evolution in order to improve properties which are difficult to predict rationally.

1.3.4. Directed evolution

An alternative to rational protein design is directed evolution [20-22]. It does not require detailed knowledge about the protein of interest, so for enzyme classes which are poorly characterized this presents the only option. Similarly to rational protein design, the gene encoding the enzyme of interest has to be available, as well as a suitable expression system. Additionally, a mutagenesis strategy and a high-throughput screening or selection system are needed. Basically, directed evolution strategies are based on the introduction of random mutations at random locations of a gene; the most time-consuming and challenging step is typically the screening for (or selection of) an improved mutant.

There are two main approaches to directed evolution: non-recombining methods create point mutations within one parental gene, while recombining methods yield a library of chimaeras of several parental genes. For recombining methods it is typically required to have parental genes with a high homology.

The most widely known non-recombining method is the so-called error-prone PCR [23]. Mutations are achieved through the use of a non-proof-reading polymerase (e.g. *Taq* polymerase) in combination with altered reaction conditions (e.g. Mn^{2+} instead of Mg^{2+}, unbalanced composition of dNTPs). A major drawback of this method is its bias in the exchange of nucleotides and the low probability of neighboring mutations, meaning that some amino acid substitutions are much more likely than others [24]; using the standard protocol one obtains approximately five times as many mutants where A or T were replaced than mutants where C or G were replaced [25]. Also, genes or gene areas with a high GC content are difficult to mutate with epPCR. Still, the technique is easy to employ and thus widely used, often as a starting point of subsequent rounds of evolution (e.g. followed by saturation mutagenesis of hot spots identified *via* epPCR). An example for the combination of epPCR and saturation mutagenesis is the inversion of hydantoinase enantioselectivity from D (40% ee) to L (20% ee), which is industrially interesting for the production of L-methionine [26].

DNA shuffling is an example of a recombining method [27]. The parental genes which may stem from different organisms or from a previous round of directed evolution are degraded with DNaseI and then recombined in a PCR, yielding a library of chimaeras. This process is similar to natural recombination and only requires a sequence homology of at least 70% [28]; an example for successful application was the generation of subtilisin chimaeras with enhanced stability against organic solvents, thermostability, activity and a more suitable pH profile [29]. Further recombining methods include ITCHY [30], StEP [31] SCRATCHY [32] and SHIPREC [33].

A major drawback of directed evolution methods is the large library size which has to be screened in order to cover a significant percentage of possible mutations (see table 1-1).

Table 1-1: Example for the number of possible combinations and the associated screening effort for the random mutagenesis using NNK codons

Positions	Number of possible combinations	Number of mutants to be screened for 95% coverage
1	20	94
2	400	3 066
3	8 000	98 163
4	160 000	3 141 251
5	3 200 000	100 520 093

While the methods for screening and selection become more and more sophisticated and amenable to a higher throughput, efforts are also made to decrease the library size and thus the screening effort through the creation of higher-quality libraries. One way to achieve this goal is to focus the mutations to certain parts of the gene; focused directed evolution is discussed below. Other possibilities include the substitution of NNK codons for saturation mutagenesis with codons such as NDT. While NNK produces 32 codons coding for all 20 amino acids, NDT only produces 12 codons, each of them coding for a different amino acid, including polar and nonpolar, aliphatic, aromatic and negatively and positively charged amino acids. While some amino acids are excluded, duplicate phenotypes due to the codon degeneracy are excluded, yielding a smaller, higher-quality library [34].

1.3.5. Focused directed evolution

Focused directed evolution aims to combine the strengths of rational protein design and directed evolution. Some data on the protein's structure and mechanism is required, but it is mostly used to identify hotspots within a gene which are likely to influence the desired property (e.g. enantioselectivity), often close to the active site (as closer mutations are often better according to Morley and Kazlauskas [35]). Rather than predicting only a handful of mutants rationally, the identified gene cassettes or residues are randomized, enhancing the chances of finding mutants with a correct fold and facilitating the discovery of synergistic effects between mutations which would be difficult to predict rationally. The main advantage over classic directed evolution is the decreased library size (i.e. the number of clones which has to be screened to statistically cover 95% of all possible mutants) and thus the decreased screening efforts.

Focused directed evolution has been successfully applied for the inversion of the enantioselectivity of the *Bacillus subtilis* esterase BS2. Three residues brought up by a docking study were subjected to CASTing (basically the simultaneous saturation of several

residues whose side chains point in the direction of the active site) [36] and a double mutant with inversed enantioselectivity was found, with E_S=64 (the starting mutant had E_R>100) [37]. A method for focused directed evolution which has recently been developed by Dr. Hidalgo in our working group is dubbed OSCARR for Onepot, Simple Cassette Randomization and Recombination [38], a schematic representation is shown in Figure 1-4.

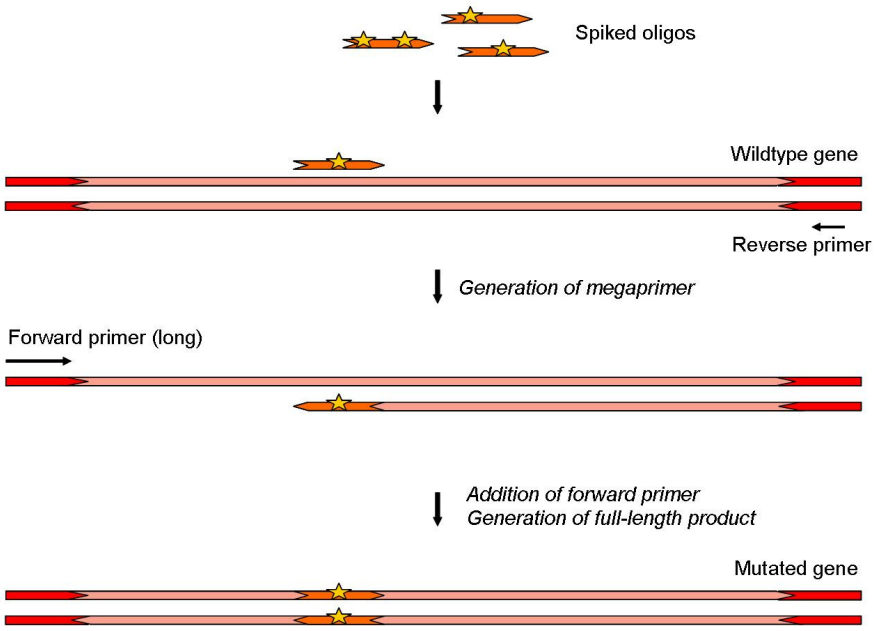

Figure 1-4: Schematic representation of the OSCARR method

OSCARR is based upon the Megaprimer PCR method developed by Kammann *et al.*[39] and refined by Ke and Madison[40] who proposed the use of outer primers differing in their T_M to forego the intermediate purification step. The idea of Datta *et al.* to include asymmetric cycles before the addition of the forward primer was also included [41]. In order to avoid the bias inherent in many methods, so-called spiked oligonucleotides are used as mutagenic primers. These spiked oligos are designed using an algorithm[42] requiring as input the original sequence, the number of desired mutations and any specific mutations which are desired or forbidden (e.g. an active site residue which may not be mutated). When data is available from homologous enzymes (e.g. from a database such as 3DM [10]), it is possible to specify a probability for a certain amino acid in a defined position, according to the frequency in which this amino acid occurs in related enzymes. Overall, the use of spiked oligos allows a tight control over the nature of the mutants by choosing allowed codons, avoiding “disallowed” codons such as stop codons, eliminating the bias and by allowing the introduction of several mutations in close proximity. It is possible to generate a triple mutant in a cassette of only ten amino acids; this kind of mutant is extremely unlikely to be found with a technique such as epPCR where the mutations are distributed statistically throughout

the gene. Additionally, one is virtually independent of the properties of the original sequence, which may, for example, be GC rich and thus difficult to mutate otherwise.
Figure 1-5 depicts a comparison between rational protein design and directed evolution.

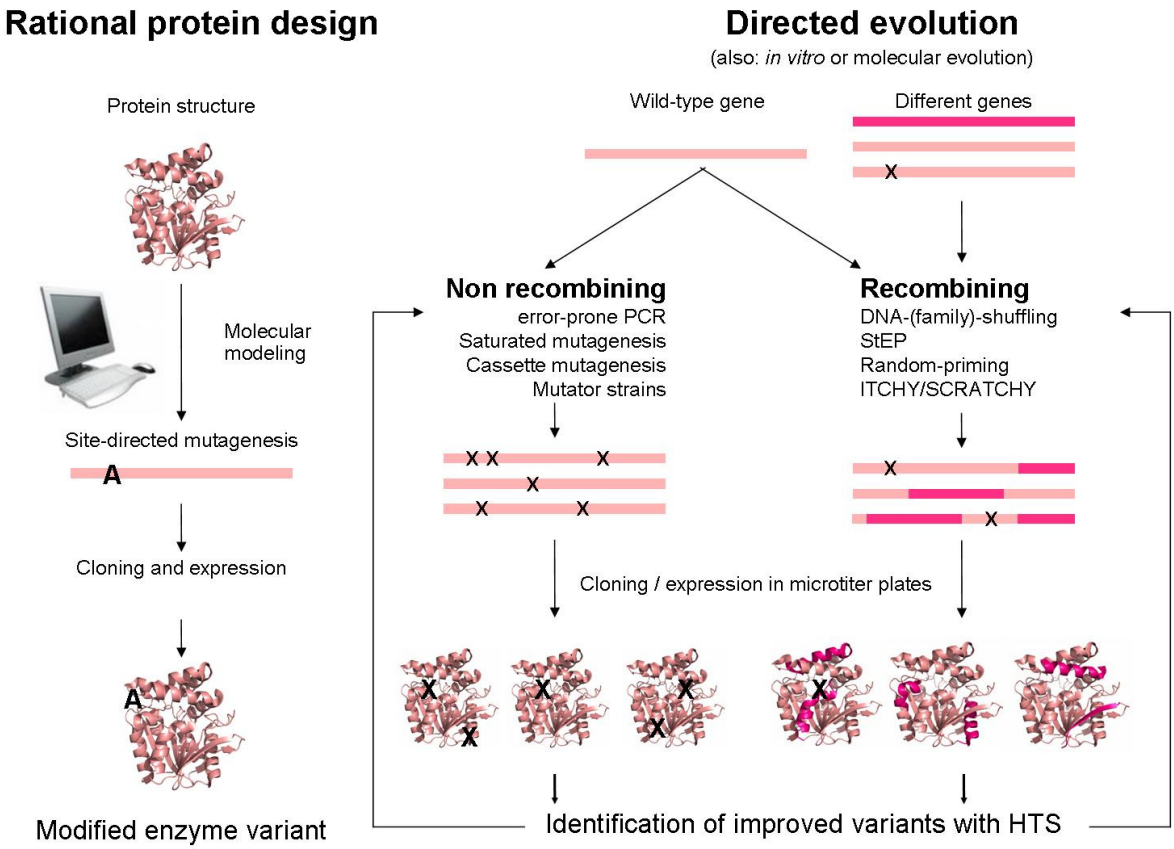

Figure 1-5: Schematic comparison of rational protein design and directed evolution; A: specific mutation, X: random mutation, HTS: High throughput screening

1.4. Screening and selection systems

Commonly, the activity of hydrolases is determined by automated acid-base titration carried out in a pH-Stat. The hydrolysis takes place under controlled conditions and the pH shift caused by the release of free acid is compensated through titration with a base. Enantioselectivity is usually determined using chiral GC or HPLC analytics. However, the above-mentioned methods can only be applied to a limited number of enzymes, as they are rather time-consuming. In order to identify target phenotypes in large mutant libraries, suitable systems for the screening or selection of variants bearing desirable traits are needed, in many cases this is the bottleneck of the endeavour to find improved enzyme variants. Several reviews are available which provide good overviews over this broad subject [43-45]. In short, a useful assay system should be

- Sensitive
- Easy to detect

- Quantitative
- Selective (no side reactions with other enzymes)
- Using substrates which are easily available
- Amenable to high throughput
- Using substrates similar to the “real” substrates

The last point is often difficult to achieve, as many real substrates are not suitable or too expensive for high-throughput assays. Thus, mutants are often identified which are optimized for surrogate substrates and their activity or selectivity against the true substrate is not necessarily affected. This problem is summed up in the so-called first law of directed evolution: “*You only get what you screen for*” [46]. An example for this is the work of Moore *et al.*, who were trying to improve esterase activity against *p*-nitrobenzyl esters. For the photometric assay, they used *p*-nitrophenyl esters as surrogate substrates and found a variant with 24 fold increased activity against the *p*-nitrophenyl ester which was only four times as active against *p*-nitrobenzyl esters [47].
Some examples of screening and selection methods for esterases and lipases are discussed below.

1.4.1. Selection

Selection systems usually provide the possibility for screening large numbers of mutants with relatively little time and effort, however, they can only be used for questions related to metabolic pathways, and one has to make sure that the host organism does not contain enzymes which interfere with the assay. Frequently used selection methods are agar plate based growth assays [48], phage-display, FACS (fluorescence activated cell sorting) [49] and *in-vitro* compartmentalization (IVC) combined with FACS analysis [50]. An example for an agar plate growth assay was the identification of an esterase mutant with activity against a sterically hindered 3-hydroxy ester. The mutant libraries were replica plated onto minimal medium plates containing the 3-hydroxy glycerol ester and a combination of pH indicators. Colonies with an active esterase were stained red due to the pH change and they could grow larger than other colonies, as the glycerol cleaved from the ester served as carbon source [48].

1.4.2. Screening

Screening methods are often carried out in microtiter plates, they usually allow quantification and the measurement of kinetics, but more effort is associated with screening methods when compared to selection methods. The principle of detection is often photometric or fluorimetric, but high-throughput methods including mass spectrometry or NMR have also been developed [51, 52]. These methods require expensive equipment which is not

accessible to the vast majority of researchers, so they will not be discussed in detail in this introduction.

A method which is very simple and suitable for virtually any substrate is a pH assay. When an ester or amide bond is cleaved, an acid is liberated which lowers the medium pH. A pH indicator with an appropriate transition pH is added to the wells of a microtiter plate and the reaction can be monitored photometrically [53]. Care has to be taken to use buffer of an appropriate concentration. It has to be strong enough to counter the influence of crude cell lysate, but it must not buffer the protons liberated by the enzymatic activity and thus suppress the signal.

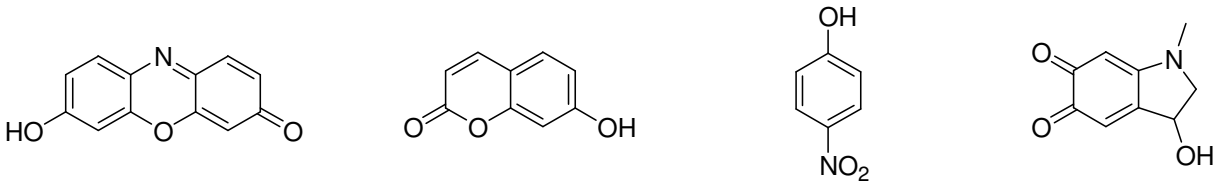

Resorufin Umbelliferone *p*-Nitrophenol Adrenochrome

Figure 1-6: Fluorophores and chromophores commonly used for high-throughput screening assays

Fluorescence-based assays are very sensitive and not very susceptible to background signals from crude cell preparations, however, fluorogenic (as well as many chromogenic) substrates are often bulky and hardly resemble the real substrates, examples of fluorophoric (resorufin, umbelliferone) and chromophoric (*p*-nitrophenol) substituents as well as a chromophoric product (adrenochrome) are shown in Figure 1-6. A very common and simple assay is the *p*-nitrophenol assay. Esterified with virtually any acid, the substrate is almost colorless. Upon cleavage of the ester bond, *p*-nitrophenol is released which appears yellow in slightly basic buffer (usually at pH 7,5). As the intensity of the color depends on the pH, care has to be taken to buffer the reaction sufficiently and to determine the so-called buffer factor, which corresponds to the molar extinction coefficient of *p*-nitrophenol at the buffer's pH.

Frequently, the chromophore or fluorophore is directly cleaved off the assay substrate to create the signal. However, as the chromophores are excellent leaving groups, the substrates are often instable at high or low pH and/or elevated temperatures. To counter this problem, alternative strategies were suggested. As an example, when umbelliferone is to be used to screen for esterase activity, the umbelliferone hydroxyl group does not participate in the ester, but forms an ether bond with a diol, which in turn is esterified with acetate. Once the ester bond is cleaved by the enzyme, sodium periodate is used to oxidize the diol to form an aldehyde, followed by a β-elimination in the presence of BSA [54, 55], the reaction is shown in Figure 1-7.

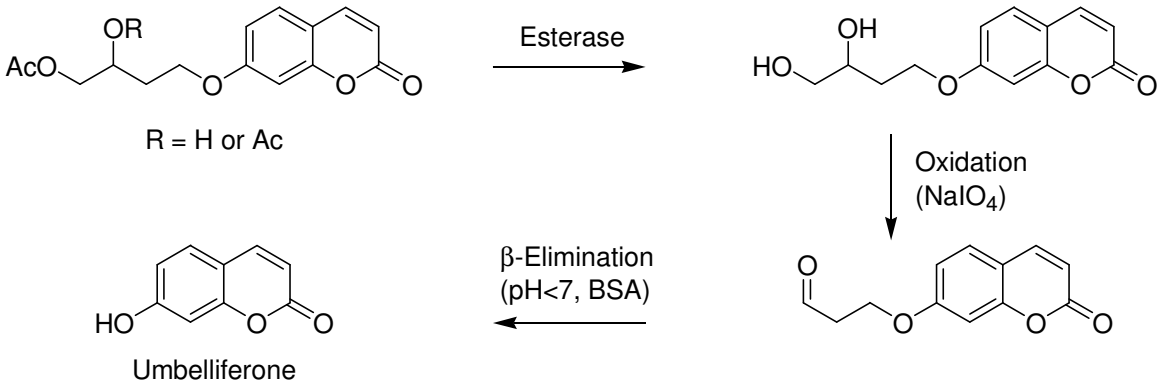

Figure 1-7: Umbelliferone assay

An elegant solution to the problem of surrogate substrates is the so-called acetate assay. Hydrolysis of a user-defined acetate liberates acetic acid, which is in turn utilized by an enzyme cascade with the final products citrate and NADH, whose concentration may be monitored photometrically at 340 nm [56, 57]. This assay eliminates the need for bulky substrates, and a kit containing all components necessary for the determination of acetic acid is commercially available. The enzyme cascade is shown in Figure 1-8.

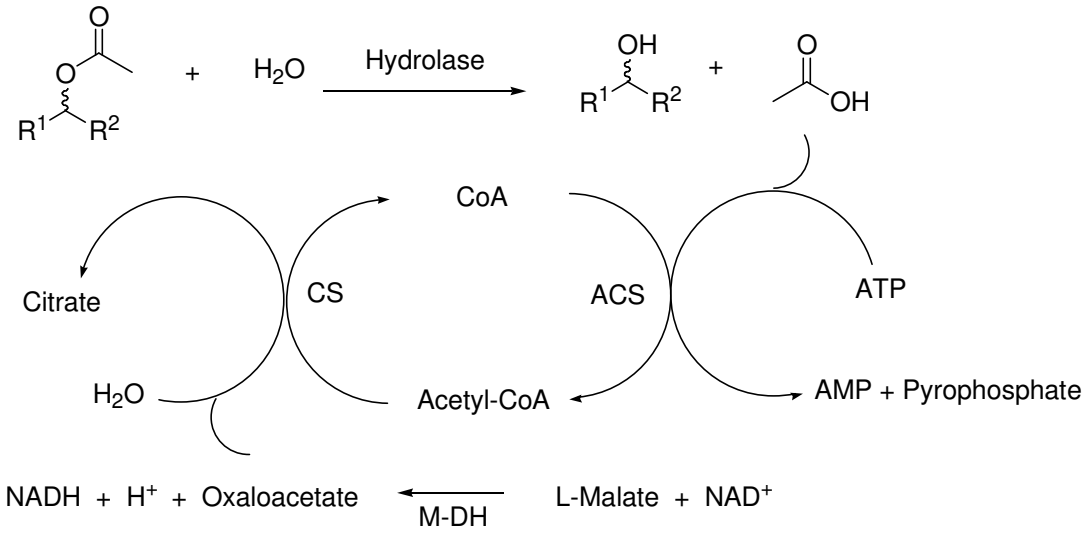

Figure 1-8: Schematic of the acetate assay. CS: Citrate synthase, ACS: Acetyl-CoA synthase, M-DH: L-Malate dehydrogenase

Another interesting assay system is the adrenalin assay. The substrate used in this assay is not sensitive to oxidation by $NaIO_4$, but the product is. After addition of a known amount of $NaIO_4$, the leftover periodate is back-titrated with adrenaline, which forms the red dye adrenochrome [58]. This assay system is used for the determination of epoxide hydrolase activity, as the epoxide is not sensitive to oxidation, while the product diol is.

When mutants are to be screened for enhanced enantioselectivity, the assay system needs to be adapted accordingly. In most cases, E_{app} – the apparent enantioselectivity – is measured, rather than E_{true} – the true value. While the true enantioselectivity is determined in

the presence of both enantiomers, for the apparent enantioselectivity the activity against each enantiomer is measured separately, thus eliminating the competition between enantiomers (i.e. neglecting K_M) and causing differences between E_{app} and E_{true}.

One of the earliest high throughput assays for hydrolase enantioselectivity was the so-called "Quick *E*" test [59]. The apparent enantioselectivity is determined by splitting the enzyme into two wells of a microtiter plate. To each well one enantiomer of the substrate linked to a chromophore such as *p*-nitrophenol is added and the initial reaction rates are measured. Simultaneously, the hydrolysis of an achiral reference compound (e.g. a resorufin ester) is measured at a different wavelength. The ratio of the reaction rates corresponds to the apparent enantioselectivity. The basic system of measuring initial reaction rates of both enantiomers separately can be applied to virtually any assay, provided that enantiopure substrates are available.

1.5. Catalytic promiscuity

Many enzymes catalyze alternate transformations in addition to their natural reaction. This so-called promiscuous behaviour is likely the starting point for the diversification of enzymes stemming from a common ancestor in natural evolution. The promiscuous activity is usually much less effective than the natural activity, so it is likely that many promiscuous activities have not been discovered yet, as many assays only cover a span of minutes or days. An example for a promiscuous activity with very low, but detectable efficiency is the aldolase activity of the *Candida antarctica* lipase B (CalB), which is one of the major workhorses of industrial biocatalysis due to its broad substrate spectrum, activity in organic solvents and often excellent enantioselectivity. The conversion of the aldol condensation of acetone and acetaldehyde was monitored over a time span of two months, as the reaction is 10^5 times slower than the hydrolysis of triglycerides. However, the activity is ten times higher than that of a catalytic antibody catalyzing the same reaction, and an improved mutant where the catalytic serine was replaced by alanine had a turnover number of 65 d^{-1}, four times higher than the turnover number of the wild type [60].

The promiscuous reaction may differ from the natural reaction in the type of bond which is formed or cleaved, and/or the catalytic mechanism. A prominent example is the hydrolysis or formation of amides by an esterase or lipase, such as the *Bacillus subtilis* esterase BS2 [61] and the *Candida antarctica* lipase B [62]. Here, the mechanism is probably similar to that of ester hydrolysis, but the type of bond formed or cleaved is different. Likewise, a *Pseudomonas aeruginosa* arylsulfatase catalyzes the hydrolysis of phosphodiesters even with a similar efficiency [63]. Pyruvate decarboxylases from *Zymomonas mobilis* and *Saccharomyces carlsbergensis* exhibit promiscuous lyase activity in the acyloin condensation of acetaldehyde and benzaldehyde [64, 65]. The condensation requires the

additional reaction step of a C-C bond formation compared to the natural decarboxylation. It is also interesting because it is an example of an industrially relevant promiscuous reaction, as the product (*R*)-phenylacetylcarbinol is a precursor to ephedrine [66].
Catalytic promiscuity is scientifically interesting because it allows insights into enzymatic reaction mechanisms and evolution, but also the identification of biocatalysts for new and possibly unnatural reactions. It is much more challenging to generate enzymatic activity *de novo* than to improve an existing activity, as it cannot be assumed that every factor which contributes to activity and substrate specificity is known.

1.6. Hydrolases

Hydrolases are enzymes which catalyze the hydrolytic cleavage of several organic compounds, for example carboxylic acid esters and amides as well as their formation, and the hydrolysis of nitriles and epoxides. Together they form the enzyme class 3 (EC 3), this Enzyme Commission number is assigned by the International Union of Biochemistry and Molecular Biology. Hydrolases are widely used in organic chemistry because they often exhibit broad substrate specificity and do not require cofactors, which are costly and difficult to regenerate, and due to the tolerance for organic solvents that many hydrolases (especially lipases) exhibit. When water is removed from the reaction medium, it is often possible to shift the equilibrium towards synthesis. Additionally, many hydrolases show a high enantioselectivity which makes them attractive for the pharmaceutical industry and for the synthesis of optically active building blocks for fine chemistry. While many esterases have been described in literature, most technical applications use lipases which often exhibit a broader substrate spectrum including water-insoluble substrates, better stability against organic solvents and excellent enantioselectivities [67, 68].

1.6.1. Esterases

Esterases are hydrolases that catalyze the cleavage, formation, or transesterification of short-chain fatty acid esters. Common features of esterases are the α/β-hydrolase fold and the G-X-S-X-G consensus motif around the active site serine, where X denotes any amino acid. The active site of serine hydrolases contains a catalytic triad composed of a nucleophilic serine, an amino acid with a catalytic carboxyl group (aspartate or glutamate) and a histidine. An additional common structural feature is the so-called oxyanion hole which stabilizes the tetrahedral intermediate. The catalysis works in a four-step mechanism, shown in Figure 1-9:

1. Nucleophilic attack of the serine oxygen on the substrate, formation of a tetrahedral intermediate stabilized by histidine and aspartate
2. Release of the alcohol, formation of an acyl enzyme complex

3. Nucleophilic attack forms another tetrahedral intermediate (the nucleophile is water in hydrolysis or an alcohol in esterification)
4. Cleavage of acyl-enzyme bond and release of the product (an acid in hydrolysis or an ester in esterification)

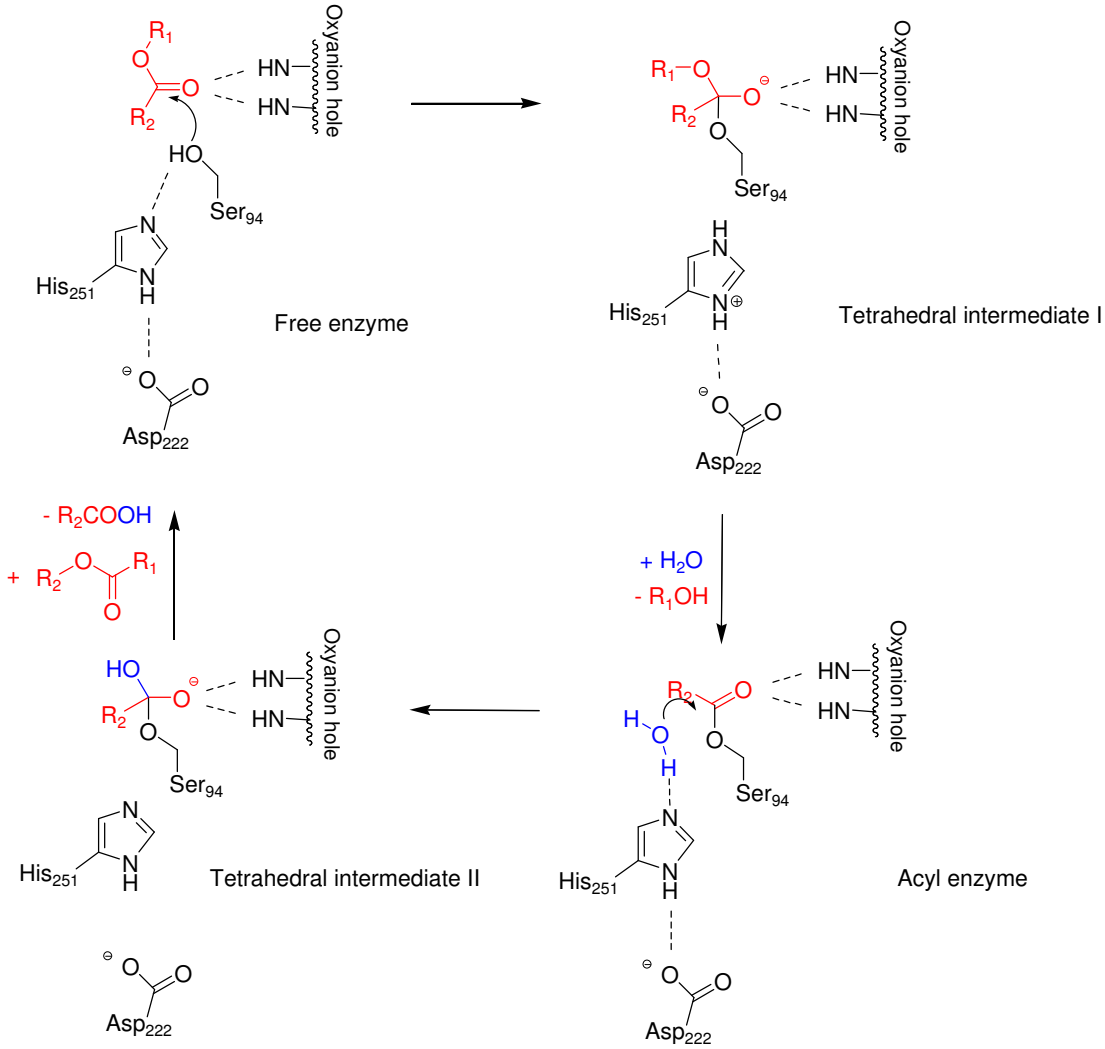

Figure 1-9: Reaction mechanism of ester hydrolysis by an esterase or lipase. The amino acid numbering corresponds to the active site of the *Pseudomonas fluorescens* esterase I.

The α/β-hydrolase fold consists of a central β-sheet whose strands are connected by helices located on each side of the sheet [69]. In a serine hydrolase, the catalytic serine sits atop β-strand 5, the catalytic acid is found after β-strand 7, and the catalytic histidine is located close to the C-terminus between β-strand 8 and helix F (see Figure 1-10). The tertiary structure is divided into the conserved main domain and a less conserved cap domain. The α/β-hydrolase fold is not only found in esterases, but also in lipases, thioesterases, proteases, haloperoxidases, epoxide hydrolases and hydroxynitril lyases [70].

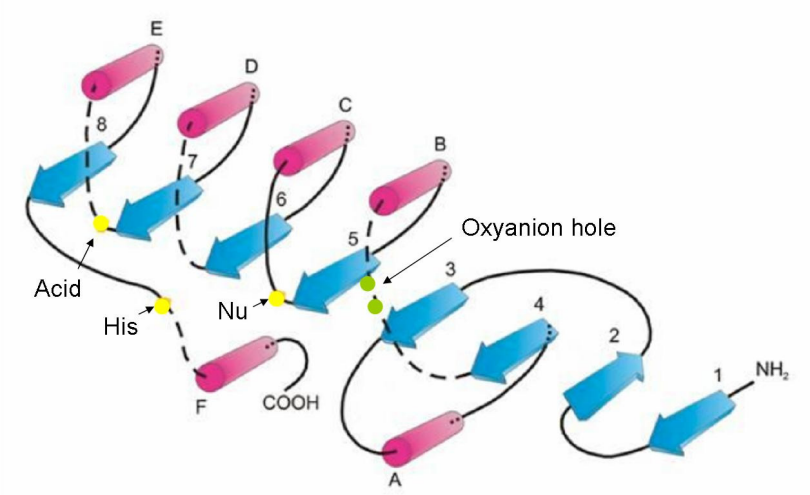

Figure 1-10: Schematic representation of the α/β-hydrolase fold; helices are shown as pink cylinders, β-strands as blue arrows. Yellow dots: catalytic residues, green dots: oxyanion hole residues. Dashed lines indicate possible insertions. Modified after [69]

1.6.2. Pseudomonas fluorescens *Esterase I*

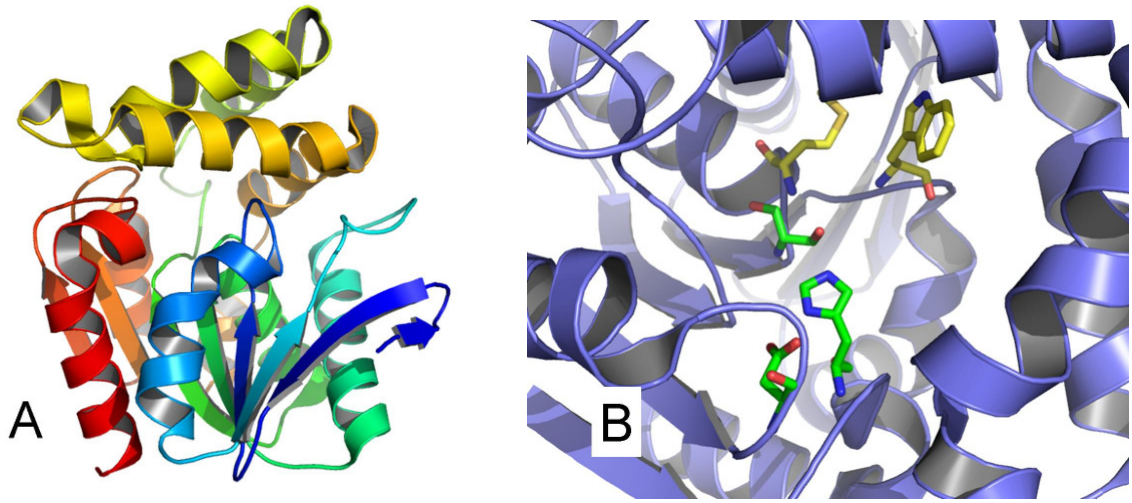

Figure 1-11: A) 3D structure of the PFE I (pdb-code 1VA4), the cap is formed by the helices in yellow and light orange B) Detail of the PFE I, active site residues are shown in green, oxyanion hole residues are shown in yellow.

The *Pseudomonas fluorescens* aryl esterase (PFE I) was first described by Choi *et al.*[71] in 1990. In 1995, Pelletier and Altenbuchner[72] cloned and expressed the enzyme and corrected the sequence to an ORF of 816 bp, corresponding to a protein with 272 amino acids and a theoretical molecular weight of 30092 Da. The crystal structure was solved in 2004 by Cheeseman *et al.* [73]. The PFE I crystallizes as a dimer of trimers, it exhibits the α/β-hydrolase fold and the typical catalytic triad Ser94-His251-Asp222. The oxyanion hole is formed by the backbone nitrogens of Trp28 and Met95, both can be seen in Figure 1-11 B. Figure 1-11 A shows the 3D structure, which consists of two domains, a cap and a core. The active site is accessible through a narrow access tunnel with a diameter of approximately 4

Å. The PFE I shares some features with non-heme haloperoxidases and has been described as a bifunctional enzyme – catalyzing both ester hydrolysis and halogenations [72].
The PFE I has been studied extensively over the past years [74-79]. Krebsfänger *et al.* [76] purified it and determined parameters such as temperature and pH preferences, revealing a broad pH profile with good activity between pH 5 and 10. The PFE I is active up to a temperature of 70°C, however, it denatures rapidly at temperatures above 50°C.
Several substrates for the PFE I have been identified. In general, the preferred length of the acyl chain is C2-C4, which is typical for an esterase [77]. While it is not very selective in the resolution of chiral arylaliphatic acids like 3-phenylbutyrate, good enantioselectivity was found in the resolution of α-phenyl ethanol. A moderate enantioselectivity was found in the resolution of methyl-3-bromo-2-methyl propanoate (MBMP), while the selectivity against methyl 2-chloropropionate (MCP) is rather low [77].
The PFE I wild type cannot hydrolyze sterically hindered 3-hydroxy esters, but mutagenesis using the mutator strain *Epicurian coli* XL1-Red yielded the double mutant A209D/L181V which accepts 3-hydroxy esters, albeit with moderate activity and low enantioselectivity [80]. Further mutants were constructed using the mutator strain and epPCR, for example L181Q which hydrolyses 3-phenylbutyric acid methyl ester with an E-value of 6,6; up from 3,5 in the wild-type[81]. The mutant T229I displays an enhanced enantioselectivity against MBMP (E=19, wild type E=12)[74]; after the structure was solved, in an approach focusing on residues close to the active site, variants with fivefold higher selectivity than the wild type (E=60) could be identified [82].

1.6.3. (-)-γ-Lactamase from Microbacterium spec.

In 1993, the company Chiratech (Now Dr. Reddy's, Slough, UK) discovered lactamase activity in an *Aureobacterium spec*. (now classified as *Microbacterium* [83]). Line *et al.* isolated and overexpressed the corresponding enzyme, purified it and solved its three-dimensional structure [84]. The coding sequence of 837 bp translates into a protein with 279 amino acids and a molecular weight of 30977 Da. The enzyme crystallizes as a trimer and exhibits the α/β-hydrolase fold and a high homology with cofactor free haloperoxidases; bromoperoxidase activity was observed at pH 4. The active site is comprised of residues Ser98-Asp230-His258; the backbone nitrogen atoms of Tyr32 and Met99 form the oxyanion hole.

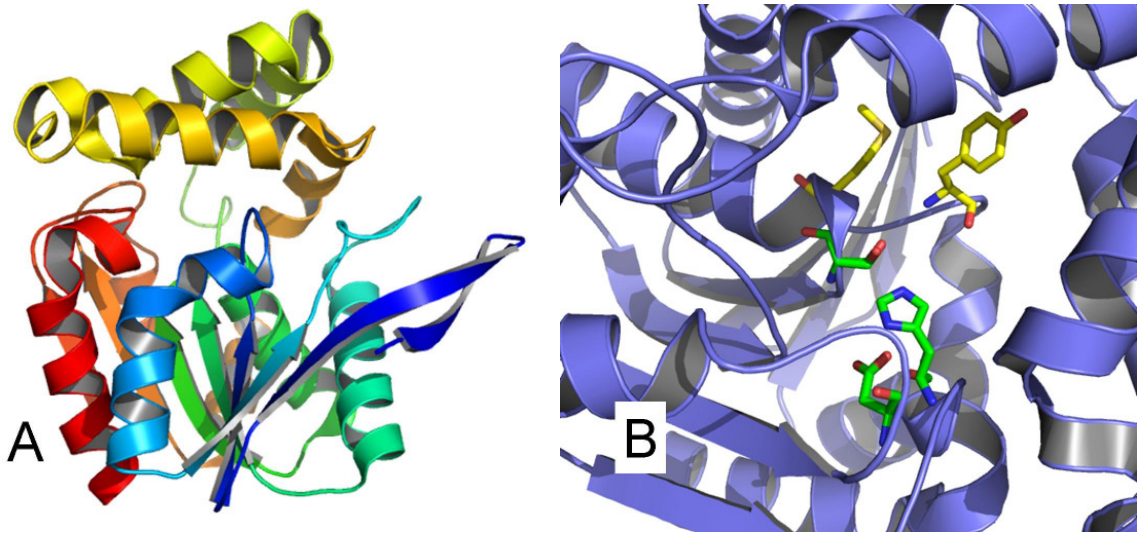

Figure 1-12: A) 3D structure of the lactamase (pdb-code 1HKH), the cap is formed by the helices in yellow and light orange B) Detail of the lactamase, active site residues are shown in green, oxyanion hole residues are shown in yellow.

The enzyme's natural function has not yet been determined; the name was assigned due to the industrially relevant hydrolysis of Vince lactam (2-Azabicyclo[2.2.1]hept-5-en-3-one) which is catalyzed by the enzyme with high selectivity (see Figure 1-13). Racemic 2-Azabicyclo[2.2.1]hept-5-en-3-one is prepared *via* cycloaddition of cyclopentadiene and chlorosulfonylisocyanate. Both stereoisomers are precursors to pharmaceutically active compounds; they were initially used for the synthesis of carbocyclic nucleosides intended for antiviral (e.g. anti-HIV) therapies [85], but the scope of applications has widened significantly in the past years [86], therefore efficient processes for the resolution are needed. Some pharmaceuticals containing 2-Azabicyclo[2.2.1]hept-5-en-3-one as a synthon are shown in Figure 1-14 [86].

The (-)-lactam is accessible using (+)-γ-lactamases from *Pseudomonas fluorescens* [87], *Pseudomonas cepacia* [86] or *Comamonas acidovorans* [88]; while the (-)-γ-lactamase from *Microbacterium* can be used for the preparation of the (+)-lactam.

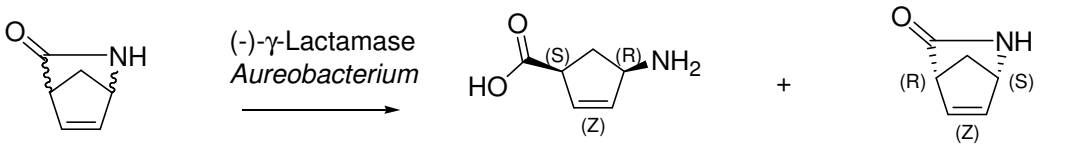

(+/-)-Lactam (1*S*,4*R*)-(-)-Amino acid (1*S*,4*R*)-(+)-Lactam

Figure 1-13: Stereoselective hydrolysis of Vince lactam

The Vince lactam contains two stereocenters, however, only two stereoisomers of the bicyclic lactam exist. The (1*R*,4*S*)-lactam is hydrolyzed to the (1*S*,4*R*)- amino acid, which is not due to an inversion of the chiral information but rather to the different numbering in mono-

and bicyclic systems. As this circumstance can lead to confusion, most publications do not name the absolute configurations but rather use the +/- terminology.

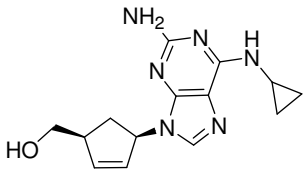

Abacavir, GlaxoSmithKline
Anti-HIV, launched

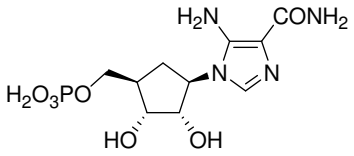

ICA-1, Inhibition Therapeutics
Oncolytic, preclinical

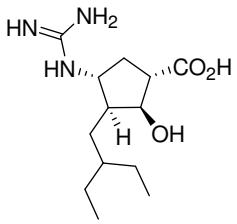

Peramivir, BioCryst
Anti-influenza virus, PIII

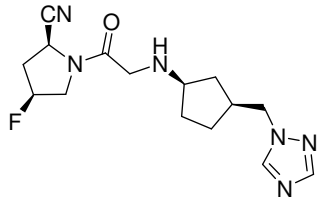

Melogliptin, Glenmark
Type 2 diabetes, PIII

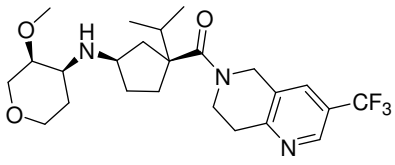

MK-0812, Merck
Multiple Sclerosis, PII

Figure 1-14: Examples for pharmaceutical compounds derived from 2-Azabicyclo[2.2.1]hept-5-en-3-one. The top row uses the (-)-lactam as synthon, the bottom row uses the (+)-lactam.

1.7. Biogenic amides

The term biogenic amides refers to amides which are found in nature, for example in plants. However, there is no precise definition, and so amides containing a biogenic amine are also referred to as biogenic amides. The so-called avenanthramides are produced by oats (*Avena sativa*) as phytoalexins to defend the plant against infections; they are amides of cinnamic acid derivatives and anthranilic acid derivatives.

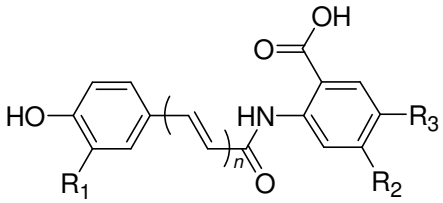

Avenanthramide	R_1	R_2	R_3	n
A	H	H	OH	1
B	OMe	H	OH	1
D	H	H	H	1
G	H	OH	H	1
L	H	H	OH	2

Figure 1-15: Structure of selected avenanthramides

Biogenic amides, and especially avenanthramides, have been researched intensively, as many biogenic amides display favourable properties for the use in cosmetics and therapeutic drugs, including anti-oxidant [89, 90], anti-inflammatory [91] and anti-microbial [92] activities. Cell tissue studies indicate that avenanthramides may help prevent atherosclerosis [91, 93]. Ferulic acid amides are being studied as potential anti-diabetes drugs, as they have been

shown to stimulate insulin secretion *in vitro* [94]. Additionally, their natural origin allows their use in organic cosmetics.

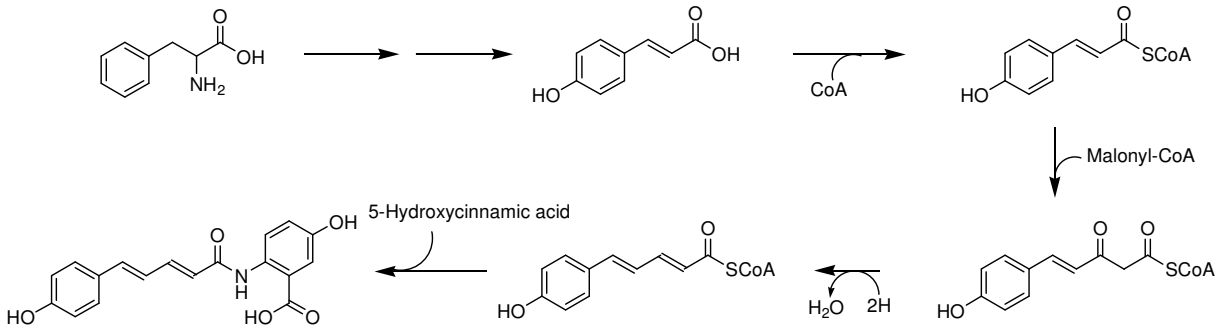

Figure 1-16: Proposed mechanism of avenanthramide synthesis exemplified for avenanthramide L [95]

The chemical synthesis of avenanthramides is challenging, as several functional groups have to be protected in order to obtain the correct product. Additionally, toxic *N*-nitrosamines may be formed; together these factors limit the potential for application in cosmetics. Some formulations employ oat extracts, however, the concentration of avenanthramides in healthy plants is rather low, so that extraction from plants is not feasible in a larger scale. A biosynthesis pathway for avenanthramides has been proposed [95], it includes activated intermediates, which in turn require ATP for synthesis. Mimicking this route in a biocatalytic process is difficult, as the expression of plant enzymes often requires complex expression systems and whole cells would be needed to regenerate the expensive cofactors. It would be very convenient to develop an enzyme capable of catalyzing the synthesis of avenanthramides from the acid and amide precursors. A major challenge is the low reactivity of the carboxyl group of cinnamic acid derivatives which is due to the conjugated double bond.

2. Aims

One aim of this work was the validation of the OSCARR technique. In previous work it had been proven that it is possible to generate mutant libraries with one to three mutations in a gene cassette of only ten amino acids. It is virtually impossible to generate this type of mutant using standard directed evolution methods such as epPCR. Additionally, using spiked oligonucleotides it is possible to mutate all positions of one codon, allowing access to all amino acids in each position. In order to prove the quality of the resulting mutants, an OSCARR library was to be constructed and screened for improved activity against medium-chain substrates, shown in Figure 2-1. The wild type PFE I displays a strong activity against pNPA and pNPB. The activity against pNPB is about 40 fold higher than against pNPC and 750 fold higher than against pNPL.

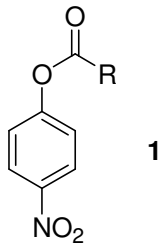

1

	Substituent R	Name (*p*-Nitrophenyl-)	Abbreviation
a	CH_3	acetate	pNPA
b		butyrate	pNPB
c		caprylate	pNPC
d		laurate	pNPL

Figure 2-1: Substrates used to screen for altered chain-length selectivity

Another goal was to enhance the understanding of mechanisms for the enantioselectivity of the PFE I and to investigate the possibility of generating promiscuous amidase activity in the PFE I.

Additionally, possibilities for the biocatalytic synthesis of biogenic amides were to be researched. The company Dr. Rieks Healthcare supplied samples of industrially interesting amides. Analytics were to be established and enzymes capable of the synthesis of compounds of interest were to be identified.

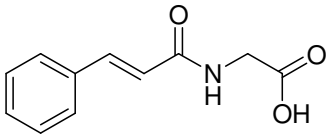

Cinnamic acid glycin amide

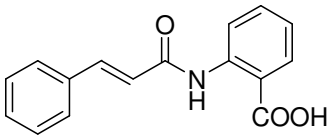

Cinnamic acid anthranilic acid amide

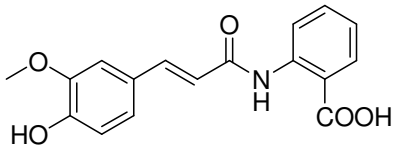

Ferulic acid anthranilic acid amide

Figure 2-2: Avenanthramide-derived biogenic amides

3. Results

3.1. Chain-length selectivity

In previous work by Dr. Hidalgo, cassettes (termed CAS) close to the active site of the PFE I were identified as possible target sequences for focused directed evolution. Cassettes 1, 2, 3, 6, and 7 are located within a 10 Å radius of the active site, 4 and 5 within a 15 Å radius, the location of the cassettes is visualized in Figure 3-1.

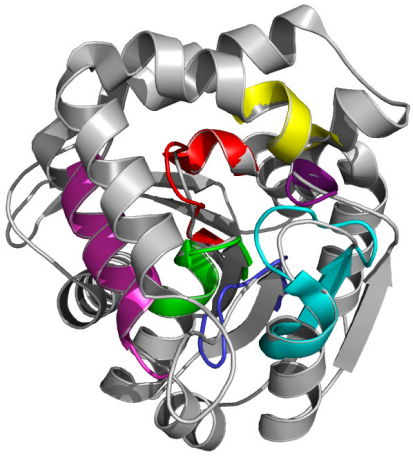

```
1     MSTFVAKDGT QIYFKDWGSG KPVLFSHGWL LDADMWEYQM EYLSSRGYRT
51    IAFDRRGFGR SDQPWTGNDY DTFADDIAQL IEHLDLKEVT LVGFSMGGGD
101   VARYIARHGS ARVAGLVLLG AVTPLFGQKP DYPQGVPLDV FARFKTELLK
151   DRAQFISDFN APFYGINKGQ VVSQGVQTQT LQIALLASLK ATVDCVTAFA
201   ETDFRPDMAK IDVPTLVIHG DGDQIVPFET TGKVAAELIK GAELKVYKDA
251   PHGFAVTHAQ QLNEDLLAFL KRGS
```

Figure 3-1: PFE I model and protein sequence with cassettes marked by color: CAS1 in red, CAS2 in green, CAS3 in blue, CAS4 in yellow, CAS5 in pink, CAS6 in cyan, CAS7 in purple

An OSCARR library was constructed using a spiked oligo for cassette 3 of the PFE I. The full-length product was purified from an agarose gel, digested with NdeI and BamHI and ligated into pGaston. After transformation into DH5α competent cells, the mutants were plated out on LB Amp agar plates.

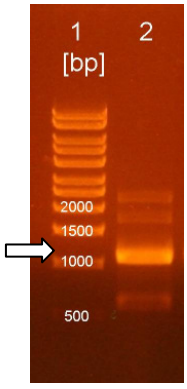

1. 1 kb ladder
2. OSCARR reaction

Figure 3-2: Agarose gel showing a sample of the OSCARR reaction used for the construction of the library. The arrow shows the size of the expected product.

A total of 8000 clones were picked into master microtiter plates, which were used to inoculate expression plates (see materials and methods for details, a graphical overview is given in Figure 3-3). After expression, cell pellets were lysed, and the lysate was split up into four microtiter plates used for photometric assays with four different esters of *p*-nitrophenol which differ in the length of the acid chain, they are shown in Figure 2-1.

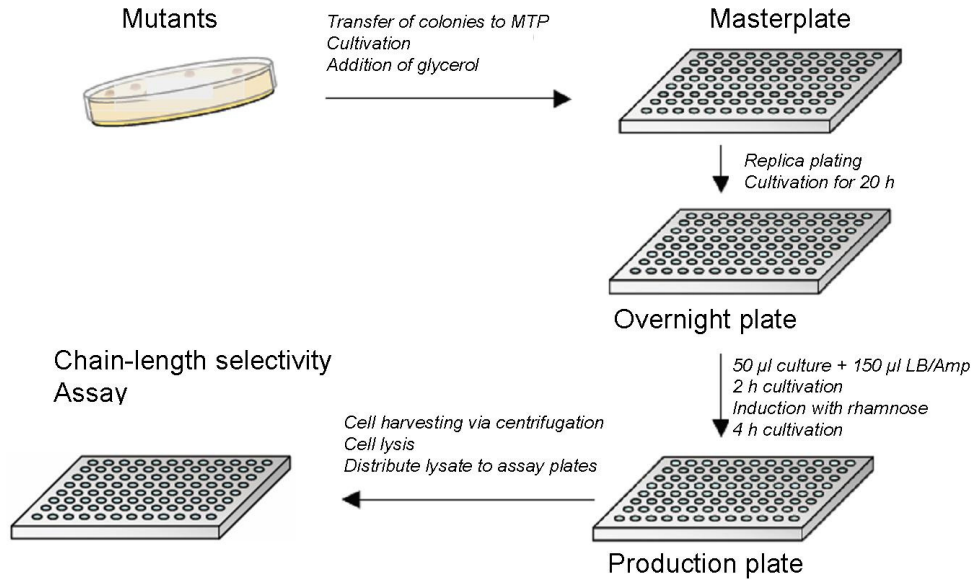

Figure 3-3: Overview of the mutant library expression and screening process in microtiter plate scale

The assay was carried out according to the procedure described in the materials and methods section. Slopes of OD_{410} over time were calculated for each well, and the slope of the autohydrolysis was subtracted from them. The slopes belonging to each mutant were then normalized by division through the slope of substrate **1a**. Mutants which differed significantly from the wild type pattern were collected on a new master plate and measured again. The differences were accepted as significant when then the value for **1c** was higher than 20% of the value for **1a** or when the activity against **1d** was clearly measurable above autohydrolysis.

The most interesting clones were then cultivated in 100 ml scale for a more thorough investigation and their mutations analyzed to determine the amino acid substitutions which had led to such a change. Interestingly, all five mutants which were sequenced contained the mutation F126I, one carried the additional mutation G120S.

Both mutants and the PFE I wild type were purified *via* immobilized metal ion affinity chromatography (IMAC), and K_M and k_{cat} values for substrates **1a-d** were determined. Interestingly, the mutants not only feature a higher catalytic efficiency in case of the medium-chain substrates, they also possess a decreased efficiency in the hydrolysis of the short-

chain substrates **1a** and **1b**. The data which was gathered is summarized in table 3-1, Figure 3-4 shows a graphical representation of chain length selectivity.

Table 3-1: K_M and k_{cat} values for the PFE I wild type and mutants F126I and G120S/F126I

Variant	pNPA			pNPB			pNPC			pNPL		
	k_{cat} [s^{-1}]	K_M [mM]	k_{cat}/K_M [$s^{-1}mM^{-1}$]	k_{cat} [s^{-1}]	K_M [mM]	k_{cat}/K_M [$s^{-1}mM^{-1}$]	k_{cat} [s^{-1}]	K_M [mM]	k_{cat}/K_M [$s^{-1}mM^{-1}$]	k_{cat} [s^{-1}]	K_M [mM]	k_{cat}/K_M [$s^{-1}mM^{-1}$]
wt	243	0.45	544	77	0.10	749	16	0.81	19	2	1.5	1.1
F126I	113	0.37	303	96	0.23	420	74	0.36	203	40	3.3	12
G120S/ F126I	56	0.26	215	56	0.14	385	57	0.25	230	14	1.1	13

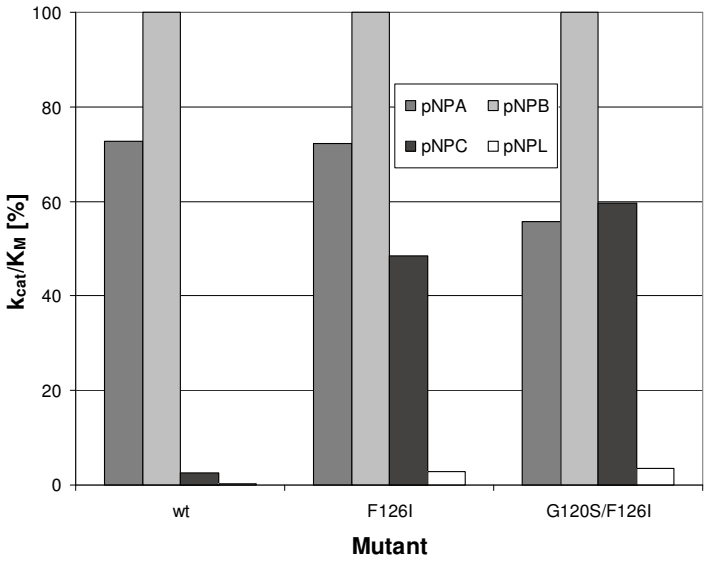

Figure 3-4: Graphical representation of chain-length selectivity expressed through k_{cat}/K_M. The value for pNPB of each mutant was set to 100%

The crystal structure of the PFE I reveals that F126, in combination with several other bulky, hydrophobic amino acids, forms a narrow entrance ("bottleneck") to the active site. Replacing F126 with an isoleucine widens the entrance, thus facilitating diffusion and binding of medium- and long-chain substrates.

The mutation G120S introduces a possible catalytic tetrad together with the other active site residues. Catalytic tetrads with an additional serine or cysteine are observed in several enzymes such as *B. subtilis* esterase BS2, subtilisin-type proteases and α/β-hydrolase fold proteases [96]. Figure 3-5 shows the geometry of this fourth residue in relation to the "classic" catalytic triad. In the BS2, the additional serine is situated closer to the catalytic acid than it would in the PFE I, as the BS2 has a glutamate, while the PFE I has an aspartate in its catalytic triad.

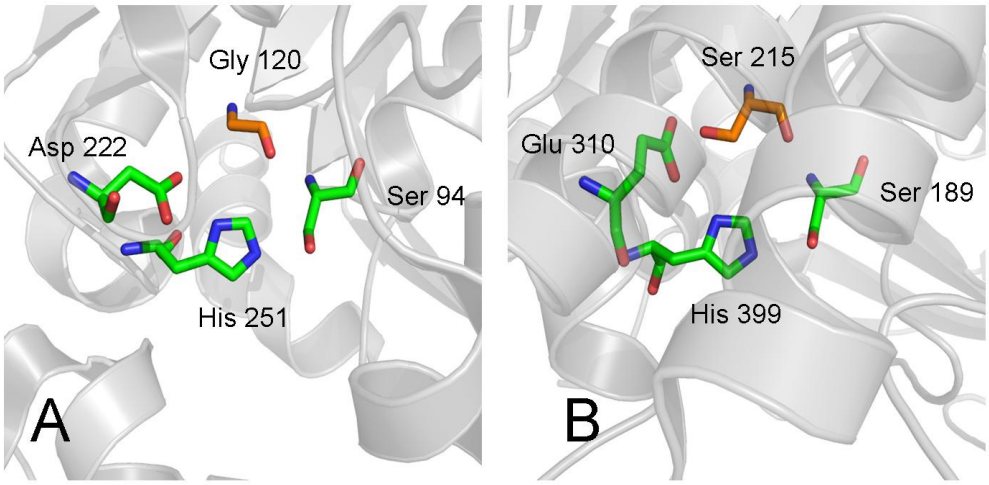

Figure 3-5: Comparison of the active sites of A) PFE I and B) BS2; green: "classic" catalytic triad, orange: additional residue which completes the catalytic tetrad.

It has been reported that reverting the tetrad to a triad in these cases raises the enzyme's K_M [96]. This is in agreement with this study's results, as G120S lowers the K_M slightly in the PFE I mutant. In serine proteases, the additional serine is involved in the induced fit rearrangement that the enzyme undergoes upon substrate binding. Additionally, it interacts with the catalytic aspartate to hold it in a favourable position [96]. However, in the PFE I the G120S mutation compromises the catalytic function, as is evident from the lower k_{cat} value [38].

F126 and the other residues forming the bottleneck (F144, F159, I225) were subjected to saturation mutagenesis to probe whether the chain-length selectivity might be altered further. It could be shown that replacing the original, bulky amino acids with smaller, yet still hydrophobic ones, has a tremendous effect on the acceptance of longer-chain substrates (Aurelio Hidalgo, personal communication). Table 3-2 lists the mutants which were constructed:

Table 3-2: List of bottleneck mutants

Designation	Mutations	Designation	Mutations
S1	F126V	D2	F126L/F144L
S2	G120S	D3	F144L/F159L
S3	I225F	D4	F144L/I225L
S4	I225L	D5	F159L/I225L
S5	F144V	D6	F126L/F159L
S6	F144L	T1	F126L/F144L/I225L
S7	F159L	T2	F126L/F159L/I225L
S8	F126L	T3	F126L/F144L/F159L
D1	F126L/I225L	Q	F126L/F144L/F159L/I225L

The single mutant S2 (G120S) did not have a noticeable influence on substrate selectivity, the position was thus not investigated further. Figure 3-6 makes it clear by how much the bottleneck is widened in mutant Q after the mutation of four residues.

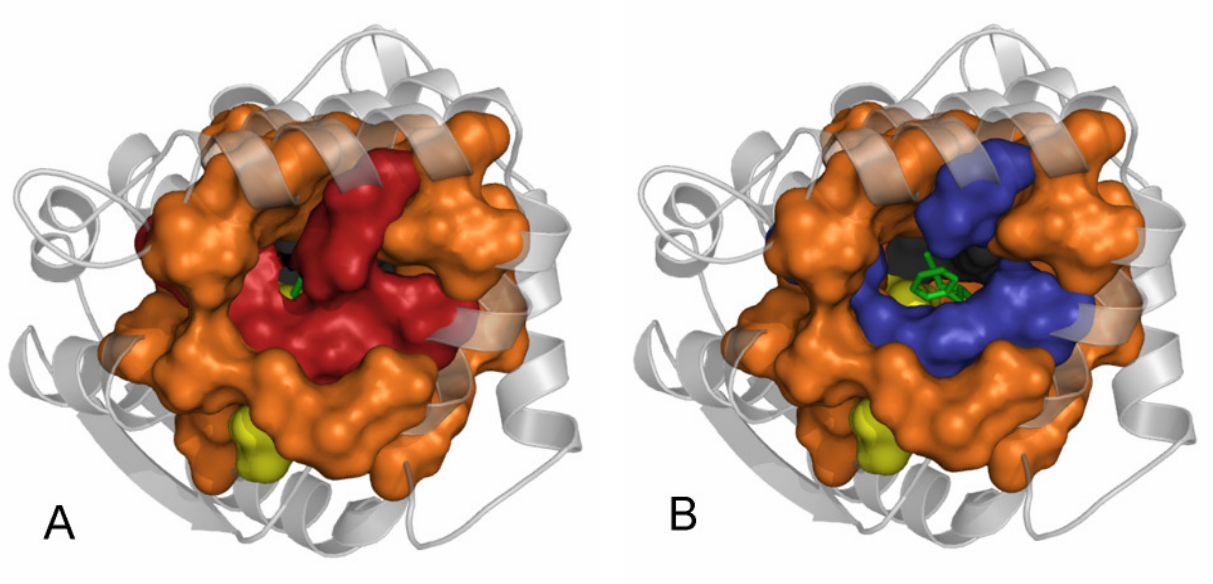

Figure 3-6: A) Wild-type PFE I, B) PFE I mutant Q; yellow: active site, green: substrate (*R)*-1-phenyl-2-propyl acetate), orange: binding pocket. Bottleneck residues are shown in red (wild-type) and blue (mutant Q)

In previous experiments (Dr. Hidalgo, unpublished results) it could be shown that the CAS3 region of the PFE I is impossible to mutate using standard epPCR protocols, probably due to the high GC content of 76,7%. It is thus not surprising that screening of an epPCR library of approximately 1500 clones did not yield mutants with comparable changes in selectivity [38]. The results gathered here clearly show that using the OSCARR method it is possible to generate high-quality libraries with mutants displaying the desired properties, where traditional techniques such as epPCR cannot be applied due to the properties of the sequence to be mutated. This case study also supports the postulate that closer mutations are better. Of the residues forming the bottleneck, F126 is located within CAS3, F159 in CAS4 und I225 in CAS6. All but one relevant position (F144) could have been found in further OSCARR libraries focused on other cassettes or combining several cassettes.

3.2. Enantioselectivity

The broadened substrate entrance provided an exciting opportunity to probe its influence on enantioselectivity [97]. Due to the proximity of the bottleneck residues to the active site, they may influence binding of the substrate enantiomers or their diffusion into the active site.

All bottleneck mutants could be expressed in *E. coli* DH5α cells at 37°C as described in materials and methods. Samples were taken when the cultures were harvested to monitor the success of the expression, both soluble and pellet fractions were subjected to

SDS-PAGE, in Figure 3-7 it can be seen that the overexpression was successful in all cases. Very little protein is found in the insoluble pellet fraction except in the case of mutant Q; even there the majority of recombinant protein is found in the soluble fraction.

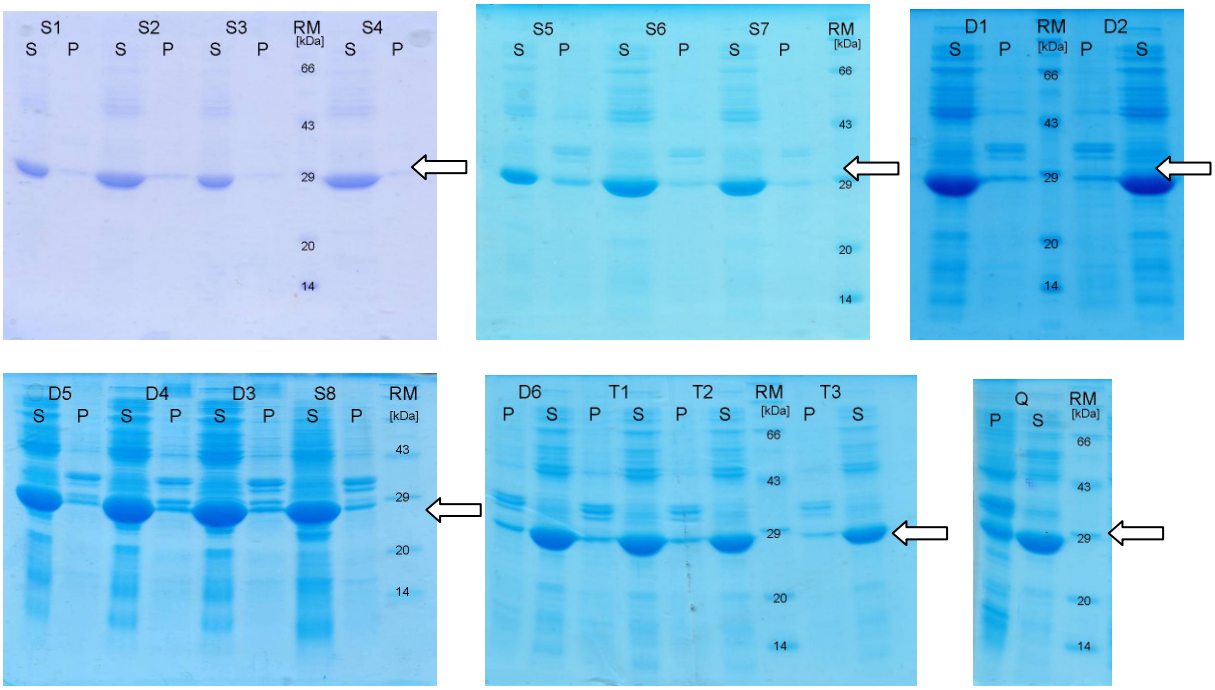

Figure 3-7: SDS-PAGE of mutant expressions, the arrow denotes the expected size of the protein. S: soluble fraction, P: pellet fraction, RM: Roti Mark Standard ®

The crude lyophilisates of the bottleneck mutants were then used for biocatalysis experiments with acetates of chiral secondary alcohols and ethyl esters of chiral acids to study both the influence of individual mutations and synergistic effects of mutation combinations. Gas chromatography was used to determine ee_S and ee_P, conversion and enantioselectivity were calculated according to Chen *et al.* [5].

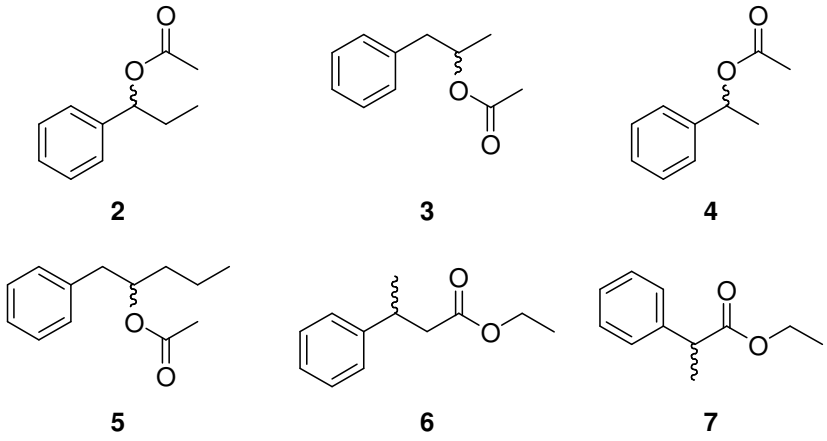

Figure 3-8: Chiral substrates employed for probing the enantioselectivity of bottleneck mutants: **2** 1-phenyl-1-propyl acetate, **3** 1-phenyl-2-propyl acetate, **4** 1-phenyl-1-ethyl acetate, **5** 1-phenyl-2-pentyl acetate, **6** 3-phenylbutyric acid ethyl ester, **7** 2-phenylpropionic acid ethyl ester

After all substrates shown in Figure 3-8 had been tested with all bottleneck mutant lyophilisates, it became obvious that substrates **5** and **7** are hardly accepted by wild type and mutants, conversions stayed very low and were completely unselective, so no further research was conducted in that regard. In the case of **6**, the wild type has a slight (*R)* preference (E_R=3.5) which can also be found in most mutants. S3 and Q, however, display a slightly inversed enantioselectivity (E_S=1.3). As this effect is not very pronounced, it did not seem likely that molecular modelling would yield significant results.

For substrates **2**-**4**, several mutants were more selective than the wild type. For the sake of clarity, only four mutants and the wild type are discussed in more detail. These mutants are based on one another, meaning that the double mutant includes the single mutant and so forth, this can be seen in table 3-3.

Table 3-3: Mutants whose enantioselectivities are discussed in more detail

Designation	Combination of	Mutations
wt	-	-
S7	S7	F159L
D3	S7+S6	F144L/F159L
T3	S7+S6+S8	F126L/F144L/F159L
Q	S7+S6+S8+S4	F126L/F144L/F159L/I225L

The biocatalysis results for the mutants are listed in tables 3-4 to 3-6. In the resolution of **2**, mutants S7, D3, and T3 are significantly more selective than the wild type, all tested variants were *R* selective. It is obvious that the mutation I225L, which is the only difference between T3 and Q, is detrimental to the enantioselectivity. D3 and T3 reached their conversion of about 50% after six hours, S7, Q, and wild type did not reach 50% even after 24h. Mutants S6, S8, and S4 were not selective, S4 (I225L) showed a very low conversion (data not shown). It is likely that F159L is responsible for the high conversion of D3 and T3, while I225L slows down mutant Q.

Table 3-4: Biocatalysis results for substrate **2**

Mutant	Enantiomeric excess		C	E
	[% ee_s]	[% ee_P]	[%]	[ ]
S7	33.4	94.2	26.2	46.8
D3	84.5	87.2	49.2	39.0
T3	84.2	89.1	58.6	46.2
Q	8.9	66.2	11.9	5.4
wt	0.6	8.6	6.2	1.2

Interestingly, the biocatalysis results for **3** are very different; they can be seen in table 3-5. Again, all mutants were (*R)* selective like the wild type. The same enzyme solutions and

amounts were used as for substrate **2**, and the reactions were carried out in parallel on the same day, so the difference in conversion indicates a difference in substrate selectivity between mutants. The most striking difference between **2** and **3** is the influence of the mutation I225L. While it destroys enantioselectivity against substrate **2**, it increases enantioselectivity against substrate **3** substantially. The single mutant S4 (I225L) displayed a moderate enantioselectivity (E=21), but the conversion was very poor, similar results were found for D4 and D5 (double mutants containing S4, data not shown). So again, I225L seems to slow the enzyme's reaction rate, which can be countered by the additional mutations. The enantioselectivity is obviously due to synergistic effects, as no single mutant surpasses the wild type's E value.

Table 3-5: Biocatalysis results for substrate **3**

Mutant	**Enantiomeric excess**		**C**	**E**
	[% ee_S]	**[% ee_P]**	**[%]**	**[ ]**
S7	79.9	83.0	49.1	26.2
D3	71.7	76.1	48.5	15.6
T3	72.0	65.1	52.5	10.0
Q	90.0	89.2	50.2	54.0
wt	34.1	92.0	27.0	33.4

In the resolution of **4**, the wild type already shows a good selectivity, however, all mutants possess excellent enantioselectivities (see table 3-6). Even after prolonged periods of time, the conversion did not rise further, which is also an indicator for excellent selectivity. All tested variants were *(R)* selective.

Table 3-6: Biocatalysis results for substrate **4**

Mutant	**Enantiomeric excess**		**C**	**E**
	[% ee_S]	**[% ee_P]**	**[%]**	**[ ]**
S7	99.99	95.2	50.6	>100
D3	99.99	93.1	48.5	>100
T3	99.99	95.6	51.1	>100
Q	99.99	86.9	53.5	>100
wt	99.99	69.9	58.9	51.7

Docking calculations were then performed with substrates **2** and **3** using the program YASARA [98] and visualized using PyMOL [99]. Each substrate enantiomer was docked into the wild type and into the best mutant (T3 for substrate **2**, Q for substrate **3**). Figures 3-9 and 3-10 below show the docking results. The numbers indicate the bottleneck residues.

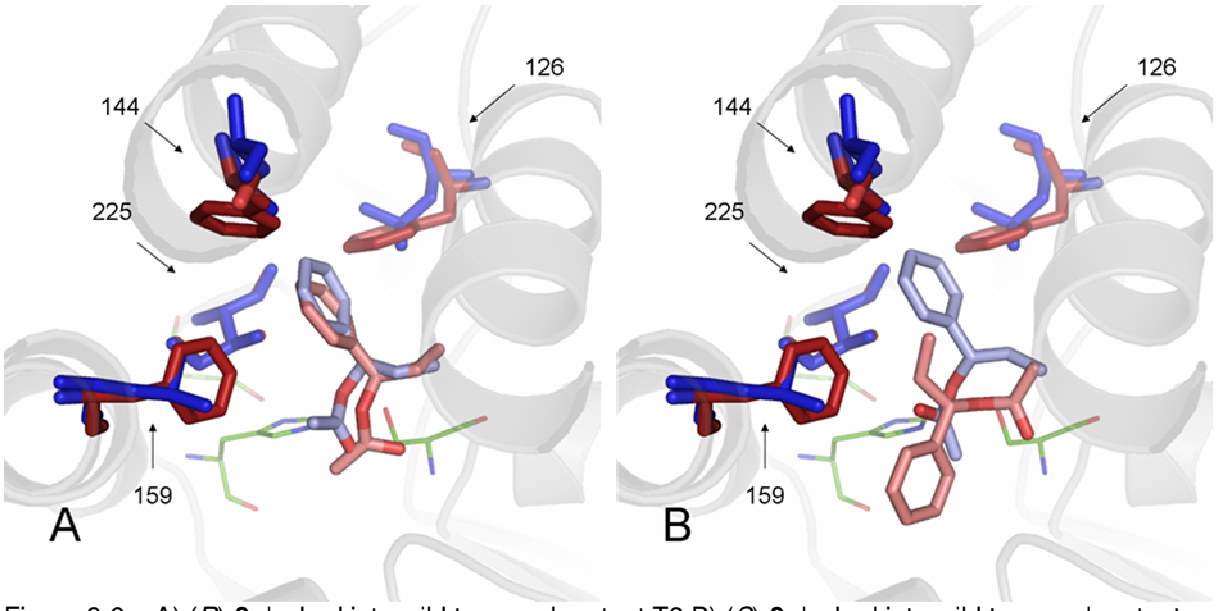

Figure 3-9: A) (*R*)-**2** docked into wild type and mutant T3 B) (*S*)-**2** docked into wild type and mutant T3. green: catalytic triad, dark red: wild type bottleneck, dark blue: mutant T3 bottleneck, light red: (*R/S*)-**2** in wild type, light blue: (*R/S*)-**2** in mutant T3.

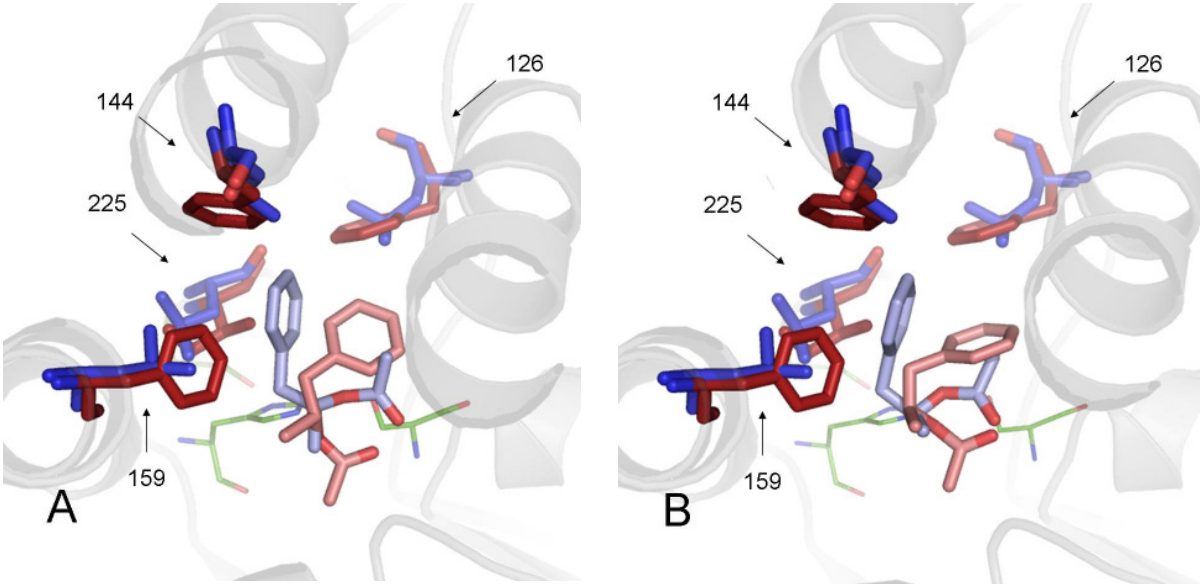

Figure 3-10: A) (*R*)-**3** docked into wild type and mutant Q, B) (*S*)-**3** docked into wild type and mutant Q. green: catalytic triad, dark red: wild type bottleneck, dark blue: mutant Q bottleneck, light red: (*R/S*)-**3** in wild type, light blue: (*R/S*)-**3** in mutant Q.

The docking studies show that residues 126 and 144 do not make close contact with the substrates, leading to the conclusion that they influence the diffusion of substrates into the active site rather than the binding of the substrate or stabilization of the tetrahedral intermediate [100]. Residues 159 and 225, on the other hand, are likely to influence binding of the substrates by opening or closing binding pockets.

In the case of both mutants, the substrates' phenyl moieties point towards the broadened bottleneck; basically, in the mutants, the enantiomers of both substrates dock in virtually the same positions – in the case of **3**, the hydrogen and the methyl group exchange places. The

enantiomers of **2** are docked like image and mirror image. Only (*R*)-**2**'s phenyl moiety points to the bottleneck in the wild type.

Mutant T3's enantioselectivity against **2** can be explained by the absence of a productive binding mode for (*S*)-**2** in the mutant. Shown above is the best docking solution available, and the carbonyl oxygen is not stabilized by the oxyanion hole.

Substrate **3** cannot occupy the same position in the wild type as in mutant Q because of the steric hindrance of the methyl group of I225 and the phenyl ring of F159.

3.3. Amidase activity

A search for structural homologues of the PFE I was conducted using the DALI server [101, 102]. Many similar structures are esterases, dehalogenases, epoxide hydrolases and nitrile hydratases, which is not surprising, as these enzymes display the α/β-hydrolase fold. The first hits with obvious amidase activity are listed in table 3-7.

Table 3-7: Proteins with amidase activity and structural similarity with the PFE I

Pdb code	EC Number	Enzyme name	Organism
1MTZ	3.4.11.5	Proline iminopeptidase	*Thermoplasma acidophilum*
1QTR	3.4.11.5	Proline iminopeptidase	*Serratia marcescens*
1AZW	3.4.11.5	Proline iminopeptidase	*Xanthomonas campestris*
2OAE	3.4.14.5	Dipeptidyl peptidase	Rat (*Rattus norvegicus*)
2AJD	3.4.14.5	Dipeptidyl peptidase	Pig (*Sus scrofa*)
3G0B	3.4.14.5	Dipeptidyl peptidase	Human (*Homo sapiens*)

They could be divided into two categories – microbial prolyl iminopeptidases and eukaryotic dipeptidyl peptidases. The former cleave the N-terminal proline off polypeptide chains, while dipeptidyl peptidases cleave dipeptides; the main difference between the substrates is their size. Both groups of enzymes share the α/β-hydrolase fold which aligns reasonably well with the main domain of the PFE I; the cap domain of the dipeptidyl peptidases is a beta-propeller with eight β-sheets, the cap domain of the proline iminopeptidases has no specific motif.

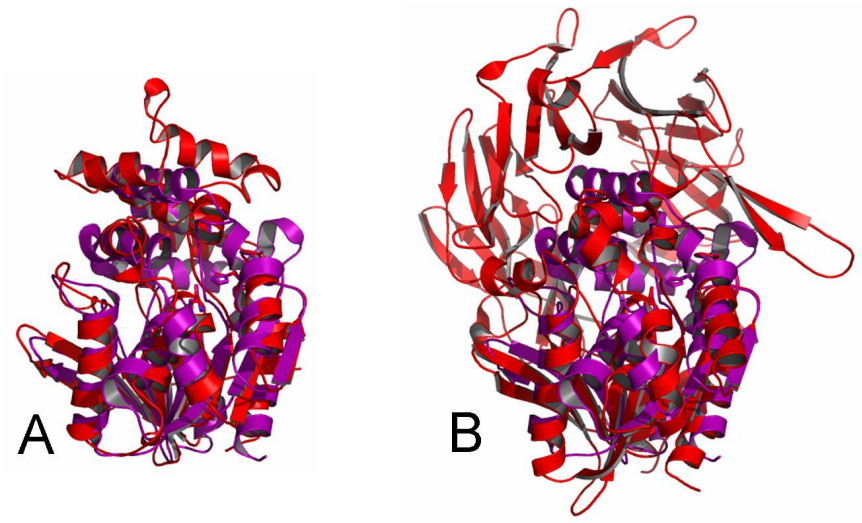

Figure 3-11: A) Alignment of PFE I (magenta) and 1AZW (red, prolyl iminopeptidase from *Xanthomonas campestris*) B) Alignment of PFE I and 2AJD (red, porcine dipeptidyl peptidase)

This similarity to existing amidases led to the conclusion that hydrolytic activity against dipeptides or, more general, amides with proline or other amino acids as carboxyl donor, could be introduced in the PFE I. Aminonaphthalene derivatives were chosen as assay substrates, as they allow agar-plate staining with Fast Blue RR. L-Proline-β-aminonaphthalene and D-alanine-β-aminonaphthalene were chosen as suitable substrates in addition to acetyl-β–aminonaphthalene, a standard amidase substrate commonly used in our laboratory (see Figure 3-12). L-alanine-β-aminonaphthalene was also tested, but this substrate is cleaved by enzymes native to the *E. coli* DH5α strain which was used.

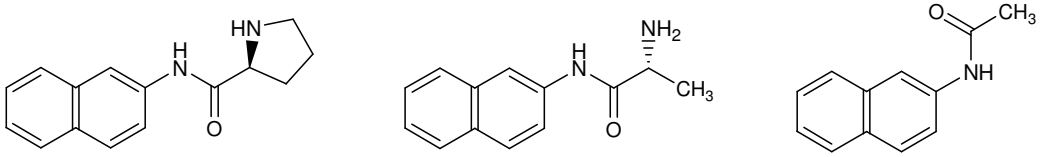

8 **9** **10**

Figure 3-12: Amides used as substrates for the agarose overlay assay **8** L-Proline-β–aminonaphthalene, **9** D-Alanine-β–aminonaphthalene, **10** Acetyl-β–aminonaphthalene

In previous work in our group common motifs of prolyl iminopeptidases were analyzed and introduced into the PFE I. The resulting mutants were used as starting mutants for epPCR, however, no mutant with activity was found. This rational approach in combination with a classic directed evolution was not successful, so focused directed evolution was to be applied to the problem.

As the OSCARR library generated before had proven to be of high quality (that is, mutants with correct fold and altered selectivities had already been found), it was now additionally screened for amidase activity. Three LB Amp/Rha agar plates were inoculated from each master microtiter plate using a replicator. After 20 hours at room temperature, the plates were overlaid with agarose containing Fast Blue RR and one of three amide substrates **8**-**10** (see Figure 3-12).

Each expression plate was also inoculated with the PFE I wild type and the *Bacillus subtilis* esterase BS2, each cloned into *E. coli* DH5α as negative and positive control, respectively. Pictures of sample plates can be seen in Figure 3-13.

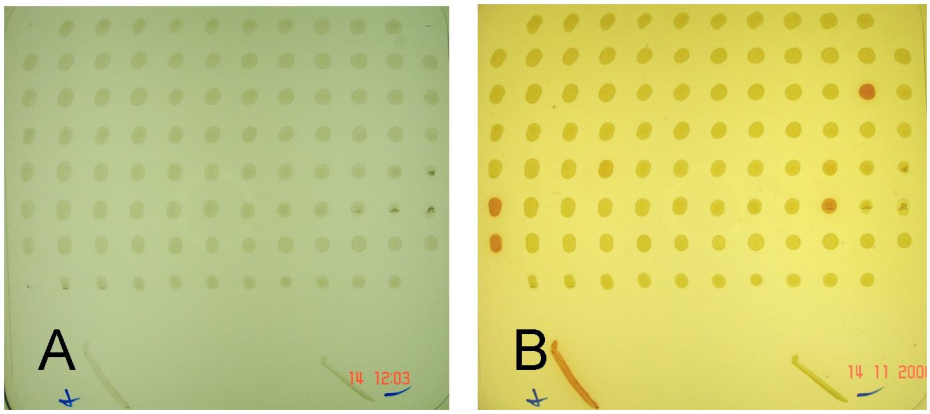

Figure 3-13: A) Expression agar plate before staining B) Expression agar plate after staining. The positive control is marked as +, the negative control is marked as -

Of the 8000 clones which were screened, a few clones appeared to give a faint stain in the overlay assay. However, when the experiment was repeated no activity was found, the stains were probably artefacts.

The question arose whether the substrates which had been used for screening were indeed suitable for finding amidase activity in the PFE I, so that other possibilities were investigated. A new similarity search with the DALI server brought up a high homology with the (-)-γ-lactamase (pdb code 1HKH) from *Microbacterium sp*. (formerly *Aureobacterium sp*.) which was not included in the previous alignment. The natural function of this enzyme is unknown, it was named after the industrially relevant enantioselective resolution of 2-azabicyclo[2.2.1]hept-5-en-3-one (Vince lactam). This lactamase is an α/β-hydrolase like the PFE I. Even though the PFE I is an enzyme from *Pseudomonas*, a gram negative bacterium, and the lactamase stems from *Microbacterium*, which is a gram positive bacterium, the structural similarity is striking. An amino acid sequence alignment using VectorNTI® showed 37,8% identity and 53,7% positives (meaning similar amino acids). The enzymes are of a very similar size and the crystal structures can be superimposed quite well, as shown in Figure 3-14. Some structural elements are shifted with relation to the other

enzyme, but in general not only the conserved α/β-hydrolase core is similar, but also the more variable cap domain and even the more flexible loops. The alignment is far better than the alignment with the proline iminopeptidases and the dipeptidyl peptidases.

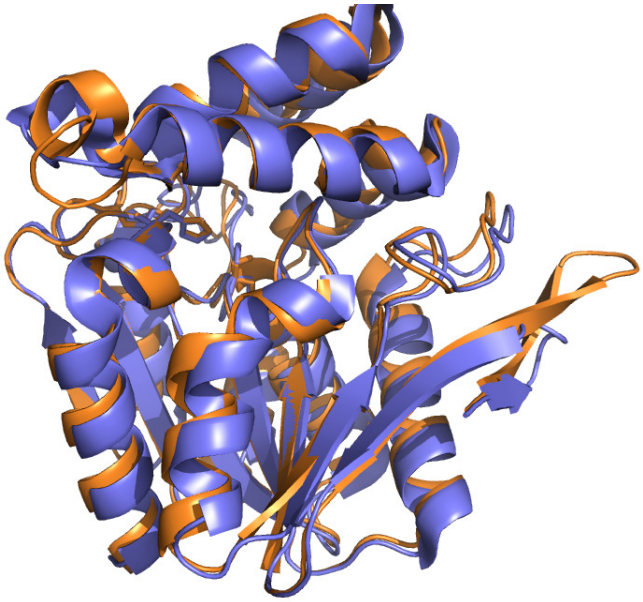

Figure 3-14: Alignment of PFE I (blue) and lactamase (orange)

In pre-tests it was found that the PFE I wt displays hydrolytic activity against 2-azabicyclo[2.2.1]hept-5-en-3-one (**11**, see Figure 3-15). To confirm that this activity stems from the esterase and not from *E. coli* background, control reactions were performed using *E. coli* DH5α wild type lyophilisate, which did not hydrolyse the lactam. In order to compare the PFE I to the lactamase in terms of enantioselectivity and activity, it was desirable to obtain the lactamase gene.

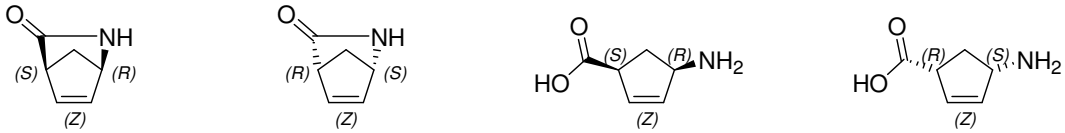

(-)-**11** (+)-**11** (-)-**11a** (+)-**11a**

Figure 3-15: **11** 2-azabicyclo[2.2.1]hept-5-ene-3-one **11a** 4-aminocyclopent-2-ene carboxylic acid

At our request, the lactamase gene was supplied by Dr. Reddy's (Slough, UK) in an unknown vector using unknown restriction sites, so primers were designed to amplify the gene and to introduce an N-terminal NdeI cleavage site as well as a C-terminal BamHI cleavage site. The stop codon was also mutated to allow the expression of a C-terminal His-tag. The PCR product had the expected size of approximately 900 bp, so it was digested with NdeI and BamHI and ligated into pGaston. This allowed the transformation and overproduction of the lactamase in *E. coli* DH5α as well as the purification of the protein *via* IMAC. The cultivation

was carried out at 37°C with induction at OD_{600} 0.5, the cell pellet was harvested 24 hours after induction. Samples were applied to an SDS gel to confirm the successful expression. As can be seen in Figure 3-16, there was a strong overexpression band in the soluble fraction and no inclusion bodies were formed.

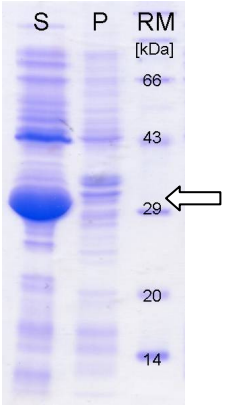

Figure 3-16: SDS-PAGE of the g-lactamase cultivation, S: soluble fraction, P: pellet fraction, RM: Roti Mark Standard® The arrow shows the size of the expected product

An analytical method for the separation of the stereoisomers had to be established. As the water solubility of **11** is > 1 kg/l, it was decided that it would be advisable to use a reversed-phase chiral HPLC column, for which aqueous mobile phases can be used. It was possible to separate the substrate peaks on a Chiralcel® OD-RH column with a mobile phase of 5% acetonitrile and 95% water with 0,1% TFA; however, it was not possible to resolve the product peaks. It can be assumed that racemization of the product occurs under the analytical conditions, so that up to four peaks can be distinguished.

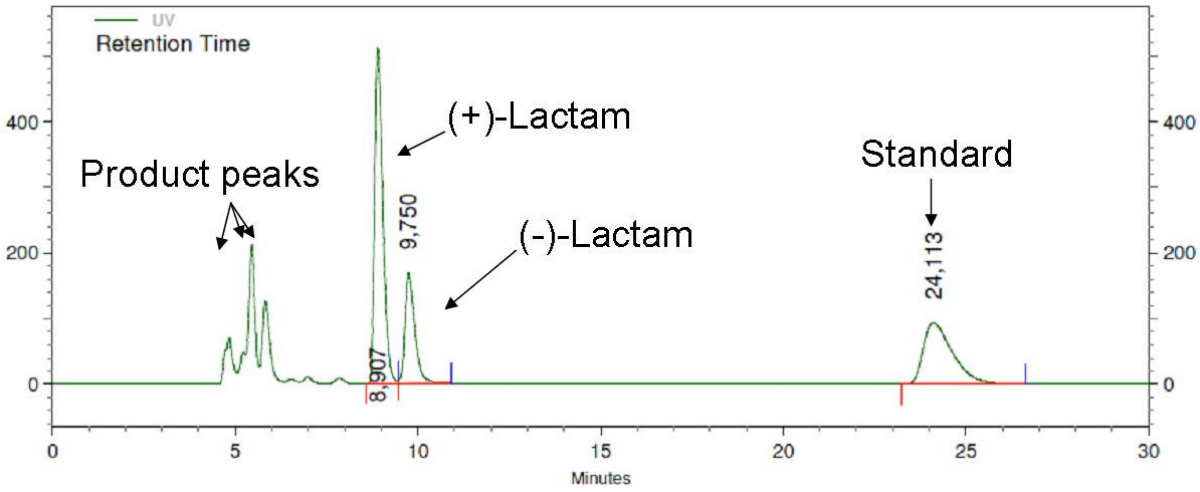

Figure 3-17: Sample chromatogram of a biocatalysis with **11**

In order to determine the enantioselectivity, it is necessary to determine two values out of ee_s, ee_p and conversion. As ee_p is not accessible *via* this method, an internal standard was

used to calculate the conversion. *p*-Aminobenzoic acid has a reasonably good absorbance at 225 nm and can easily be separated from the lactam peaks under the analytical conditions. A standard curve was measured to determine the analytical limits.

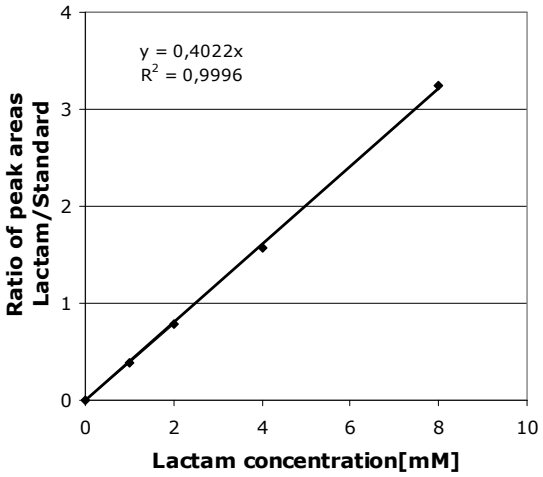

Figure 3-18: Calibration curve of lactam and internal standard

Figure 3-18 shows a good linear correlation between the concentration of **11** and the ratio of the peak areas of lactam and internal standard. At concentrations above 8 mM the peak area of the lactam no longer shows a linear increase, so 8 mM is the maximal substrate concentration which can be measured accurately.

In order to increase the method's reproducibility, some factors were improved over time. During the first biocatalysis attempts, the standard was added to the reaction mixture after the reaction time had elapsed and conversion was calculated based on the slope of the calibration curve. The idea was to prevent the standard from interfering with the reaction; however, this leads to imprecision if small pipetting errors occur when the reactions are set up or when the standard is added. While the error is small, it would especially influence parallel reactions (e.g. for a pH profile). Additionally, while it is possible to store a stock solution of the standard, the substrate solution must be freshly prepared for every round of biocatalysis. Even though a special accuracy weighing machine was used for weighing, a small margin of error remains which would offset the ratio of lactam to standard peak areas. To avoid these errors, a master mix was prepared for serial biocatalysis experiments. This master mix contained all ingredients which were identical in the series, most importantly substrate and standard. A sample of this master mix was analyzed on the HPLC to determine the ratio of lactam to standard peak areas at 0 % conversion. Additionally, this measurement allows the verification of highly selective mutants through the comparison of peak ratios between (+)-lactam and standard. As selective mutants will only convert the (-)-lactam, the aforementioned ratio stays the same over the course of the reaction.

Crude lyophilisates of lactamase, PFE I wild type and bottleneck mutants described above were used for biocatalysis to determine differences in enantioselectivity. Molecular docking performed by Dr. Aurelio Hidalgo additionally suggested that the mutations C195V and F199Y would increase the enantioselectivity of the PFE I (data not shown). The lactamase contains valine instead of cysteine, but tryptophane instead of phenylalanine in the indicated positions. Additional mutants were created containing these mutations in the wild type or combined with bottleneck mutations. Mutants are named according to the bottleneck mutant list, an additional C or F in the name indicates the presence of C195V or F199Y, respectively.

Biocatalysis experiments were carried out using crude lyophilisate of the indicated mutants; the results are shown in table 3-8.

Table 3-8: Conversion, enantiomeric excess (ee_S, ee_P) and enantioselectivity of bottleneck mutants against **11**

	Conversion	**Enantiomeric excess**		**E**
	[%]	**[%ee_S]**	**[%ee_P]**	**[ ]**
Lactamase	87.3	100.0	14.6	8
PFE I wt	56.3	100.0	77.6	74
CF	51.8	78.8	73.5	16
S7+CF	46.0	85.9	100.0	>100
D2+CF	35.2	54.1	99.6	>100
D6+CF	13.3	12.9	83.9	13
S1	51.9	100.0	92.6	>100
S2	69.7	96.1	41.8	9
S3	47.2	72.6	81.2	21
S4	92.9	97.1	7.4	3
S5	54.6	96.3	80.2	36
S6	51.7	98.0	91.6	>100
S7	51.7	100.0	93.4	>100
S8	46.1	65.1	76.0	14
D1	68.0	100.0	47.1	23
D2	49.7	95.0	96.1	>100
D3	49.2	96.7	100.0	>100
D4	52.5	92.1	83.5	36
D5	58.8	100.0	69.9	52
D6	51.5	100.0	94.2	>100
T1	51.9	87.5	81.1	27
T2	52.6	88.4	79.6	26
T3	28.1	36.7	94.2	48
Q	6.1	3.2	49.9	3

According to this data, the PFE I wild type appears to be more selective than the lactamase. Additionally, several mutants reach excellent enantioselectivities of >100. The most interesting mutations are F144L (S6), F159L (S7) and F126V (S1), as they confer selectivity not only to the single mutants, but also to double mutants they are included in.

The most interesting mutants were expressed in 500 ml scale to provide fresh lyophilisate in sufficient amounts for purification. After purification *via* IMAC, the purified proteins were stored in 30% glycerol at -20°C. Protein contents of these enzyme solutions were determined using the Bradford method, this data is displayed in table 3-9 and samples were applied to SDS gels to estimate protein purity. In most cases only very faint bands were visible in addition to the protein of interest, with the exception of D3. This is likely due to the fact that the protein concentration was very low in the case of D3 so that the enzyme solution was applied undiluted. In general the SDS gels show that the purifications were successful.

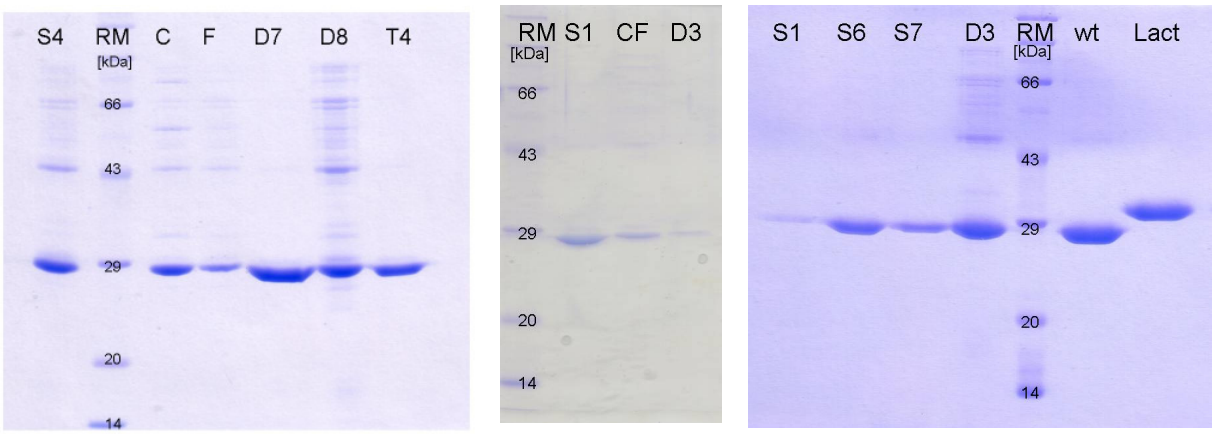

Figure 3-19: SDS-Gels showing the purity of the IMAC-purified proteins

Table 3-9: Protein content of the IMAC-purified protein solutions

Mutant	**Protein content [µg/ml]**
S1	506
S6	2340
S7	1010
D3	314
CF	91
PFE I wt	3174
Lactamase	26497
C	199
F	131
S4	309

Even though similar amounts of lyophilisate were used for purification and the expression levels were similar, the yield of purified protein varied greatly, even between purifications which were carried out on the same day, under the same conditions.

While the first results with crude lyophilisate indicated that the lactamase is less selective than the PFE I wild type and mutants, biocatalysis experiments with purified proteins show E values above 100 for all tested proteins including the lactamase. This is somewhat surprising, as lyophilisate of wild-type *E. coli* does not possess lactam-hydrolyzing activity; the source of the interference is unknown.

Biocatalysis reactions were carried out in a larger scale to allow the analysis of samples at several points in time. Care was taken to choose data points in the linear range for the calculation of the specific activity (see Figure 3-20). Great differences in specific activity may be observed between mutants. While most mutants are much less active against **11** than the lactamase, the mutant CF seems to possess a similarly high activity, both mutants C and F are more active than the wild type.

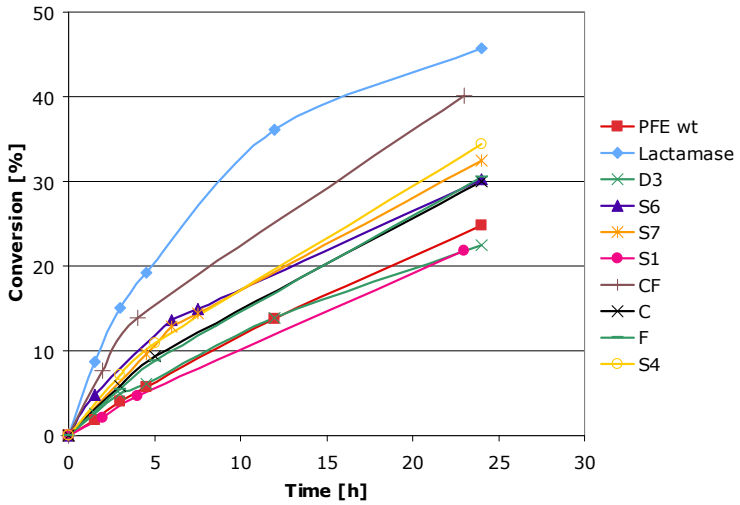

Figure 3-20: Progress of conversion over time of various mutants

Table 3-10: Specific activities of purified proteins

Mutant	Protein amount [µg]	Time [h]	Lactam [µmol]	Specific activity [U/mg]
S1	63.3	4	0.37	0.024
S6	35.1	6	1.10	0.086
S7	15.2	4.5	0.77	0.189
D3	26.9	3	0.39	0.081
CF	11.4	4	1.11	0.406
PFE I wt	13.2	24	1.98	0.104
Lactamase	13.2	1.5	0.70	0.584
S4	17.7	3	0.57	0.179
C	11.4	3	0.47	0.229
F	7.5	3	0.44	0.324

As has been published before [76], the PFE I wild type is active over a broad pH range, this is also true for lactam hydrolysis. Little differences in conversion were observed between pH 6 and pH 10, with a drop in activity above pH 10. Several mutants' pH profiles were also characterized, and some displayed a narrowed pH preference, with the highest activity usually between pH 9 and pH 10. Here, the lactamase differs markedly from the PFE I and its mutants, as it is highly active at pH 11, where all PFE I variants lose activity.

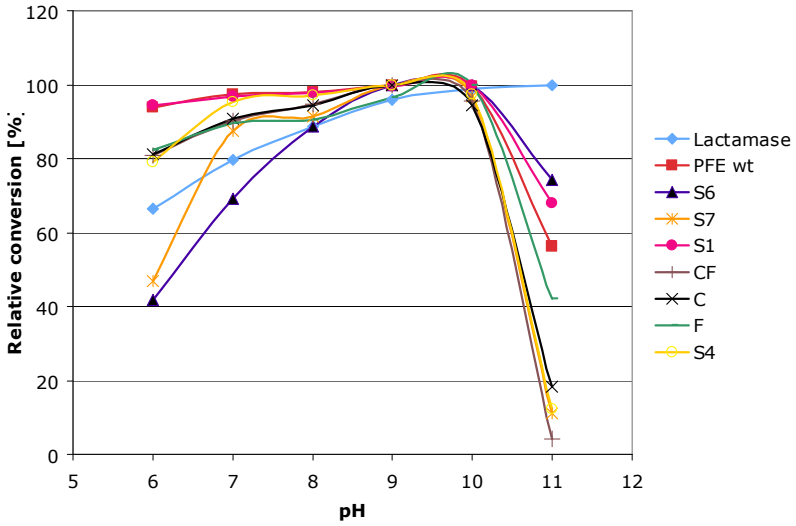

Figure 3-21: Relative conversion of **11** depending on pH

The standard buffer used for determination of enantioselectivity and specific activity had a pH of 7,5; this probably had an influence on the values for specific activity. Thus, measurements were repeated in order to confirm the high activity of the mutant CF compared to the lactamase at pH 9. However, it was impossible to reproduce the mutant's high activity at either pH 7.5 or 9. The mutant's expression was repeated to obtain fresh lyophilisate, which was then used for a new purification. While the success of this repeated purification could be monitored *via* SDS PAGE, in the biocatalysis reactions using **11** only a low activity could be found, while the lactamase, which was also purified for a second time, retained its high activity. Unfortunately the protein content of the first purification of CF was so low that almost all protein had already been used for the time course and pH profile, so that there was not enough remaining to repeat the experiments with the original solution. Protein inactivation through contaminated buffers or insufficient cooling may be ruled out as a factor, as specific activities against **1a** were determined as reference activity from both purifications; while the first purification yielded CF with a specific activity of 10 U/mg, the second yielded 13 U/mg, which may be due to a higher purity.

It is difficult to explore the amide substrate spectrum of the PFE I, as few bicyclic lactams are commercially available. The saturated form of Vince's lactam

(2-azabicyclo[2.2.1]heptan-3-one, **12**) is not available as a racemate, but only as the enantiomerically pure (1*S*, 4*R*) - lactam.

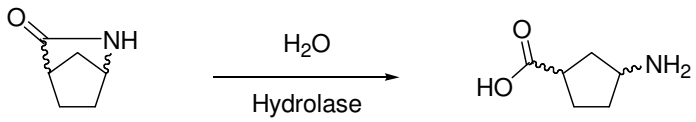

(+/-)-**12** (+/-)-**12a**

Figure 3-22: Hydrolysis of 2-azabicyclo[2.2.1]heptan-3-one (**12**) to 4-aminocyclopentane carboxylic acid (**12a**)

Unfortunately, this configuration of the unsaturated lactam is hardly converted by PFE I or lactamase, so if there is no conversion it is impossible to prove whether it is due to the lack of the double bond or due to the enzyme's stereoselectivity. If it is converted, nothing can be said about the enantioselectivity of the reaction.

Several publications describe the reduction of **11** using hydrogen and Pd/C as catalyst, however, the product is supposed to be a white solid and after three attempts at the synthesis always turned out as yellow oil. Still, NMR and GC/MS spectra confirm that saturated lactam was generated, so biocatalysis reactions were prepared and analyzed *via* thin-layer chromatography, as the HPLC analytic is not established.

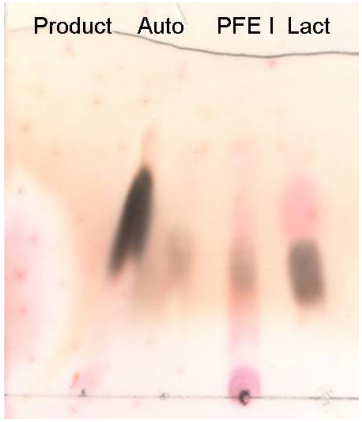

Figure 3-23: thin-layer chromatogram of biocatalysis with saturated lactam stained with ninhydrin reagent. From left to right: product standard, autohydrolysis, PFE I wt, lactamase

Unfortunately the product standard did not migrate straight, probably due to a flaw in the silica coating. Still, it can be seen that the amount of product after biocatalysis with the PFE I hardly differs from the autohydrolysis reaction, while the lactamase shows a distinct stain of the right color at approximately the same height as the product standard. Thus, it appears that the PFE I does not convert the saturated lactam well, while the γ-lactamase does.

The bicyclic structure seems to be important, as the monocyclic lactam 2-pyrrolidinone which is essentially one cycle of Vince lactam is not converted either by the PFE I nor by the lactamase. This was confirmed *via* thin-layer chromatography and staining with ninhydrin

reagent, which stains amines such as γ-aminobutyric acid, the hydrolysis product of 2-pyrrolidinone.

To determine the substrate acceptance of the lactamase, it was tested for activity against esters **1a-d** and amides **13a-c**. The results are shown in table 3-11.

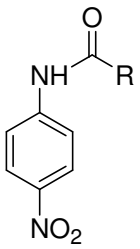

13

	Substituent R	Name (- *p*-nitro-anilide)	Abbreviation
a		Butyric	BpNA
b	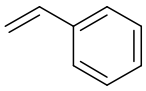	Cinnamic	CpNA
c	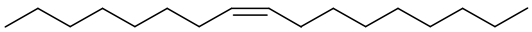	Oleic	OpNA

Figure 3-24: Chromogenic amide substrates

Table 3-11: Specific activity of purified g-lactamase against chromogenic standard esters and amides

Substrate	Specific activity [mU/mg]
1a	446.1
1b	1.1
1c	0.2
1d	-
13a	-
13b	-
13c	-

Like the PFE I and esterases in general, the γ-lactamase prefers short-chain esters. However, its activity against **1a** is very low compared to the PFE I wild type (approximately 200 fold lower), and its activity against **1b** and **1c** are both very low and surprisingly similar. When the chain-length selectivity of the PFE I was determined, it was found that it is more active against **1b** than against **1a**, while **1c** is converted slowly. It can thus be said that the "cut-off" of different chain-lengths is lower in the lactamase. Neither **1d** nor any of the amides **13a-c** were converted by the lactamase. In the cases of **13b** and **13c** this is not surprising, as the reactions with the esters suggest that substrates with large sidechains are not accepted, however, **13a** and **1b** share the same substituent, and the lactamase is efficient at hydrolyzing amides, so it could be expected that the lactamase is able to hydrolyze **13a**.

3.4. Biogenic amides

Furthermore, possibilities for the synthesis of biogenic amides were researched. In his diploma thesis, Gunnar Schmidt tested a wide range of commercially available enzymes for hydrolytic activity against **14a-c**, as well as several enzymes commonly used in our

laboratory; he also established analytics for these substrates [103, 104]. As the avenanthramides (**15a-b, 16a**) were added to the project at a later point in time, analytics needed to be established and enzymes had to be identified with activity against avenanthramides.

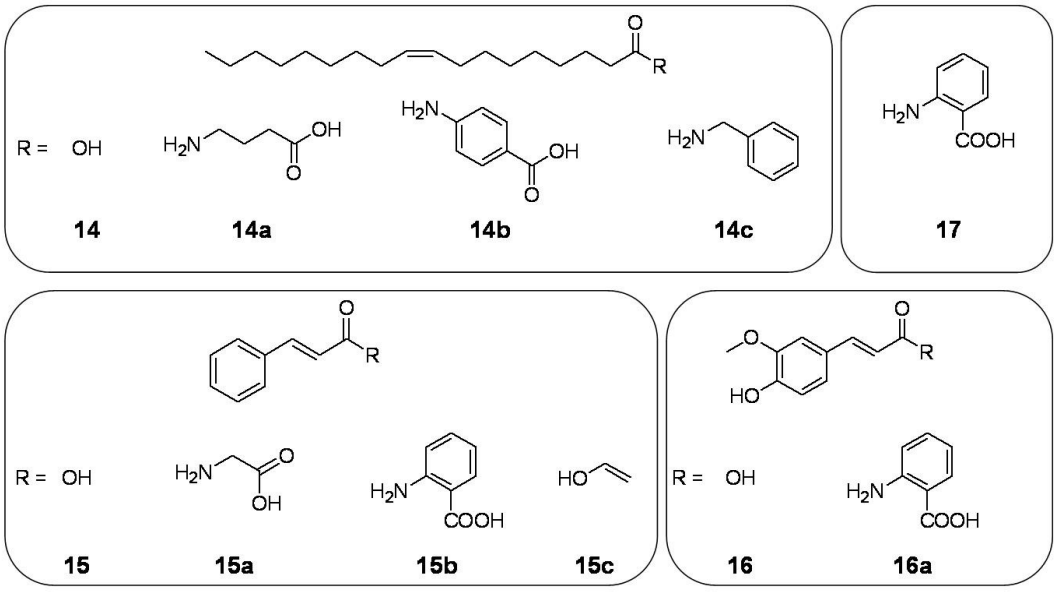

Figure 3-25: Biogenic amides and the corresponding acids supplied by Dr. Rieks Healthcare, **14** oleic acid **14a** oleic acid γ-aminobutyric acid amide **14b** oleic acid *p*-aminobenzoic acid amide **14c** oleic acid benzylamide 15 cinnamic acid **15a** cinnamic acid glycin amide **15b** cinnamic acid anthranilic acid amide **15c** vinyl cinnamate **16** ferulic acid **16a** ferulic acid anthranilic acid amide **17** anthranilic acid

Most enzymes did not convert the oleic acid amides at all, among the more promising candidates was the *Bacillus subtilis* esterase BS2 (4% conversion in the hydrolysis of **14b** after 65,5h [103]), however, the amidase activity of the BS2 is approximately 10 000 fold lower than its esterase activity [61]. In order to find a mutant with enhanced amidase activity, a 20 MTP BS2 CASTing library randomizing positions 188, 190, and 193 (all pointing toward the active site) which had been constructed by Sebastian Bartsch of our working group was screened using as substrate **13a**. The assay plates were incubated at 37°C for 20 hours and then measured at 410 nm.

During the screening a problem emerged: In other experiments, slight differences in expression or cell lysis did not have a large influence on the results, as the relation between the activities against different substrates was determined. Now, absolute values for activity were needed, and it became obvious, that the standard cell lysis technique used in the laboratory did not lyse the wells evenly enough. Attempts were made to optimize the conditions, using fresh lysozyme and DNase, higher concentrations of these enzymes, varying incubation times and temperatures, and using deep-well MTPs to increase the

volume, but an even cell lysis could not be achieved. In the end the BugBuster™ kit from Novagen was used as it yielded very uniform results (see Figure 3-26).

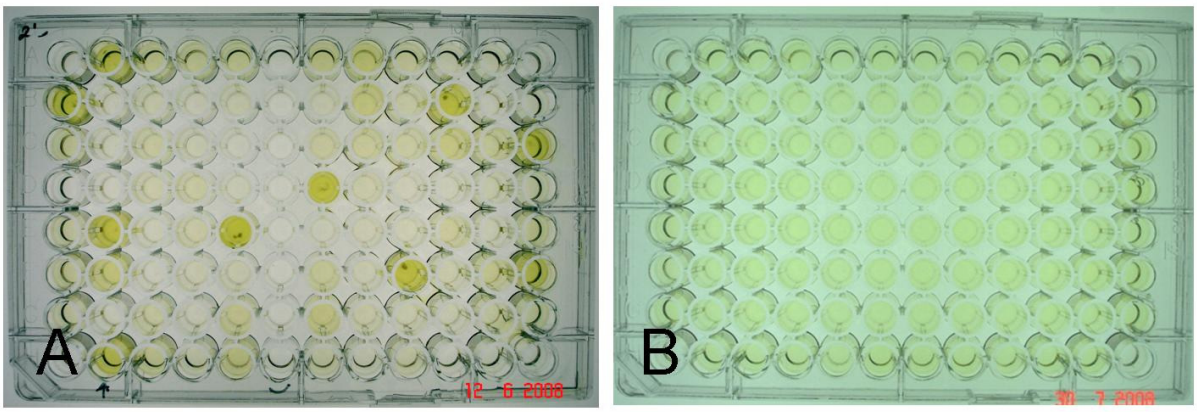

Figure 3-26: Microtiter plates used for the assay with **13a**, all plates contain the BS2 wild type A) Cell lysis *via* freeze/thaw cycle and lysozyme B) Cell lysis using BugBuster™

All clones which displayed a slightly higher activity than the wild type were gathered in a new master plate and measured again, but no clone displayed an activity higher than the wild type plus the standard deviation of 7.4% which was determined using BugBuster™ on a wild type MTP. While some mechanisms involved in amide hydrolysis in the BS2 have been researched, no mutant was found with overall increased amidase activity [61].

A metagenome library of approximately 2000 clones from the group of Prof. Streit was also screened for amidase activity. The DNA was extracted from biofilms in fresh water tubes [105]. The library was expressed at 37°C according to the procedure described in materials and methods, but using 0,1 µM IPTG (final concentration) as inducer. Pellets were lysed using the BugBuster™ kit and 40 µl of lysate was used for the colorimetric assay. As substrates, standard amidase substrates **13a-c** were used, plates were read after 24 hours of incubation at 37°C. Unfortunately no clone was found with activity higher than the background; however, it is possible that the expression and/or assay temperature was too high for proteins derived from a biofilm from fresh water tubes.

3.4.1. Avenanthramides

In order to characterize enzymatic activity against avenanthramides, precise analytics are needed, so an HPLC program was developed for the separation of substrates and product. The specifications can be found in the materials and methods section.

Table 3-12: Retention times of avenanthramides and their educts

Substance	Retention time [min]
15	8.95
16	6.59
17	5.60
15c	16.11
15b	12.84
16a	9.29

If one wants to screen many enzymes or enzyme variants, a fast and easy screening or selection system is needed. UV/VIS spectra were recorded of the substrates and their components. **16a** is yellow at pH 7,5; the products of hydrolysis are colorless. To ensure that **16** and **17** do not interfere with the detection, mixtures were measured which simulate the course of a reaction, with increasing amounts of amide and decreasing amounts of **16** and **17**. The spectra were recorded using standard phosphate buffer and 20% DMSO as cosolvent. It is possible to monitor the reaction at 380 or 390 nm, both cuvette and microtiter plate scales were tested.

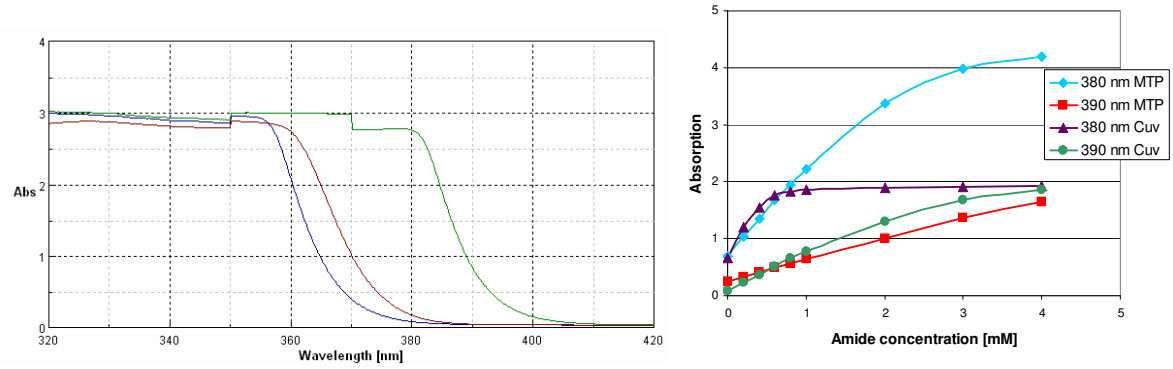

Figure 3-27: Spectra of **16** (blue), **17** (red) and **16a** (green) and standard curves for the assay at different wavelengths in microtiter plate (MTP) and cuvette (Cuv)

At 390 nm, there is a linear correlation for amide concentrations up to 4 mM both in cuvette and MTP. At 380 nm, the linear range only goes up to 1 mM, but in the microtiter plate the absorption is much better than at 390 nm, so this wavelength is more sensitive for the detection of small amounts. The big advantage is that the real substrate is used, eliminating the danger of identifying enzymes with activity towards the assay substrate which do not accept the substrate of interest.

Unfortunately, no positive control for an assay is available, so it is difficult to verify the validity of the assay. It would best be applied for the screening of a directed evolution library of a wild type enzyme with some confirmed activity against the substrate.

In literature, many examples of feruloyl esterases and chlorogenate esterases from bacteria [106, 107] and fungi [108-111] are found which can be classified into groups according to their substrate specificity [112]. In general, feruloyl esterases hydrolyze ester bonds between hydroxycinnamic acids and sugars present in plant cell walls, chlorogenate esterases are named after their activity in the cleavage of chlorogenate (an ester of caffeic acid and quinic acid). So far most have not been screened for amidase activity, but their natural substrates resemble the avenanthramide structure, and several examples of esterases or lipases with promiscuous amidase activity are known. One chlorogenate esterase from *Aspergillus japonicus* was found to be commercially available from Kikkoman (Noda, Japan); it is used to control bitterness and to prevent enzymatic browning in the preparation of juice, wine, and coffee.

Selected enzymes which are commercially available or recombinantly available in our laboratory were tested for synthetic activity, using anthranilic acid as amino component and cinnamic acid or vinyl cinnamate as acyl donor. Both strategies work with very little or no water in the system, favoring synthesis over hydrolysis but possibly compromising enzyme activity.

The first attempt at avenanthramide synthesis was carried out using tertiary amyl alcohol as solvent, 100 mM of **15** and **17**, and 20 mg/ml enzyme preparation. After six days at 40°C and 1400 rpm, samples were withdrawn and analyzed on the HPLC. Of all enzymes tested, only the CAL-B (*Candida antarctica*) showed a conversion of 16.7%. This promising result prompted another attempt using altered, hopefully better, reaction conditions, using vinyl cinnamate as acyl donor and solvent. This reaction is favored thermodynamically by the large excess of one of the substrates, shifting the equilibrium towards the products. Additionally, vinyl esters are activated acyl compounds, their reactivity favors the reaction kinetics. Vinyl ester cleavage is virtually irreversible, as tautomerization to acetaldehyde occurs spontaneously with the equilibrium strongly on the side of the aldehyde. Also, when an alcohol such as amyl alcohol is used as solvent in reactions including esterases or lipases, transesterifications with this alcohol may occur as unwanted side reactions.

The reactions were performed at 40°C and 1400 rpm using 5 mg/ml enzyme in 900 µl **15c** and 100 µl **17** (10 mg/ml in DMSO), samples were analyzed on the HPLC after 96 hours; the results are summarized in table 3-13.

Table 3-13: Biocatalysis results using **15c** as acyl donor and solvent and **17** as amino component, conversion was calculated based on decrease of anthranilic acid concentration only when a product peak was found

Enzyme (origin)	Conversion [%]	Cinnamic acid formation
Amano Ps (*Pseudomonas cepacia*)	-	+
Lipase (*Mucor miehei*)	-	+
L3 (*Candida rugosa*)	-	-
L7 (porcine pancreas)	-	+
L8 (*Thermomyces lanuginosus*)	3	+
CAL-B (*Candida antarctica*)	2.5	+
Chlorogenate esterase (*Aspergillus japonicus*)	-	-
BS2 (*Bacillus subtilis*)	-	-
PFE I (*Pseudomonas fluorescens*)	-	+
BsteE (*Bacillus stearothermophilus*)	-	+
BsubE (*Bacillus subtilis*)	-	-
SDE (*Streptomyces diastratochromogenes*)	2.7	+

Most enzymes apparently accept **15c** as substrate, however, even at low water concentrations, hydrolysis (the unwanted side reaction) is favored over amide formation. Only three enzymes showed a measurable conversion which included the decrease of anthranilic acid concentration and product formation, but also liberation of cinnamic acid. Of these three enzymes, only the *Streptomyces diastratochromogenes* esterase is recombinantly available in our laboratory. While optimization of reaction conditions may help improve the conversion, the values which were obtained so far appeared to be too low to be raised sufficiently for an efficient preparative scale process, so it was decided to search for a more suitable wild type enzyme with a higher starting activity.

3.4.2. Chlorogenate esterase from Acinetobacter bailii ADP1

If protein engineering is to be applied for the generation of an improved enzyme variant, the gene coding for the enzyme must be available and recombinant expression has to be possible. A gene cluster responsible for chlorogenate and hydroxycinnamate catabolism has been identified in *Acinetobacter bailii* ADP1, the sequences of the enzymes involved are published [113]. Genomic DNA from *Acinetobacter bailii* ADP1 was isolated using the GenomiPhi DNA amplification kit (GE Healthcare). The *hcaG* gene, which codes for a chlorogenate esterase, was then amplified using the nested PCR method, meaning that first a larger fragment of DNA is amplified using so-called outer primers. In an entire genome, it is possible that these outer primers bind at unspecific sites, amplifying unwanted regions of the bacterial chromosome. This first PCR product was then isolated using the PCR purification kit (Qiagen) and used as template in a second PCR with inner primers, which only amplify the gene of interest, as the likelihood of the inner primers binding within unspecific products

from the first round of PCR is extremely low. These inner primers also introduce mutations which generate an N-terminal NdeI restriction site (forward primer) and a C-terminal BamHI restriction site (reverse primer) which is useful for subcloning into expression vectors. The PCR product of the second round of PCR was treated with *Taq* polymerase to create poly-A overhangs, purified and cloned into the TOPO vector using the TOPO-TA® cloning kit (Invitrogen). After transformation into Top10 competent cells and a blue/white screening according to the kit's manual, colonies containing an insert (which remain white because the insert destroys the β-galactosidase gene capable of hydrolysing X-gal) were selected and subjected to colony PCR. When the correct size of the insert was verified, three plasmid samples were sequenced and the correct nucleotide sequence confirmed.

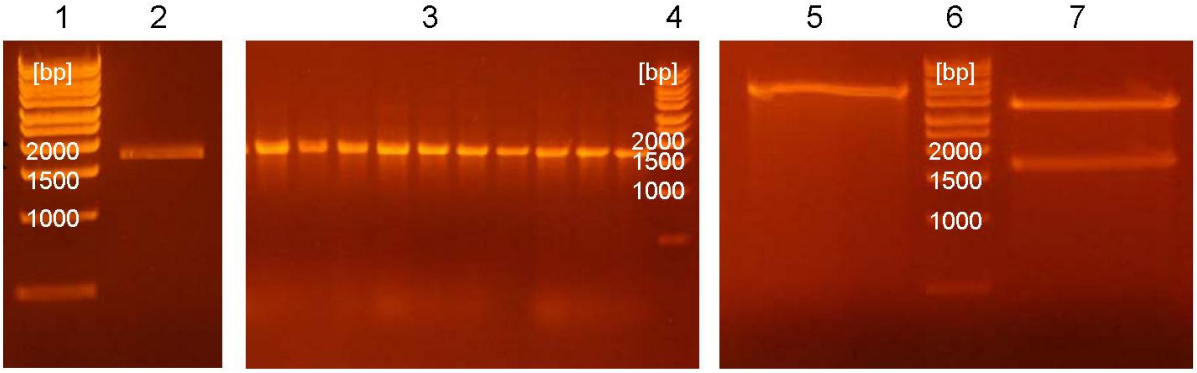

Figure 3-28: Agarose gels from various stages of the cloning, 1) 1kb ladder 2) PCR product after PCR with inner primers, 3) result of colony PCR after TOPO cloning and blue/white selection 4) 1kb ladder 5) pET15 digested with NdeI/BamHI 6) 1kb ladder 7) TOPO vector with chlorogenate esterase insert, digested with NdeI/BamHI

HcaG was described to be membrane-associated, whether it is translocated to the periplasm or remains within the inner membrane is unknown [113]. As *Acinetobacter* and *E. coli* are both gram negative, it is possible that the localization within the cells is similar. The SignalP 3.0 server [114] was used to identify possible signal peptide cleavage sites in *E. coli*. Two different calculations methods are used by the server; while the NN (neural network) predicts a cleavage site between residues 21 and 22 (SVA | ACN), the HMM (hidden Markov models) predicts the most likely cleavage site to be between residues 24 and 25 (ACN | DNN).

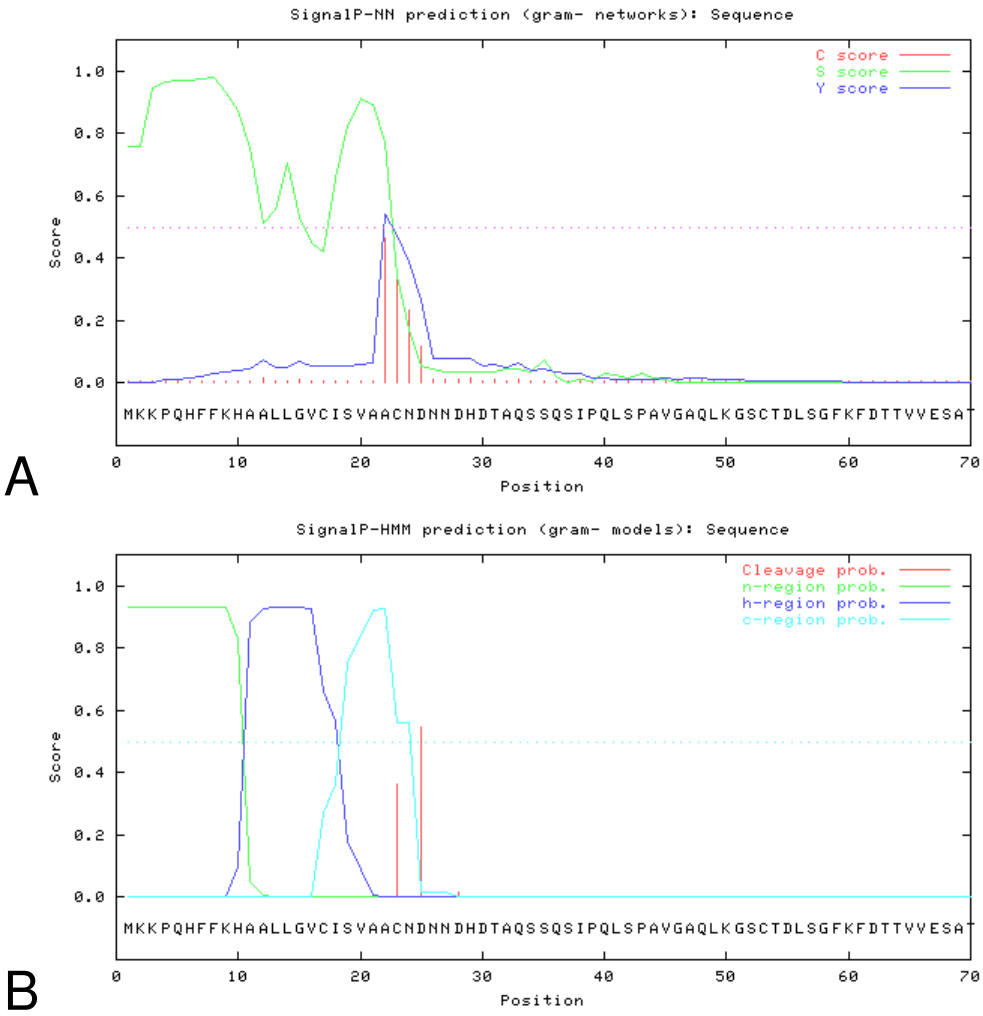

Figure 3-29: Graphical representation of SignalP results for the chlorogenate esterase (*hcaG*) sequence, A) calculation with neural network, B) calculation using hidden Markov models

Three constructs of the chlorogenate esterase were then created and cloned into two different vectors. The native sequence was cloned into pET22 to enable expression without a His-tag. Additionally, in a QuikChange reaction, the stop codon of the chlorogenate esterase was mutated, and the mutant cloned into pET22 to enable the expression with a C-terminal His-tag. A truncated version of the protein was also created using a primer which introduced an NdeI cleavage site between residues 31 and 32. After digestion with NdeI and BamHI, the smaller fragment was cloned into pET15 to yield a chlorogenate esterase mutant with an N-terminal his-tag and lacking a signal peptide which would cause the his-tag to be cleaved off. All three constructs were then transformed into *E. coli* BL21(DE3) competent cells.

Table 3-14: Overview of chlorogenate esterase constructs

Construct	Vector	His-tag	Signal peptide
pET15 CE	pET15	N-terminal	-
pET22 CE	pET22	C-terminal	+
pET22 CE stop	pET22	-	+

Expression of all three constructs was attempted at 20 °C, 30 °C and 37 °C and samples were subjected to SDS-PAGE to monitor the success of the expressions. Sample SDS-gels of expressions at 30 °C can be seen in Figure 3-30. A band of the appropriate size appears after induction; however, it is only clearly visible in the insoluble pellet fraction. This may be due to the fact that the protein is membrane-associated in *Acinetobacter bailii*, as one product of chlorogenate hydrolysis is metabolized outside the inner cell membrane (quinate), while the other remains inside the cell (caffeate) [113].

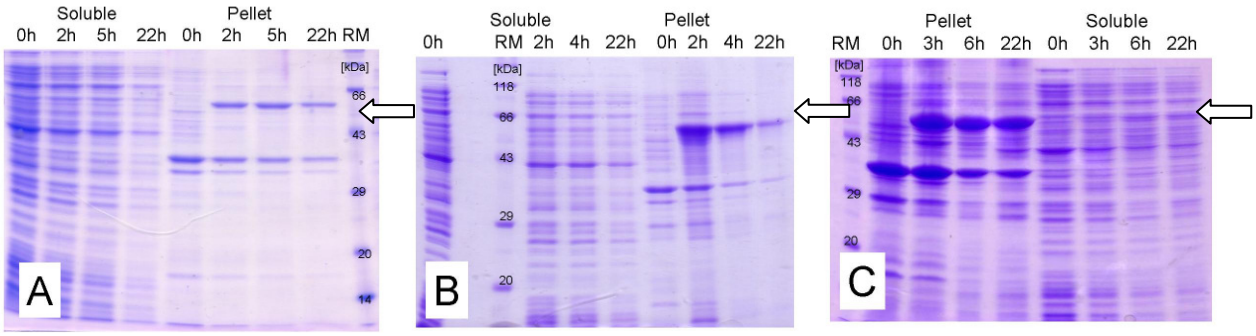

Figure 3-30: SDS-PAGE gels showing various stages of expression at 30 °C, arrows indicate the size of the expected product (64 kDa) A) pET15 CE, B) pET22 CE, C)pET22 CE stop

As the majority of recombinant protein was found in the pellet fraction, it was not separated from the soluble fraction after cell disruption and before lyophilization. The lyophilisate was then tested for activity against **16a**. The activity of the lyophilisate was so low that it was not possible to record reaction kinetics, but after a few hours the yellow biocatalysis solution was decolored, which is a qualitative confirmation of activity (*E. coli* lyophilisate without chlorogenate esterase did not decolor the solution). This hydrolytic activity was also confirmed *via* HPLC analysis of the biocatalysis. As there was a possibility of the enzyme being translocated due to the signal peptide, samples of the culture supernatant were concentrated and also used for biocatalysis, however, there was no activity.

For focused directed evolution or rational protein design of the chlorogenate esterase, a model of the structure needs to be generated. This was attempted using the Phyre server [115, 116] which compares the amino acid sequence of the unknown protein with those of solved structures and assesses the compatibility using a scoring function (“threading”), and the SWISS-MODEL server, which searches for homologous proteins (“homology modelling”) [117, 118]. Unfortunately, so far only structures of class A feruloyl esterases have been solved, and the *Acinetobacter* chlorogenate esterase has been classified as type C feruloyl esterase [112], so neither attempt to generate a homology model was successful. If properties of the chlorogenate esterase are to be improved, directed evolution may be applied (e.g. epPCR).

As the expression was difficult, but the initial activity test quite promising, work on the chlorogenate esterase from *Acinetobacter bailii* ADP1 is now continued by a diploma student

with the aim of an optimized soluble expression and a more precise characterization of the substrate spectrum.

4. Discussion

For the generation of suitable biocatalysts for various industrial applications, it is necessary to develop and characterize methods for protein engineering. While methods which rely entirely upon random mutagenesis events (such as epPCR) are very easy to employ, the library size which needs to be screened in order to find a certain mutant with 95% probability is enormous. Additionally, using the original protocols, these techniques exhibit an inherent bias influencing the position and type of the mutations which are introduced. On the other hand, knowledge-based approaches still suffer from the lack of complete understanding of enzyme mechanisms, so that important residues or synergistic effects may be overlooked due to the focus on a very small number of mutated residues. Focused directed evolution aims to combine the advantages of both methods: while randomization allows for the discovery of mutants which are challenging to predict (especially when synergistic effects occur), focusing this randomization to certain parts of the gene which are likely to influence the desired characteristic keeps the library size manageable.

OSCARR (Onepot, simple cassette randomization and recombination) was developed to suit these needs. In previous work [119], it could be proven that OSCARR allows the incorporation of the mutagenic oligo into the PCR product with high efficiency, it was also shown that the use of a spiked oligo enables the elimination of the mutational bias inherent to other mutagenesis methods such as epPCR. As it had already been demonstrated that the PCR functions, in this work, OSCARR was to be further validated through the generation of mutants with altered properties, such as modified substrate specificity or enhanced enantioselectivity, thus proving that interesting mutants can be found in a relatively small OSCARR library. In an excellent review, Morley and Kazlauskas discuss in which cases it is better to mutate residues close to the active site, and when distant mutations are as effective [35]. They present data collected from various publications and conclude, that closer mutations are often better in terms of influence on substrate selectivity, enantioselectivity, or enhanced catalytic promiscuity. Other properties such as thermostability or catalytic activity are influenced equally by mutations close to or far from the active site, so in order to modify these properties, directed evolution methods targeting the entire gene are more suitable.

The *Pseudomonas fluorescens* esterase I is a well studied enzyme which is easy to express recombinantly in *E. coli*. It displays the α/β hydrolase fold which is a widespread structural scaffold among hydrolases. In the past it could be shown that mutations close to the active site have a stronger influence on enantioselectivity than distant mutations [82], in agreement with the theory of Morley and Kazlauskas [35]. Together these features make the PFE I a suitable model enzyme.

In previous work conducted in our group, cassettes close to the active site of the PFE I were identified as target sequences for OSCARR. In this work, an 8000 clone OSCARR library based on CAS3 was constructed, cloned into *E. coli* DH5α and expressed in microtiter format. Cell lysates were used for a high-throughput screening using substrates **1a**-**d**, and mutants bearing an altered substrate specificity were found. Sequencing results showed that all of these mutants contained the mutation F126I, one mutant additionally bore the mutation G120S.

The crystal structure of the PFE I reveals the role of the mutations which were found. G120S introduces a serine capable of forming hydrogen bonds with the catalytic aspartate. In serine proteases such as thrombin, a serine in this position promotes the productive formation of the enzyme-substrate complex. This was proven by mutating the serine and measuring kinetic parameters. While k_{cat} remains largely unchanged in the mutants, K_M increases substantially [96]. The data gathered for the PFE supports the role as facilitator of substrate binding by lowering K_M, however, it was detrimental for catalytic activity as the k_{cat} was simultaneously lowered.

The major change in selectivity was caused by F126I. F126, in combination with F144, F159, and I225, forms a narrow tunnel through which substrates and products diffuse into and out of the active site of the PFE I. When the phenylalanine in position 126 is replaced by isoleucine (or leucine), the hydrophobic nature of the tunnel is preserved, but it is widened, thus facilitating the diffusion and binding of sterically more demanding substrates such as longer-chain acids.

The importance of access tunnels to the active site of hydrolases has also been found by other groups. The group of Jirí Damborsky is interested in the access tunnels of haloalkane dehalogenases, which are also α/β hydrolases. Applying focused directed evolution, they introduced bulky hydrophobic residues to the access tunnel of a haloalkane dehydrogenase from *Rhodococcus rhodochrus*, thereby increasing the activity against a non-natural substrate 32-fold, while the activity against the natural substrate 1,2-dichloroethane remained largely unchanged [120]. In this case narrowing the access tunnel led to improved activity by displacing inhibitory water molecules.

The discovery of the F126I mutant invited further studies on the influence of the size of the PFE I's bottleneck. Dr. Hidalgo pursued the idea that widening the bottleneck by mutating other bottleneck residues, and by combining these mutations, would further improve the activity against medium- and long-chain esters. Indeed, his research shows that F158L is especially active against **1c**, while the double mutant F143L/F158L is more active against **1d** than all other mutants (personal communication).

The "bottleneck" mutants were then studied with respect to their enantioselectivity towards the esters of some chiral alcohols (**2**-**5**) and acids (**6**, **7**). Like the PFE I wild type, the mutants

were not selective against the chiral acids, however, for substrates **2**-**4** mutants with enhanced selectivity were found. Even though the substrates are structurally related, different mutations are required to confer upon the PFE I selectivity against different substrates. The most obvious difference is the influence of the mutation I225L – while it eliminates selectivity against **2**, it is crucial for increased selectivity against **3**. This example shows that it is challenging to design enantioselectivity rationally, as isoleucine and leucine have similar side chains and the substrates do not differ greatly in the structure. Additionally, synergistic effects are indispensable for the selective resolution of **3**, as the corresponding single mutant (S4) alone exhibits only a moderate enantioselectivity (E=21), and the reaction progresses very slowly; this slowing effect is obviously negated by the presence of the other mutations. I225L also slows down the reaction rate against **2**, even combined with other mutations in mutant Q. While the same amount of enzyme is sufficient to reach 50% conversion after 6 hours for **3**, even after 24 hours only 12% conversion was reached for **2**. Essentially this means, that not only the enantioselectivities were altered but also the substrate selectivity.

Several other publications also focus on the importance and engineering of access tunnels [121-127]. The group of Stefan Lutz strives to improve catalytic properties of the *Candida antarctica* lipase B (CAL-B) through circular permutation [128] and incremental truncation [129]. When mutants with enhanced activity were crystallized and their structures analyzed, they found that mutant cp283 (a mutant whose N- and C-terminus correspond to the wild type's amino acids 283 and 282), which possesses a tenfold increased activity against **1b** when compared to the wild type, has a wide cleft instead of a narrow access tunnel leading to the active site. The group assumes that the enhanced activity is due to faster substrate binding and product release [129]. Guieysse *et al.* modelled the trajectories of substrate enantiomers through the access tunnel of a *Pseudomonas cepacia* lipase to the active site and found this to be the factor determining enantioselectivity in their enzyme, as docking into the active site did not yield conclusive results [100]. Bordes *et al*. describe the improvement of *Yarrowia lipolytica* lipase activity and enantioselectivity through mutations in the substrate binding site which cause changes in substrate positioning [130]. In the case of the PFE I, docking simulations were performed with substrates **2** and **3**. They show that the substrates are oriented differently in the active site of the wild type, which is why they are influenced in different ways by the same mutation. In all cases the mutant's widened bottleneck allows the phenyl moiety of the substrate to point towards the access tunnel, while only (*R*)-**2** does so in the wild type. Thus, the different positioning of substrates is certainly a factor contributing to enantioselectivity, similarly to the results described by Bordes *et al*. [130]. Residues126 and 144, which are further away from the substrate, are more likely to influence substrate and

product diffusion, which would be in agreement with the results of Stefan Lutz' group for the CAL-B [129].

Pursuing the long-standing goal of generating promiscuous amidase activity in the PFE I, a homology search was performed with the PFE I crystal structure (1VA4) as input. The DALI server returned procaryotic prolyl iminopeptidases and eukaryotic dipeptidyl peptidases as closely related enzymes with amidase activity. It was thus decided that it would be feasible to introduce amidase activity against suitable substrates designed to mimic the natural substrates of prolyl iminopeptidases or dipeptidyl peptidases by using amino acids as acyl components. The amino component was 2-naphthylamine, which forms a red dye in combination with Fast Blue RR after it is released. While it does not mimic an amino acid, the PFE I is known to accept 2-naphthyl esters and thus is able to accommodate 2-naphthylamine in its active site. As mutations close to the active site are likely to influence catalytic promiscuity, the CAS3 library which had been constructed to screen for altered chain-length selectivity was additionally screened for amidase activity with substrates **8**-**10**. Unfortunately, no mutant with activity was found. For future work it would be interesting to construct the mutant F93E as base mutant for another library, as it could be shown that in the *Bacillus subtilis* esterase BS2, a glutamate adjacent to the active site serine is implicated in promiscuous amidase activity, and replacing the glutamate with a phenylalanine drastically reduces the amide hydrolyzing capacity of the BS2 [61].

When the homology search was repeated, an additional enzyme with amidase activity was included as close structural neighbour, namely the γ-lactamase from *Microbacterium* sp. This enzyme is very active and highly selective in the hydrolysis of the Vince lactam (**11**), which is a precursor to important pharmaceuticals. As the lactamase is closely related to the PFE I, comparing their substrate spectra can yield interesting information on how to influence the PFE I's substrate spectrum. The activity against standard amide substrates such as **13a**-**c** is not detectable; the monocyclic lactam which is contained in **11** is also not hydrolyzed. The thin-layer chromatography of a biocatalysis with saturated lactam **12** suggests that activity is not dependent on the double bond, but rather on the bicyclic structure. Unfortunately, bicyclic lactams other than **11** are not available commercially from standard suppliers, so it was not possible to investigate the lactamase's substrate selectivity in more detail. Like the PFE I, the lactamase contains a phenylalanine adjacent to the catalytic serine, a residue which virtually destroyed amidase activity in the BS2 [61]. It could be interesting to investigate the mutant F97E with respect to substrate specificity.

Based on the high similarity with a lactamase, biocatalysis experiments using the PFE I and substrate **11** were conducted and analyzed using a newly developed HPLC method. All mutants which were assayed, including the wild type, displayed activity against **11**, the wild type and several mutants hydrolyse the compound with excellent stereoselectivity. The pH

profiles of PFE I variants and γ-lactamase show that the lactamase is active even at a high pH, while most PFE I variants have a broad pH optimum between pH 8 and 10. While no tested PFE I variant displays a specific activity higher than that of the lactamase, some variants come quite close. Unfortunately, when the biocatalysis experiments were repeated, the high activity of the CF mutant could not be confirmed.

Industrially, lactamases are employed for the preparation of enantiopure **11** or **11a** [86]. In other studies, lipases from *Candida antarctica* (CAL-A and CAL-B), *Pseudomonas cepacia*, *Pseudomonas fluorescens*, *Candida rugosa* as well as the porcine pancreatic lipase (PPL) were used for the kinetic resolution of **11** [131]. Examples for patented enzymatic resolutions are patents held by Chirotech ltd (now Dr. Reddy's, Slough, UK), which claim enzymes from *Rhodococcus spec*.[132] and *Comamonas acidovorans* [133]; Lonza (Basel, Switzerland) holds a patent including several proteases and lipases [134]. While Dr. Reddy's utilizes lactamases from different organisms to access both enantiomers, Lonza uses proteases such as subtilisins which hydrolyze the (+)-lactam and lipases such as the CAL-B which hydrolyze the (-)-lactam. The active sites of proteases and lipases can be described as image and mirror image [69], which is obviously a major factor influencing enantioselectivity against **11**. The PFE I might present an alternative to enzymes or enzymatic routes which have already been patented for the resolution of **11**, it is also the first esterase with confirmed activity against **11**.

Another field of study was the synthesis of biogenic amides. A broad range of commercially and recombinantly available enzymes had previously been screened for activity against **14a**-**c** in our group [103], but the results were not satisfactory. A metagenome library of approximately 2000 clones was screened for amidase activity against standard amidase substrates **13a**-**c**, but no hit was found. Additionally, a 2000 clone CASTing library of the *Bacillus subtilis* esterase BS2 was screened for enhanced amidase activity, as this enzyme was one of the more promising candidates which were brought up during the initial study. Unfortunately, no mutant featured an enhanced rate of hydrolysis against **13a**; a study from our group identified mutants with strongly decreased promiscuous amidase activity but no evidence which points towards other regions implicated in amide hydrolysis [61].

Additional biogenic amides were added to the project by the industrial partner Dr. Rieks Healthcare. For these amides, HPLC analytics could be established. Additionally, a colorimetric assay suitable for high-throughput screening was developed for substrate **16a**. Several commercially available enzymes were employed in biocatalysis reactions to attempt the synthesis of **15b**; however, most enzymes did not convert the substrates at all. If the project is continued in a future, it would be interesting to attempt the biocatalysis again under varying conditions, such as lower substrate concentration, and monitor the time course of the

reactions to rule out that the low conversions were caused by enzyme deactivation in the early stages of the reaction or by substrate or product inhibition.

For biogenic amides **15a**-**b** and **16a**, it was proposed that a chlorogenate esterase whose natural substrates are structurally very similar would be a suitable starting point, as no enzyme is known which catalyzes the synthesis of these amides directly from simple precursors without the use of ATP. The chlorogenate esterase from *Acinetobacter bailii* was cloned from genomic DNA into different pET vectors with and without N- or C-terminal His-tags. The functional expression proved to be challenging, probably due to the membrane association which is postulated for the enzyme in *Acinetobacter bailii*. However, even with the low expression which could be achieved in *E. coli* BL21, it could be shown that the esterase is hydrolytically active against **16a**. The basis for further research could be established including a high-throughput colorimetric assay and HPLC analytics, so it was decided to continue this project in a diploma thesis focusing on the optimization of the expression and the characterization of the substrate spectrum of the chlorogenate esterase.

5. Summary

The first goal of this work was to validate the OSCARR method for focused directed evolution. While it was shown before that the PCR functions well, with high incorporation rates of the mutagenic oligo, an example of a successful application was desirable. An OSCARR library of PFE I mutants was constructed and screened for altered chain-length selectivities. Mutants containing the F126I mutation were found to accept medium-chain length substrates better than the wild type; additionally, the G120S/F126I double mutant was found which introduces a catalytic tetrad which is found in several hydrolases. An epPCR library did not yield comparable results, which is not surprising since the region which was mutated in the OSCARR library has a high GC content, making it virtually impossible to mutate *via* epPCR. Thus it can be said that OSCARR affords the creation of high-quality libraries containing active mutants with altered properties.

The mutant F126I pointed towards the relevance of a so-called bottleneck for the substrate selectivity of the PFE I. A subsequent investigation on the role of the four residues forming the bottleneck revealed their influence on enantioselectivity. F126 and F144 are probably involved in controlling a substrate's diffusion into the active site, while F159 and I225 come closer to the substrate and can thus influence substrate binding. The individual influence of residues depends strongly upon the substrate. While 1-phenyl-1-propyl acetate and 1-phenyl-2-propyl acetate are structurally relatively similar, their orientation in the active site of the PFE I differs, so that mutations in bottleneck residues influence the selectivities against different substrates in different ways, e.g. in the case of 1-phenyl-1-propyl acetate, the mutation I225L is detrimental to the selectivity, while it contributes to selectivity against 1-phenyl-2-propyl acetate. This data suggests that it is challenging to design enantioselectivity rationally, as isoleucine and leucine have similar side chains and the substrates do not differ greatly in the structure. The OSCARR method uses structural data to define possible hotspots, but allows a certain degree of randomization to include mutations which would not seem likely to alter the desired property in a purely rational approach.

The OSCARR library was also screened for amidase activity. However, the substrates which were used due to the PFE I's similarity to prolyl iminopeptidases were not converted by any mutant. When the striking similarity between the PFE I and a γ-lactamase was revealed by a repeated search for structural homologues, it was found that the PFE I wild type already possesses promiscuous amidase activity. However, the substrates used in previous screenings were not suitable, and thus the activity was never found. The lactam which is converted with excellent stereoselectivity by the PFE I and its mutants is highly interesting for the pharmaceutical industry as a chiral precursor for antiviral drugs.

Additionally, possibilities for the synthesis of biogenic amides, most importantly avenanthramides, were researched. Although a preparative scale synthesis was not achieved, the basis for further research could be established through the development of a high-throughput colorimetric assay and HPLC analytics and the identification and cloning of a chlorogenate esterase from *Acinetobacter bailii* with hydrolytic activity against avenanthramides. This project is being continued in a diploma thesis in our working group.

6. Materials and Methods

6.1. Materials

6.1.1. Bacterial Strains

E. coli DH5a fhuA2 Δ(argF-lacZ)U169 phoA glnV44 Φ80 Δ(lacZ)M15 gyrA96 recA1 relA1 endA1 thi-1 hsdR17

E. coli BL21 (DE3) *E. coli B* dcm ompT hsdS($r_B^-m_B^-$) gal λDE3

6.1.2. Plasmids

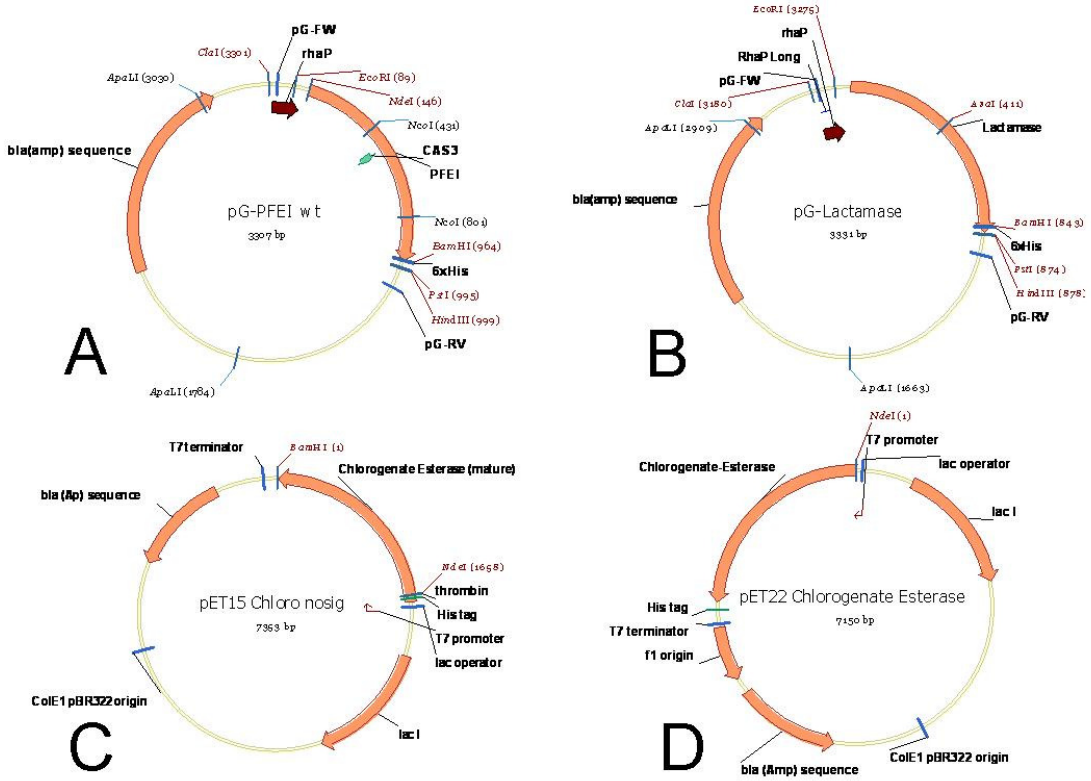

Figure 6-1: Plasmid maps of A) pG-PFE I wild type (the position of CAS3 which was mutated in order to change chain-length specificity is highlighted) B) pG-lactamase C) pET15 CE D) pET22 CE

pGaston[135] (Abbreviation: pG) was used for gene expression of the PFE I and the lactamase. It is a high-copy number plasmid harboring a rhamnose-inducible promoter (rhaP), a β-lactamase gene which confers ampicillin resistance, and a C-terminal His-tag. The lactamase from *Microbacterium spec*. as well as the *Pseudomonas fluorescens* esterase I (see Figure 6-1) were cloned into the vector using NdeI and BamHI restriction sites.

The chlorogenate esterase from *Acinetobacter bailii* ADP1 was cloned into pET15 (Novagen) without signal peptide, and into pET22 (Novagen) with signal peptide using NdeI and BamHI restriction sites. The pET vectors are low-copy number plasmids using a T7 polymerase

promoter and terminator. They require expression strains bearing the DE3 prophage, which allows expression of the T7 polymerase under control of the lac promoter. To prevent premature expression, the pET vectors contain the gene for the lac repressor (lacI). When IPTG is added as inductor, expression of the T7 polymerase is de-repressed; the polymerase may then transcribe the genes under control of the T7 promoter of the plasmid. Both pET15 and pET22 carry a β-lactamase gene for ampicillin resistance, additionally pET15 contains an N-terminal His-tag, while pET22 includes a C-terminal His-tag.

6.1.3. Chemicals and Disposables

All chemicals and disposables were purchased in their highest purity from Fluka (Buchs, Switzerland), Sigma (Steinheim) Merck (Darmstadt), VWR (Hannover), Roth (Karlsruhe) and StarLab GmbH (Ahrensburg), unless marked otherwise.

Qiagen GmbH (Hilden)	QIAquick™ Gel Extraction Kit (including PCR purification kit)
Fermentas (St. Leon-Rot)	GeneJet™ Plasmid Miniprep Kit
BD Biosciences Clontech (Heidelberg)	BD Talon™ Metal Affinity Resin
Millipore GmbH (Schwalbach)	Centricons® 30kDa
GE Healthcare (München)	GenomiPhi DNA amplification kit

6.1.4. Enzymes

Restriction enzymes and ligase were purchased from New England Biolabs GmbH (Frankfurt am Main) and Fermentas (St. Leon-Rot). DNA Polymerases were purchased from Roboklon (Berlin).

(-)-γ-Lactamase from *Aureobacterium spec*. was kindly supplied by Dr. Reddy's (Slough, UK).

6.1.5. Primers

The composition of the spiked oligo used for the generation of the OSCARR library may be found in the appendix.

Table 6-1: Sequences of primers used in this work. Primers used for generation of mutants *via* QuikChange are named after the mutation they introduce. pG-FW and pG_RV are the sequencing primers for pGaston. Lact_FW and Lact_RV were used for the amplification of the lactamase gene. rrnB_rv and RhaP_FW_long are the outer primers for the OSCARR PCR. Primers beginning with CE were used for the cloning and QuikChange modification of the chlorogenate esterase.

Primer name	**Sequence**
G120S_FW	GGCCGGCCTGGTGCTGCTGTCCGCCGTCACCCCGCTGTTC
G120S_RV	GAACAGCGGGGTGACGGCGGACAGCAGCACCAGGCCGGCC
F126L_FW	CGCCGTCACCCCGCTGTTGGGCCAGAAGCCCGAC
F126L_RV	GTCGGGCTTCTGGCCCAACAGCGGGGTGACGGCG
F126V_FW	GTCACCCCGCTGGTCGGCCAGAAGC
F126V_RV	GCTTCTGGCCGACCAGCGGGGTGAC
F144V_FW	CGATGTGTTCGCAAGGGTCAAGACTGAGCTGCT
F144V_RV	AGCAGCTCAGTCTTGACCCTTGCGAACACATCG
F144L_FW	GCTCGATGTGTTCGCAAGGCTCAAGACTGAGCTGCTGAAGG
F144L_RV	CCTTCAGCAGCTCAGTCTTGAGCCTTGCGAACACATCGAGC
F159L_FW	CGCGCAGTTCATCAGCGATTTGAACGCACCGTTCTATGGCATC
F159L_RV	GATGCCATAGAACGGTGCGTTCAAATCGCTGATGAACTGCGCG
I225L_FW	CGATGGCGACCAGCTCGTGCCGTTCGA
I225L_RV	TCGAACGGCACGAGCTGGTCGCCATCG
I225F_FW	CATGGCGATGGCGACCAGTTCGTGCCGTTCGAGACCACC
I225F_RV	GGTGGTCTCGAACGGCACGAACTGGTCGCCATCGCCATG
pG_FW	CTTTCCCTGGTTGCCAATGG
pG_RV	GCTTCTGCGTTCTGATTTAATC
Lact_FW	AAAAAAAAAACATATGGGTTACATCACCGTCGG
Lact_RV	AAAAAAAAAAGGATCCCTTCGCGAGGAAGGTCTTCAG
rrnB_rv	CCGCCAGGCAAATTCTGT
RhaP_fw_long	GCAAATTGTGAACATCATCACGTTCATCTTTCCCTGGTTGCCAATGGCCC
CE_Outer_FW	CATGGTCTTGGCACATGCATAAATTCA
CE_Outer_RV	AGCTAAAACAAAAAGAGAGCGATTAGTCG
CE_Inner_FW_Nde	CATATGAAAAAACCTCAACATTT
CE_Inner_RV_Bam	GGATCCTTATTTACAAGTGAAATTCTCG
CE_signal	CAATAACGATCATCATATGGCACAGTCGAG
CE_QC_stop_FW	CGGAGCTCGAATTCGGATCCTTGTTTACAAGTGAAAT
CE_QC_stop_RV	ATTTCACTTGTAAACAAGGATCCGAATTCGAGCTCCG

6.1.6. Laboratory Equipment

Autoclave	V-120, Systec (Wettenberg)
Incubators	Friocell and Incucell, MMM Medcenter-Einrichtungen GmbH (Gräfelfing)
	Unitron, Infors AG (Bottmingen, Switzerland)
DNA electrophoresis	Sub-Cell ® and Mini Sub-Cell GT, BioRad (München)
Fine balances	R180D and AC120S, Sartorius (Göttingen)
Gas chromatography	GC-14A Gaschromatograph, Shimadzu (Duisburg)
	GC 2010 Gaschromatograph, Shimadzu (Duisburg)
	GC 2010 coupled with QP 2010 mass spectrometer, Shimadzu (Duisburg)
HPLC	LaChrom Elite, Hitachi (Tokyo)
Fluorimeter	Fluostar Galaxy and Fluostar Optima, BMG (Offenburg)
Lyophilizer	Alpha 1-2, Christ (Osterode am Harz)
PCR machines	Progene and Touchgene Gradient, Techne (Cambridge, UK)
pH Meter	Microprocessor HI 9321, Hanna Instruments (Kehl am Rhein)
SDS-PAGE	Minigel-Twin, Biometra GmbH (Göttingen)
Clean Bench	HeraSafe KS15, Thermo Electron (Langenselbold)
Thermomixer	Thermomixer comfort, Eppendorf (Hamburg)
Ultrasound device	Sonoplus HD 2070 and UW 2070, Bandelin (Berlin)
UV-VIS spectrophotometer	UV mini 1240, Shimadzu (Duisburg)
Vortex mixer	Vortex-Genie ® 2, Scientific Industries (Bohemia, NY, USA)
Centrifuges	Multifuge 3 S-R, Labofuge 400R, Biofuge fresco and Biofuge pico, Heraeus (Hanau)
Colony Picker	BioPick, Biorobotics (Cambridge, UK)
Pipetting Robot	Miniprep 75, Tecan (Crailsheim)

6.1.7. Computer Programs and Databases

Visualization of protein structures	PyMol (www.pymol.org/)
Substrate Docking	YASARA (www.yasara.org/)
Handling of nucleotide sequences	VectorNTI (Invitrogen)
Drawing of chemical structures	ChemDraw (CambridgeSoft)
Homology searches	BLAST (http://www.ncbi.nlm.nih.gov/BLAST/)
	DALI (http://ekhidna.biocenter.helsinki.fi/dali_server/)
Identification of signal peptides	SignalP (http://www.cbs.dtu.dk/services/SignalP/)

Creation of homology models	Phyre (http://www.sbg.bio.ic.ac.uk/phyre/html/help.html)
	SWISS-MODEL (http://swissmodel.expasy.org/)
Comparison of superfamilies	3DM (http://fungen.wur.nl/sfamlist.php)

6.1.8. Cultivation Media, Buffers and Solutions

For all buffers the pH is adjusted through the addition of NaOH or HCl, then the volume is adjusted to 1 l, unless noted otherwise

Sodium phosphate buffer 50 mM (standard)

14.50 g Na_2HPO_4 x 12 H_2O
1.31 g NaH_2PO_4 x H_2O
pH 7.5

Assay buffer for pNPC and pNPL

14.50 g Na_2HPO_4 x 12 H_2O
1.31 g NaH_2PO_4 x H_2O
1% (v/v) Triton X-102
pH 7.5

Washing buffer for IMAC

10.14 g Na_2HPO_4 x 12 H_2O
3.00 g NaH_2PO_4 x H_2O
17.4 g NaCl
pH 7.0

Elution buffer for IMAC

10.14 g Na_2HPO_4 x 12 H_2O
3.00 g NaH_2PO_4 x H_2O
17.4 g NaCl
20.42 g Imidazol
pH 7.0

MES buffer for IMAC

20 mM 2-(N-Morpholino)-ethanesulfonic acid
100 mM NaCl
pH 5.0

Lysis buffer

17.91 g Na_2HPO_4 x 12 H_2O
17.4 g NaCl
pH 8.0

DNase stock solution (1000x)

1 mg/ml DNase in 60 % Glycerol

Bradford reagent (5x)

0.1 g Coomassie-Brilliant-Blue G 250
50 ml 50% Ethanol
100 ml 85% Phosphoric acid
250 ml H_2O

Ninhydrin staining solution

1.5 g Ninhydrin
97 ml n-butanol
3 ml acetic acid

Cultivation Media and Additives

LB (Lysogeny Broth) Medium

10 g NaCl
10 g Tryptone
5 g Yeast extract
15 g Agar agar (only for preparation of Petri dishes)
autoclave

SOB Medium

2% (w/v) Trypton
0.5% (w/v) Yeast extract
0.05% (w/v) NaCl
1% (v/v) 250 mM KCl-solution
pH 7.0; autoclave
add 0.5% (v/v) sterile 2 M $MgCl_2$-solution

10x SOC Medium

0.2 % (w/v) KCl

2 % (w/v) $MgCl_2$

2 % (w/v) $MgSO_4$

4 % (w/v) Glucose

Ampicillin stock solution

100 mg/ml Ampicillin in H_2O dest.

Rhamnose solution for induction

20% (w/v) rhamnose in H_2O dest., sterile (stock solution)

0.2% (w/v) final concentratin for induction

IPTG solution for induction

0.1 M in H_2O dest., sterile (stock solution)

0.1 mM final concentration for induction

Buffers for the preparation of chemocompetent cells

RF1

100 mM RbCl

30 mM CH_3COOK

10 mM $CaCl_2$

50 mM $MnCl_2$

15% (v/v) Glycerol

pH 5.8 (adjust with acetic acid), sterile filtered

RF2

10 mM RbCl

10 mM 3-(N-Morpholino)-propansulfonic acid

75 mM $CaCl_2$

15% (v/v) Glycerol

pH 6.9, sterile filtered

Buffers for pH profiles (50 ml volume)

Sodium phosphate buffer pH 6 50 mM

0.345 g NaH_2PO_4 x H_2O

Sodium phosphate buffer pH 7 50 mM

0.207 g NaH_2PO_4 x H_2O

0.358 g Na_2HPO_4 x 12 H_2O

Tris/HCl buffer pH 8 50 mM

0.303 g Tris

Glycin buffer pH 9-11 50 mM

0.188 g Glycin

Buffers for SDS-PAGE

4x Upper Tris

0.5 M Tris-HCl

0.4 % (w/v) SDS

pH 6.8

4x Lower Tris

1.5 M Tris-HCl

0.4 % (w/v) SDS

pH 8

APS stock solution

10 % (w/v) Ammoniapersulfate in H_2O dest.

Sample buffer

20 % (v/v) Glycerol

6 % (w/v) 2-Mercaptoethanol

0.0025 % (w/v) Bromophenol blue

Dissolved in 1x Upper Tris

10x Running buffer

30.3 g Tris
144 g Glycin
10 g SDS
pH 8.4

Protein Marker

RotiMark ® Standard from Roth (Karlsruhe)

Coomassie staining solution

0.1 % (w/v) Coomassie brilliant blue
30 % (v/v) Ethanol
10 % (v/v) Glacial acetic acid

Destaining solution

30 % (v/v) Ethanol
10 % (v/v) Glacial acetic acid

Agarose gel electrophoresis buffers

50x TAE buffer

242 g Tris
57.1 ml Acetic acid
50 mM EDTA
pH 8

Loading buffer

10x TAE buffer
0.25 % (w/v) Bromophenol blue
30 % (v/v) Glycerol

DNA Marker

1 kb DNA-ladder from Roth (Karlsruhe)

6.2. Methods

6.2.1. Microbiological Methods

Storage of strains and overnight cultures

For long-term storage, overnight cultures are mixed with sterile glycerol up to a final glycerol concentration of 30%. These glycerol stocks are kept at -80°C.

For temporary storage and for frequently used mutants, LB agar plates containing the appropriate antibiotic are inoculated. These plates are kept at 4°C for four to six weeks before fresh plates are prepared.

For the preparation of overnight cultures, 3-5 ml of appropriate medium are inoculated with a single colony from an agar plate or with 1 µl of glycerol stock, followed by incubation at 37°C for 15-18 hours.

Preparation of chemocompetent cells

Chemocompetent cells are prepared according to the RbCl method. 50 ml of SOB medium are inoculated using an overnight culture of the desired strain and incubated at 37°C until an OD_{600} of 0.3-0.5 is reached. The cells are then incubated on ice for 15 min and centrifuged (25 min, 3500 g, 4°C). The cell pellet is resuspended in 8 ml RF1 buffer, incubated on ice for 15 min and centrifuged again (25 min, 3500 g, 4°C). The cell pellet is then resuspended in 2 ml RF2 buffer, incubated on ice for 15 min. Aliquots of 50 µl were shock-frozen on dry ice and stored at -80°C.

Transformation

An aliquot of competent cells is thawed on ice. The DNA sample is carefully added to the surface, mixing is achieved by tapping the reaction vessel with a finger. After 30 min of incubation on ice, the cells are submitted to a heat shock of 30 s at 42°C, followed by 5 min of incubation on ice. Then, 250 µl of LB-SOC are added and the cells are incubated at 37°C for one hour. Subsequently, 150 µl are plated out on LB Agar plates containing the appropriate antibiotics; the plates are incubated at 37°C over night.

Protein Expression

Protein expression is carried out in *E. coli* DH5α using the plasmid pGaston or in *E. coli* BL21 (DE3) using pET vectors. The culture medium is supplemented with ampicillin and inoculated 1:100 with an overnight culture of the desired mutant. Cells are grown at 37°C up to an OD of 0.5; at this point the inductor rhamnose is added up to a final concentration of 0,2 % (for pGaston) or IPTG is added up to a final concentration of 0,1 mM (pET vectors). The cultivation is then continued at the desired temperature, the cells are harvested 20 hours

after induction by centrifugation at 4000 g, the pellet is washed with phosphate buffer and centrifuged again at 4000 g.
To monitor the success of the expression, 5 ml/OD samples are taken which are later analyzed *via* SDS-PAGE.

Cell disruption

The pellet is resuspended in ice cold phosphate buffer and subjected to 10 min sonication at 50% pulse and 50% power. After a centrifugation step (15 min 4000 g), the supernatant is transferred to a Petri dish, placed at -80°C for 1 hour and subsequently lyophilized over night. The lyophilisate is stored at 4°C.

Sample preparation for SDS-PAGE

The pellet from the 5 ml/OD samples is washed with phosphate buffer, centrifuged and then resuspended in 300 µl phosphate buffer. After 30 s of sonication at 50% pulse and 50% power, cell debris is pelleted by centrifugation at 855 g. The pellet is discarded and the supernatant is centrifuged at 4000 g to pellet the unsoluble protein fraction (inclusion bodies). After this step the supernatant can be used for the SDS-PAGE, it contains the soluble protein fraction. The pellet is incubated with phosphate buffer containing 1% Triton X-100 for 10 min at room temperature, then centrifuged and washed twice with phosphate buffer. It is then resuspended in 100 µl of phosphate buffer. This fraction is also applied to the SDS-PAGE, it contains the unsoluble proteins.

Creation of microtiter master plates

The wells of sterile 96-well microtiter plates are filled with 150 µl of LB/Amp medium. Colonies are transferred from agar plates into wells using sterile toothpicks or using the colony picking robot. The four corner wells are left empty to serve as blanks or to allow growing a standard in the expression plate. The plates are incubated at 37°C over night, 60 µl of 60% (v/v) sterile glycerol is added to each well and plates are stored at -80°C.

Protein expression in microtiter plates

To facilitate uniform expression in all wells, the steady-state method is used for protein expression in microtiter plates. The wells of sterile 96-well microtiter plates are filled with 200 µl of LB/Amp medium; they are then inoculated from a master plate using a 96-needle replicator. The plates are then incubated at 37°C for 20 h, after which all wells have reached the stationary phase and thus virtually the same cell density. The wells of a fresh microtiter plate are then filled with 150 µl of LB/Amp medium and 50 µl of overnight culture is added to each well. Protein expression is induced by addition of sterile rhamnose solution (final

concentration 0,2 % (w/v)) after two hours, cells are harvested four hours after induction by centrifugation at 3000 g for 30 min. The supernatant is removed and the plates may be stored at -80°C until used for cell disruption.

Cell disruption in microtiter plates

BugBuster reagent (Novagen) is diluted 1:100 with lysis buffer, DNase stock solution is added and 100 µl are dispensed into the wells of the microtiter plate containing the cell pellets. The plate is then incubated at 30°C for one hour and centrifuged at 3000 g for 30 min. The supernatant can then be used for assays.

Agarose overlay assay

The library master microtiter plates are thawed in the fridge. Large LB/Amp/Rha agar plates are then inoculated using a sterile 96-needle replicator. Three replica plates are created from each master plate, and a positive and negative control are applied to each plate (*E. coli* DH5α containing pGASTON with BS2 and PFE I as inserts). The colonies are then allowed to grow at room temperature for approximately 20 hours. For the overlay agarose assay, 0.5% agarose in water is molten and thermostatized at 42°C. To 10 ml of agarose, 150 µl of DMSO containing 8.9 mg Fast Blue RR is added in addition to one of the three substrates (see below).

Table 6-2: Amounts of substrates used for the agarose overlay assay

Substrate	Amount [mg]	Solvent
N-Acetyl-aminonaphthalene	3.2	80 µl DMF
L- Proline-β-aminonaphthalene	3.7	80 µl DMSO
D-Alanine-β-aminonaphthalene	4.1	160 µl DMSO

After overlaying plates with agarose, they are read after approximately 30 minutes. Staining is regarded successful, if the negative control (PFE I wild-type) remains unstained and the positive control (BS2 wild-type) is stained red. Mutant colonies which are stained are noted as possible positive clones.

6.2.2. Molecular Biology Methods

Plasmid isolation

An overnight culture of bacteria harbouring the desired plasmid is centrifuged to pellet the cells. The DNA is then extracted according to the instructions of the GeneJet™ Plasmid Miniprep Kit (Fermentas).

Digestion with NdeI/BamHI

The following is added to a sterile PCR tube:

10 µl DNA (Plasmid or purified PCR fragment)

76 µl sterile H_2O

10 µl Fast Digest buffer

2 µl Fast Digest BamHI

2 µl Fast Digest NdeI

The digestion is carried out at 37°C for one hour, then the enzymes are inactivated at 80°C for 10 min.

Ligation

The following is added to a sterile PCR tube:

11.5 µl insert

1 µl vector

Depending on the concentration the molar ratio should be about 3:1. For the contruction of a mutant library, a molar ratio of 1:1 is used. The tube is then heated to 70°C for 10 min to facilitate the annealing of sticky ends. After the tube has reached room temperature again, the following is added:

1.5 µl T4 ligation buffer

1 µl T4 ligase

The reaction mix is then incubated at 16°C for 16 h in a thermocycler, followed by a 10 min cycle at 70°C to inactivate the ligase.

Standard PCR

The standard PCR is used to amplify specific fragments of DNA. The reagents listed in table 6-3 are pipetted into a sterile PCR tube and placed in a thermocycler, the temperature program is detailed in table 6-4.

Table 6-3: Composition of a standard PCR

Reagent	**Volume [µl]**
H_2O sterile	40.5
Buffer B (10x)	5
dNTP Mix	1
Primer Forward (50 pmol/µl)	1
Primer Reverse (50 pmol/µl)	1
Template (10 ng/µl)	1
Pfu+ Polymerase (5 U/µl)	0.5

Table 6-4: Temperature program of a standard PCR

Number of cycles	Segment	Time	Temperature [°C]
1	1	5 min	95
30	1	30 s	95
	2	30 s	53
	3	1 min/kb	72
1	1	10 min	72
1	1	∞	4

Megaprimer PCR (OSCARR)

The OSCARR (Onepot, simple cassette randomization and recombination) method[38] was used to generate a library of PFE I mutants. The composition of the reaction is listed in table 6-5, the temperature program is detailed in table 6-6.

Table 6-5: Composition of the OSCARR reaction

Reagent	Volume [µl]
H_2O sterile	86
Buffer B (10x)	10
dNTP Mix	1
Spiked Oligo Cassette 3 (50 pmol/µl)	0.5
rrnB_reverse (50 pmol/µl)	1
pG-PFE I (1 ng/µl)	1
Pfu+ Polymerase (5 U/µl)	0.5
After first pause in program:	
dNTP Mix	1
Pfu+ Polymerase (5 U/µl)	0.5
After second pause in program:	
RhaP_fw_long	1

Table 6-6: Temperature program of the OSCARR reaction

Number of cycles	Segment	Time	Temperature [°C]
1	1	3 min	95
30	1	45 s	95
	2	1 min	53
	3	45 s	72
1	1	10 min	72
1	1	∞	4
Pause	**Addition of dNTPs and polymerase**		
5	1	45 s	95
	2	1 min 15 s	72
1	1	∞	4
Pause	**Addition of forward primer**		
25	1	45 s	95
	2	1 min	66
	3	1 min 15 s	72
1	1	10 min	72
1	1	∞	4

QuikChange™ site directed mutagenesis

With the QuikChange ™ site directed mutagenesis strategy (Stratagene, La Jolla, USA) it is possible to introduce specific mutations at defined positions within a gene. The reactions were performed according to the manufacturer's instructions.

Agarose gel electrophoresis

Agarose gel electrophoresis is used for the separation of DNA fragments by their size. When a current is applied, the negatively charged DNA fragments migrate towards the anode. Large fragments are retarded by the gel more than small fragments are, leading to the separation. The ethidium bromide intercalates with the DNA, making it visible on a UV table.
0.8 % (w/v) agarose gels are used with 0.1 % (v/v) ethidium bromide solution. DNA samples are mixed with sample buffer prior to loading. A voltage of 80 V is applied and the electrophoresis is run until the bromophenol blue of the sample buffer has almost migrated through the gel (usually 30 min). The gel is then placed on a UV table and photographed.

DNA gel extraction

The desired band is cut out of the gel using a sharp scalpel as fast as possible, as the UV light which is necessary for visualization can damage the DNA. The extraction was performed using the QIAquick Gel Extraction Kit (Qiagen, Hilden) according to the manufacturer's instructions.

6.2.3. Biochemical and Chemical Methods

Immobilized Metal Ion Affinity Chromatography using BD Talon™ Metal Affinity Resin

Proteins containing a C- or N-terminal Polyhistidine tag can be purified *via* IMAC as the imidazol rings of the His-tag can bind to nickel or cobalt ions. In theory, this allows a one-step purification of a recombinant protein from crude extract. The purification was carried out according to the resin manufacturer's instructions; elution was achieved with imidazol-containing elution buffer. After elution, the protein is concentrated using centrifugal concentration devices (centrikon) with a cutoff of 30 kDa. After centrifugation at 4000 g for 30 min, ice-cold standard phosphate buffer is added to the concentrate and the centricon is again centrifuged for 30 min at 4000 g. This step is repeated. Now the concentrated protein is removed from the centrikon. If the desired reactions are not carried out on the same day, glycerol is added up to a final concentration of about 40% and the protein solution is stored at -20°C.

SDS-Polyacrylamide Gel Electrophoresis (SDS-PAGE)

SDS-PAGE is used to separate proteins according to their size. Prior to running the gel, the proteins are mixed with sample buffer containing denaturing agents and denatured at 95 %. The SDS contained in the gel masks the protein's own charge, so that all proteins migrate towards the anode. The pores of the gel retard larger proteins more than they do smaller proteins, leading to a separation.

The composition of stacking gel and separation gel are listed in table 6-7. While the samples migrate through the stacking gel, a current of 13 mA is applied. Once the samples have passed into the separation gel, the current is increased to 25 mA per gel. The electrophoresis is ended when the bromophenol blue from the sample buffer diffuses out of the gel. The protein bands are visualized through staining with Coomassie solution (approx. 1 hour) followed by destaining (approx. 3 hours).

Table 6-7: Pipetting scheme for SDS-PAGE, volumes are for one gel

Solution	Stacking gel (4 %)	Separation gel (12,5 %)
4x Upper Tris	1 ml	
4x Lower Trix		2 ml
30% Acrylamide solution	0,52 ml	3,33 ml
H_2O dist.	2,47 ml	2,67 ml
APS stock solution	40 µl	40 µl
TEMED (N, N, N', N'-Tetramethylethylendiamine)	4 µl	4 µl

Colorimetric assay ("pNPA-Assay") in microtiter plates

All pipetting steps may be performed by the pipetting robot. For measuring activity against **1a**, **1b**, and **13a**, 160 µl of standard phosphate buffer are pipettet into each well of a microtiter plate. The supernatant from cell disruption is diluted 1:10, and 20 µl of this dilution is added to the wells. 20 µl of substrate (10 mM in DMSO) is added, and the measurement is begun immediately (the addition of substrate may be performed by the pipetting robot or by the fluorimeter's internal pump). For **1c**, **1d**, **13b** and **13c**, the appropriate assay buffer containing Triton X-102 is used, the supernatant is not diluted prior to use and the concentration of substrate is only 5 mM. In all cases, the kinetic is measured over ten minutes at a wavelength of 410 nm. Blank wells are included on each plate so the autohydrolysis can be subtracted from the mutant activities.

Colorimetric assay ("pNPA-Assay") in cuvettes

Clones with altered chain-length selectivity which were found in the MTP assay are expressed in 100 ml scale, and either crude lyophilisate or purified protein is used for a cuvette activity assay. Prior to the measurements, the buffer factor is calculated by recording a standard curve for p-nitrophenol; the inverse of the slope is the buffer factor. Effectively, this mirrors the extinction coefficient of pNP in the buffer, as even slight changes in pH affect the color intensity.

800 µl of appropriate buffer is dispensed into the cuvettes. 100 µl of enzyme solution is added and the cuvette is placed into the spectrophotometer. 100 µl of substrate (**1a**, **1b** and **13a**: 10 mM in DMSO; **1c**, **1d**, **13b** and **13c**: 5 mM in DMSO) is then added to start the reaction, the ingredients are mixed by pipetting and the measurement is started immediately. The OD_{410} is monitored for one minute.

Determination of protein content using the Bradford method [136]

The Bradford assay is used for the determination of a sample's protein content. 5x Bradford reagent is diluted 1:5 with water and filtered. 300 µl of this solution is pipetted into the wells of a microtiter plate. 15 µl of protein samples are then added to a well, each sample is applied to three wells. Each microtiter plate contains a blank with phosphate buffer and BSA standards of defined concentrations. The absorption is measured at 600 nm, and protein concentrations are calculated with the help of the standard curve.

Biocatalysis with 2-Azabicyclo[2.2.1]hept-5-en-3-one (**11**)

Biocatalysis reactions are carried out in 10 mM of the appropriate buffer using 8 µmol of **11** per ml. Internal standard (*p*-Aminobenzoic acid) is added up to a final concentration of 50 µg/ml. Enzyme is added in form of crude lyophilisate or as purified enzyme in 30% glycerol.

The first sample is taken immediately and stored at -20°C until analyzed *via* HPLC, further samples are taken as indicated in the results section.

Biocatalysis with substrates **2-7**

1 mg of crude lyophilisate is dissolved in 1 ml phosphate buffer (50 mM, pH 7.5) and the reaction is started by the addition of 5 µl of substrate. The reaction proceeds at 37°C and 1300 rpm. 200 µl samples are taken after 4, 6, and 24 h, extracted twice with CH_2Cl_2 and dried over anhydrous Na_2SO_4.

Derivatization with TMS-Diazomethane

Samples of substrates **6** and **7** are derivatized with TMS-diazomethane (20 µL) and methanol (50 µL). After 30 min incubation time, leftover TMS-diazomethane was removed by addition of glacial acetic acid (10 µL).

Biocatalysis with substrates **15** and **17** in organic solvent

100 mM of **15** and **17**, and 20 mg/ml enzyme preparation (as listed in the results section) are dissolved in tertiary amyl alcohol and incubated at 40°C and 1400 rpm. Samples are withdrawn and analyzed on the HPLC.

Biocatalysis with substrates **15c** and **17** using **15c** as solvent

5 mg/ml enzyme and 100 µl **17** (10 mg/ml in DMSO) are dissolved in 900 µl **15c**. The reactions are performed at 40°C and 1400 rpm. Samples are analyzed on the HPLC.

Synthesis of **13a-c**

p-Nitroaniline (1 g, 7.2 mmol) in dioxane (10 ml) is added, dropwise, to a solution of the corresponding acid chloride (300 mg, 2.8 mmol) in dioxane (6 ml) and the mixture is stirred for 15 min. After stopping the reaction by adding ice-cold water (25 ml), the product is washed with diluted hydrochloric acid and water. Chromatography on silica gel (hexane/dichloromethane 25:1) yields a yellowish powder. The acid chlorides used are butyryl chloride for **13a**, cinnamoyl chloride for **13b** and oleoyl chloride for **13c**.

Synthesis of **12** [137]

0.3 g Pd/C and 0.5 g **11** in 20 ml methanol are stirred for five hours under a hydrogen atmosphere. The Pd/C is then filtered off with celite, and the celite washed thoroughly with methanol. After evaporation of the solvent, an oily yellow liquid remains as the product (according to literature, it should be a white solid).

Biocatalysis with **12**

5 mg lyophilisate are dissolved in 500 µl sodium phosphate buffer pH 7.5. 2 µl of **12** are added and the reactions are incubated at 37°C and 850 rpm for four hours. To generate a product standard (**12a**), 2 µl of **12** are simultaneously hydrolyzed in 500 µl 1 N HCl. Samples are analyzed *via* TLC, the sample of **12a** is previously neutralized using Na_2CO_3.

6.2.4. Analytical Methods

Determination of enantioselectivity *via* gas chromatography (Substrates **2**-**7**)

Substrates **2-5**, and **7** are analyzed on a Hydrodex β-3P column; **6** is analyzed on a Hydrodex β-TBDAc column (both Macherey–Nagel). All gas chromatography analyses are performed on Shimadzu (Duisburg) instruments. **2**, **3**, and **7** are analyzed on a GC-2010 gas chromatograph, using hydrogen as carrier gas and a pressure of 60 kPa. **4** and **6** are analyzed on a GC-2010 gas chromatograph coupled with a QP2010 mass spectrometer, using helium as carrier gas and a pressure of 96.6 kPa. **5** is analyzed on a GC-14A gas chromatograph, using hydrogen as carrier gas and a pressure of 89 kPa. Column temperatures and retention times are detailed in table 6-8. Enantioselectivity and conversion are calculated by using the formula derived by Chen *et al.* [5].

Table 6-8: Column temperatures and retention times for analysis of chiral substrates and products *via* gas chromatography

Substrate	**Temp. [°C]**	**Retention time [min]**			
		(*R*)-Substrate	**(*S*)-Substrate**	**(*R*)-Product**	**(*S*)-Product**
2	110	11.9	10.0	20.4	21.8
3	90	14.8	12.5	13.7	13.4
4	110	16.4	11.0	19.3	21.8
5	95	46.3	45.4	60.1	57.9
6	90	22.3	21.4	14.5	13.6
7	70	105.0	101.2	77.5	71.0

Thin-layer chromatography

Samples of biocatalysis with **12** are applied to a silica coated TLC plate. The plate is then placed in a TLC cuvette with n-butanol: acetic acid: water 9:2:1 as mobile phase. When the solvent has almost reached the top of the TLC plate, the plate is removed from the cuvette, dried, and immerged in ninhydrin staining solution. To develop the color, the TLC plate is heated with a blow-drier.

Determination of enantioselectivity *via* HPLC (Substrate **11**)

The stereoisomers of **11** are separated on a Chiralcel ® OD-RH column with a mobile phase of 95% H_2O containing 0.1 % TFA and 5% acetonitrile at a flow of 0.4 ml/min, the UV absorbance was monitored at 225 nm. As the products cannot be separated, *p*-aminobenzoic acid is added as internal standard, the ratio of the peak areas of lactam and standard was used to calculate the conversion. T0 blank values are measured to determine the initial ratio at 0 % conversion. The retention times vary for unknown reasons, but the sequence of elution remains the same, with **11a** from approximately 4 to 6 min, (-)-**11** at around 8.9 minutes, (+)-**11** at around 9.7 minutes and the standard peak after 20 to 24 minutes.

Determination of conversion *via* HPLC (Substrates **14**-**17**)

The reaction educts and products are separated on a 60 mm Kromasil C18 column. The mobile phase is made up of water with 1% (v/v) acetic acid and methanol using a gradient with increasing methanol concentration (0 min 90-10, 15 min 20-80, 25 min 0-100) at a flow rate of 1 ml/min; the UV detector is set to 254 nm. The retention times can be found in table 3-12.

7. References

1. Fox, M.A. and J.K. Whitesell, *Organische Chemie*. 1995, Heidelberg: Spektrum Akademischer Verlag GmbH.
2. Vollhardt, K.P.C. and N.E. Schore, *Organische Chemie*. 3rd ed. 2000, Weinheim: Wiley-VCH Verlag GmbH.
3. Voet, D., J.G. Voet, and C.W. Pratt, *Lehrbuch der Biochemie*. 2002, Weinheim: Wiley-VCH Verlag GmbH.
4. FDA, *FDA's policy statement for the development of new stereoisomeric drugs.* Chirality, 1992. **4**: p. 338-340.
5. Chen, C.S., et al., *Quantitative analyses of biochemical kinetic resolutions of enantiomers.* J. Am. Chem. Soc., 1982. **104**: p. 7294-7299.
6. Betancor, L., et al., *Preparation of a stable biocatalyst of bovine liver catalase using immobilization and postimmobilization techniques.* Biotechnol. Progr., 2003. **19**: p. 763-7.
7. Bornscheuer, U.T., *Enzymimmobilisierung: ein Weg zu verbesserten Biokatalysatoren.* Angew. Chem., 2003. **115**: p. 3458-3459.
8. Domínguez de María, P., et al., *Pig Liver Esterase (PLE) as Biocatalyst in Organic Synthesis: From Nature to Cloning and to Practical Applications.* Synthesis, 2007. **10**: p. 1439-1452.
9. Hummel, A., et al., *Isoenzymes of pig-liver esterase reveal striking differences in enantioselectivities.* Angew. Chem. Int. Ed., 2007. **46**: p. 8492-8494.
10. *http://fungen.wur.nl/sfamlist.php*.
11. Barth, S., et al., *The database of epoxide hydrolases and haloalkane dehalogenases: one structure, many functions.* Bioinformatics, 2004. **20**: p. 2845-2847.
12. Sakai, T., et al., *Enhancement of the enantioselectivity in lipase-catalyzed kinetic resolutions of 3-phenyl-2H-azirine-2-methanol by lowering the temperature to -40°C.* J. Org. Chem., 1997. **62**: p. 4906-4907.
13. Hirose, Y., et al., *Drastic solvent effect on lipase-catalyzed enantioselective hydrolysis of prochiral 1,4-dihydropyridines.* Tetrahedron Lett., 1992. **33**: p. 7157-7160.
14. Yang, H., E. Henke, and U.T. Bornscheuer, *The use of vinyl esters significantly enhanced enantioselectivities and reaction rates in lipase-catalyzed resolutions of arylaliphatic carboxylic acids.* J. Org. Chem., 1999. **64**: p. 1709-1712.
15. Stokes, T.M. and A.C. Oehlschlager, *Enzyme reaction in apolar solvents: the resolution of (±)-sulcatol with porcine pancreatic lipase.* Tetrahedron Lett., 1987. **28**: p. 2091-2094.

16. Böttcher, D. and U.T. Bornscheuer, *Protein engineering of microbial enzymes.* Curr. Opin. Microbiol., 2010. **13**: p. 1-9.
17. Bakker, M., F. van Rantwijk, and R.A. Sheldon, *Metal substitution in thermolysin: Catalytic properties of tungstate thermolysin in sulfoxidation with H_2O_2.* Can. J. Chem., 2002. **80**: p. 622-625.
18. Joosten, H.-J., *3DM: From data to medicine*. 2007, University of Wageningen.
19. Kuipers, R., et al., *3DM: Systematic analysis of heterogeneous super-family data to discover protein functionalities* Proteins, 2010.
20. Reetz, M.T. and K.E. Jaeger, *Enantioselective enzymes for organic synthesis created by directed evolution.* Chemistry (Weinheim an der Bergstrasse, Germany), 2000. **6**: p. 407-12.
21. Bornscheuer, U.T., *Directed evolution of enzymes.* Angew. Chem. Int. Ed., 1998. **37**: p. 3105-3108.
22. Sutherland, J.D., *Evolutionary optimization of enzymes.* Curr. Opin. Chem. Biol., 2000. **4**: p. 263.
23. Cadwell, R.C. and G.F. Joyce, *Randomization of genes by PCR mutagenesis.* PCR Meth. Appl., 1992. **2**: p. 28-33.
24. Wong, T.S., et al., *A statistical analysis of random mutagenesis methods used for directed protein evolution.* J. Mol. Biol., 2006. **355**: p. 858-871.
25. Brakmann, S. and B. Lindemann, *Generation of mutant libraries using random mutagenesis*, in *Evolutionary methods in biotechnology*, S. Brakmann and A. Schwienhorst, Editors. 2004, Wiley-VCH: Weinheim. p. 5-11.
26. May, O., P.T. Nguyen, and F.H. Arnold, *Inverting enantioselectivity by directed evolution of hydantoinase for improved production of l-methionine.* Nat. Biotechnol., 2000. **18**(3): p. 317-320.
27. Stemmer, W.P.C., *DNA shuffling by random fragmentation and reassembly: In vitro recombination for molecular evolution.* Proc. Natl. Acad. Sci. USA, 1994. **91**: p. 10747-10751.
28. Lutz, S. and U.T. Bornscheuer, eds. *Protein Engineering Handbook*. 2009, Wiley-VCH: Weinheim.
29. Ness, J.E., et al., *DNA shuffling of subgenomic sequences of subtilisin.* Nat. Biotechnol., 1999. **17**(9): p. 893-896.
30. Ostermeier, M., A.E. Nixon, and S.J. Bencovic, *Incremental truncation as a strategy in the engineering of novel biocatalysts.* Bioorg. Med. Chem., 1999. **7**: p. 2139-2144.
31. Zhao, H., et al., *Molecular evolution by staggered extension process (StEP) in vitro recombination.* Nat. Biotechnol., 1998. **16**: p. 258-261.

32. Lutz, S., et al., *Creating multiple-crossover DNA libraries independent of sequence identity.* Proc. Natl. Acad. Sci. U.SA., 2001. **98**: p. 11248-11253.
33. Sieber, V., C.A. Martinez, and F. Arnold, *Libraries of hybrid proteins from distantly related sequences.* Nat. Biotechnol., 2001. **19**: p. 456-460.
34. Reetz, M.T., D. Kahakeaw, and R. Lohmer, *Addressing the Numbers Problem in Directed Evolution.* Chembiochem, 2008. **9**(11): p. 1797-1804.
35. Morley, K.L. and R.J. Kazlauskas, *Improving enzyme properties: when are closer mutations better?* Trends Biotechnol., 2005. **23**: p. 231-237.
36. Reetz, M.T., et al., *Expanding the range of substrate acceptance of enzymes: combinatorial active-site saturation test* Angew. Chem. Int. Ed., 2005. **44**: p. 4192-4196.
37. Bartsch, S., R. Kourist, and U.T. Bornscheuer, *Complete inversion of enantioselectivity towards acetylated tertiary alcohols by a double mutant of a Bacillus subtilis esterase.* Angew. Chem. Int. Ed., 2008. **47**: p. 1508-11.
38. Hidalgo, A., et al., *A one-pot, simple methodology for cassette randomisation and recombination for focused directed evolution.* Protein Eng., Des. Sel., 2008. **21**(9): p. 567-576.
39. Kammann, M., et al., *Rapid insertional mutagenesis of DNA by polymerase chain reaction (PCR).* Nucleic Acids Res., 1989. **17**: p. 5404.
40. Ke, S.H. and E.L. Madison, *Rapid and efficient site-directed mutagenesis by single-tube 'megaprimer' PCR method.* Nucleic Acids Res., 1997. **25**(16): p. 3371-3372.
41. Datta, A.K., *Efficient amplification using 'megaprimer' by asymmetric polymerase chain reaction.* Nucleic Acids Res., 1995. **23**(21): p. 4530-4531.
42. Jensen, L.J., et al., *Scoring functions for computational algorithms applicable to the design of spiked oligonucleotides.* Nucleic Acids Res., 1998. **26**(3): p. 697-702.
43. Goddard, J.-P. and J.-L. Reymond, *Enzyme assays for high-throughput screening.* Curr. Opin. Biotech., 2004. **15**: p. 314-322.
44. Bornscheuer, U.T., *High-Throughput-Screening Systems for Hydrolases.* Eng. Life Sci., 2004. **4**: p. 539-542.
45. Schmidt, M. and U.T. Bornscheuer, *High-throughput assays for lipases and esterases.* Biomol. Eng., 2005. **22**: p. 51-56.
46. You, L. and F.H. Arnold, *Directed evolution of subtilisin E in Bacillus subtilis to enhance the total activity in aqueous dimethylformamide.* Prot. Eng., 1994. **9**: p. 77-83.
47. Moore, J.C. and F.H. Arnold, *Directed evolution of a para-nitrobenzyl esterase for aqueous-organic solvents.* Nat. Biotechnol., 1996. **14**: p. 458-467.

48. Bornscheuer, U.T., J. Altenbuchner, and H.H. Meyer, *Directed evolution of an esterase: screening of enzyme libraries based on pH-indicators and a growth assay.* Bioorg. Med. Chem., 1999. **7**: p. 2169-2173.
49. Becker, S., et al., *Ultra-high-throughput screening based on cell-surface display and fluorescence-activated cell sorting for the identification of novel biocatalysts.* Curr. Opin. Biotech., 2004. **15**: p. 323-329.
50. Aharoni, A., et al., *High-throughput screening of enzyme libraries: thiolactonases evolved by fluorescence-activated sorting of single cells in emulsion compartments.* Chem. Biol., 2005. **12**: p. 1281-1289.
51. Reetz, M.T., et al., *A Method for High-Throughput Screening of Enantioselective Catalysts.* Angew. Chem. Int. Ed., 1999. **38**: p. 1758-1761.
52. Reetz, M.T., et al., *A practical NMR-based high-throughput assay for screening enantioselective catalysts and biocatalysts* Adv. Synth. Catal., 2002. **344**: p. 1008-1016.
53. Janes, L.E., A.C. Löwendahl, and R.J. Kazlauskas, *Quantitative Screening of Hydrolase Libraries Using pH Indicators: Identifying Active and Enantioselective Hydrolases.* Chem. Eur. J., 1998: p. 2324-2331.
54. Badalassi, F., et al., *A versatile periodate-coupled fluorogenic assay for hydrolytic enzymes.* Angew. Chem. Int. Ed., 2000. **39**: p. 4067-4070.
55. Wahler, D. and J.-L. Reymond, *Novel methods for biocatalyst screening.* Curr. Opin. Chem. Biol., 2001. **5**: p. 152-158.
56. Baumann, M., R. Stürmer, and U.T. Bornscheuer, *A high-throughput-screening method for the identification of active and enantioselective hydrolases.* Angew. Chem. Int. Ed., 2001. **40**(22): p. 4201-4204.
57. Böttcher, D. and U.T. Bornscheuer, *High-throughput screening of activity and enantioselectivity of esterases.* Nature protocols, 2006. **1**: p. 2340-2343.
58. Wahler, D. and J.-L. Reymond, *The Adrenaline Test for Enzymes.* Angew. Chem. Int. Ed., 2002. **41**: p. 1229-1232.
59. Janes, L.E. and R.J. Kazlauskas, *Quick E. A Fast Spectrophotometric Method To Measure the Enantioselectivity of Hydrolases.* J. Org. Chem., 1997. **62**: p. 4560-4561.
60. Branneby, C., et al., *Carbon-carbon bonds by hydrolytic enzymes.* J. Am. Chem. Soc., 2003. **125**(874-875).
61. Kourist, R., et al., *Understanding promiscuous amidase activity of an esterase from Bacillus subtilis.* ChemBioChem, 2008. **9**: p. 67-69.
62. de Zoete, M., et al., *Lipase-catalysed ammoniolysis of lipids. A facile synthesis of fatty acid amides.* J. Mol. Catal. B: Enzym., 1996. **1**: p. 109-113.

63. Babtie, A.C., et al., *Efficient Catalytic Promiscuity for Chemically Distinct Reactions.* Angew. Chem. Int. Ed., 2009. **48**: p. 3692-3694.
64. Bringer-Meyer, S. and H. Sahm, *Acetoin and phenylacetylcarbinol formation by the pyruvate decarboxylase of Zymomonas mobilis and Saccharomyces carlsbergensis.* Biocatalysis, 1988. **1**: p. 321-331.
65. Crout, D.H.G., et al., *Studies on pyruvate decarboxylase: acyloin formation from aliphatic, aromatic and heterocyclic aldehydes.* J. Chem. Soc. Perkin Trans. 1, 1991: p. 1329-1334.
66. P.Ward, O. and A. Singh, *Enzymatic asymmetric synthesis by decarboxylases.* Curr. Opin. Biotech., 2000. **11**: p. 520-526.
67. Balkenhohl, F., et al., *Optisch aktive Amine durch Lipase-katalysierte Methoxyacetylierung.* J. Prakt. Chem., 1997. **339**: p. 381-384.
68. Bornscheuer, U.T. and R.J. Kazlauskas, *Hydrolases in organic synthesis*. 2nd ed. 2006, Weinheim: Wiley-VCH.
69. Ollis, D.L., et al., *The alpha/beta hydrolase fold.* Protein Eng., 1992. **5**(3): p. 197-211.
70. Holmquist, M., *Alpha/beta-hydrolase fold enzymes: Structures, functions and mechanisms.* Curr. Protein Pept. Sci., 2000. **1**: p. 209-235.
71. Choi, K.D., et al., *Cloning and nucleotide sequence of an esterase gene from Pseudomonas fluorescens and expression of the gene in Escherichia coli.* Agric. Biol. Chem., 1990. **54**: p. 2039-2045.
72. Pelletier, I. and J. Altenbuchner, *A bacterial esterase is homologous with non-haem haloperoxidases and displays brominating activity.* Microbiology, 1995. **141**: p. 459-468.
73. Cheeseman, J.D., et al., *Structure of an aryl esterase from Pseudomonas fluorescens.* Acta Crystallogr., Sect. D: Biol. Crystallogr., 2004. **60**: p. 1237-1243.
74. Horsman, G.P., et al., *Mutations in distant residues moderately increase the enantioselectivity of Pseudomonas fluorescens esterase towards methyl 3bromo-2-methylpropanoate and ethyl 3phenylbutyrate.* Chem. Eur. J., 2003. **9**(9): p. 1933-1939.
75. Krebsfänger, N., K. Schierholz, and U.T. Bornscheuer, *Enantioselectivity of a recombinant esterase from Pseudomonas fluorescens towards alcohols and carboxylic acids.* J. Biotechnol., 1998. **60**: p. 105-111.
76. Krebsfänger, N., et al., *Characterization and enantioselectivity of a recombinant esterase from Pseudomonas fluorescens.* Enzyme Microb. Tech., 1998. **22**: p. 641-646.
77. Liu, A.M.F., et al., *Mapping the substrate selectivity of new hydrolases using colorimetric screening: lipases from Bacillus thermocatenulatus and Ophiostoma*

piliferum, esterases from Pseudomonas fluorescens and Streptomyces diastatochromogenes. Tetrahedron: Asymmetry, 2001. **12**: p. 545-556.

78. Schmidt, M., et al., *Directed evolution of an esterase from Pseudomonas fluorescens yields a mutant with excellent enantioselectivity and activity for the kinetic resolution of a chiral building block.* ChemBioChem, 2006. **7**(5): p. 805-809.
79. Jochens, H., et al., *Converting an esterase into an epoxide hydrolase.* Angew. Chem. Int. Ed., 2009. **48**: p. 3584-3587.
80. Bornscheuer, U.T., et al., *Mutator strain Epicurian coli XL1-red generates esterase variants.* Strategies, 1998. **11**: p. 16-17.
81. Henke, E. and U.T. Bornscheuer, *Directed evolution of an esterase from Pseudomonas fluorescens. Random mutagenesis by error-prone PCR or a mutator strain and identification of mutants showing enhanced enantioselectivity by a resorufin-based fluorescence assay.* Biol. Chem., 1999. **380**(7-8): p. 1029-1033.
82. Park, S., et al., *Focusing mutations into the P. fluorescens esterase binding site increases enantioselectivity more effectively than distant mutations.* Chemistry & biology, 2005. **12**: p. 45-54.
83. Takeuchi, M. and K. Hatano, *Proposal of six new species in the genus Microbacterium and transfer of Flavobacterium marinotypicum ZoBell and Upham to the genus Microbacterium as Microbacterium maritypicum comb. nov.* Int. J. Syst. Bacteriol., 1998. **48**: p. 973-982.
84. Line, K., M.N. Isupov, and J.A. Littlechild, *The crystal structure of a (-) γ-Lactamase from an Aureobacterium species reveals a tetrahedral intermediate in the active site.* J. Mol. Biol., 2004. **338**: p. 519-532.
85. Vince, R. and M. Hua, *Synthesis of anti-HIV activity of carbocyclic 2',3'-didehydro-2',3'-dideoxy-2,6-disubstituted purine nucleosides.* J. Med. Chem., 1990. **33**: p. 17-21.
86. Holt-Tiffin, K.E., *(+)- and (-)-2-Azabicyclo[2.2.1]hept-5-en-3-one: Extremely useful synthons.* Chim. Oggi, 2009. **27**(4): p. 23-25.
87. Brabban, A.D., J.A. Littlechild, and R. Wisdom, *Stereospecific γ-lactamase activity in a Pseudomonas fluorescens species.* J. Ind. Microbiol., 1996. **16**: p. 8-14.
88. Gonsalvez, I.G., M.N. Isupov, and J.A. Littlechild, *Crystallization and preliminary X-ray analysis of a γ-lactamase.* Acta Crystallogr., Sect. D: Biol. Crystallogr., 2001. **D57**: p. 284-286.
89. Chen, C.Y., et al., *Avenanthramides and phenolic acids from oats are bioavailable and act synergistically with vitamin C to enhance hamster and human LDL resistance to oxidation.* J. Nutr, 2004. **134**: p. 1459-1466.
90. Li, L., et al., *Effects of avenanthramides on oxidant generation and antioxidant enzyme activity in exercised rats.* Nutr. Res., 2003. **23**: p. 1579 -1590.

91. Nie, L., et al., *Avenanthramide, a polyphenol from oats, inhibits vascular smooth muscle cell proliferation and enhances nitric oxide production.* Atherosclerosis, 2006. **186**: p. 260-266.
92. Mayama, S., T. Tani, and Y. Matsuura, *The production of phytoalexins by oat in response to crown rust, Puccinia coronata f. sp. avenae.* Physiol. Plant Pathol., 1981. **19**: p. 217-226.
93. Liu, L., et al., *The antiatherogenic potential of oat phenolic compounds.* Atherosclerosis, 2004. **175**: p. 39-49.
94. Nomura, E., et al., *Synthesis of amide compounds of ferulic acid, and their stimulatory effects on insulin secretion in vitro.* Bioorg. Med. Chem., 2003. **11**: p. 3807-3813.
95. Ishihara, A., Y. Ohtsu, and H. Iwamura, *Biosynthesis of oat avenanthramide phytoalexins.* Phytochemistry, 1999. **50**: p. 237-242.
96. Krem, M.M., S. Prasad, and E. Di Cera, *Ser(214) is crucial for substrate binding to serine proteases.* J. Biol. Chem., 2002. **277**: p. 40260-40264.
97. Schließmann, A., et al., *Increased enantioselectivity by engineering bottleneck mutants in an esterase from Pseudomonas fluorescens.* ChemBioChem, 2009. **10**: p. 2920-2923.
98. *http://www.yasara.org*.
99. *http://www.pymol.org*.
100. Guieysse, D., et al., *Towards a novel explanation of Pseudomonas cepacia lipase enantioselectivity via molecular modelling of the enantiomer trajectory into the active site.* Tetrahedron: Asymmetry, 2003. **14**: p. 1807-1817.
101. *http://ekhidna.biocenter.helsinki.fi/dali_server/*.
102. Holm, L., et al., *Searching protein structure databases with DaliLite v.3.* Bioinformatics, 2008. **24**: p. 2780-2781.
103. Schmidt, G., *Untersuchungen zur katalytischen Promiskuität von Esterasen*. 2006, Universität Greifswald.
104. Henke, E. and U.T. Bornscheuer, *Fluorophoric assay for the high-throughput determination of amidase activity.* Anal.Chem., 2003. **75**: p. 255-260.
105. Elend, C., et al., *Isolation and biochemical characterization of two novel metagenome-derived esterases.* Appl. Environ. Microbiol., 2006. **72**: p. 3637-3645.
106. Dalrymple, B., et al., *Cloning of a gene encoding cinnamoyl ester hydrolase from the ruminal bacterium Butyrivibrio fibrisolvens E14 by a novel method.* FEMS Microbiol. Lett., 1996. **143**: p. 115-120.
107. Donaghy, J., et al., *Purification and characterization of an extracellular feruloyl esterase from the thermophilic anaerobe Clostridium stercorarium.* J. Appl. Microbiol., 2000. **88**: p. 458-466.

108. Borneman, W., et al., *Purification and partial characterization of two feruloyl esterases from the anaerobic fungus Neocallimastix strain MC-2.* Appl. Environ. Microbiol., 1992. **58**: p. 3762-3766.
109. Crepin, V.F., C.B. Faulds, and I.F. Connerton, *A non-modular type-B feruloyl esterase from Neurospora crassa exhibits concentration dependent substrate inhibition.* Biochem. J., 2003. **370**: p. 417-427.
110. Crepin, V.F., C.B. Faulds, and I.F. Connerton, *Production and characterisation of the Talaromyces stipitatus feruloyl esterase FAEC in Pichia pastoris: identification of the nucleophilic serine.* Protein Express. Purif., 2003. **29**: p. 176-184.
111. De Vries, R.P., et al., *The faeA genes from Aspergillus niger and Aspergillus tubingensis encode ferulic acid esterases involved in degradation of complex cell wall polysaccharides.* Appl. Environ. Microbiol., 1997. **63**: p. 4638-4644.
112. Crepin, V.F., C.B. Faulds, and I.F. Connerton, *Functional classification of the microbial feruloyl esterases.* Appl. Microbiol. Biotechnol., 2004. **63**: p. 647-52.
113. Smith, M., et al., *Genes for chlorogenate and hydroxycinnamate catabolism (hca) are linked to functionally related genes in the dca-pca-qui-pob-hca chromosomal cluster of Acinetobacter sp. strain ADP1.* Appl. Environ. Microbiol., 2003. **69**: p. 524-532.
114. *http://www.cbs.dtu.dk/services/SignalP/*.
115. *http://www.sbg.bio.ic.ac.uk/phyre/html/help.html*.
116. Kelley, L. and M. Sternberg, *Protein structure prediction on the web: a case study using the Phyre server.* Nature protocols, 2009. **4**: p. 363-371.
117. *http://swissmodel.expasy.org/*.
118. Arnold, K., et al., *A web-based environment for protein structure homology modelling.* Bioinformatics, 2006. **22**: p. 195-201.
119. Schließmann, A., *Developing methods for focused directed evolution*. 2007, Universität Greifswald.
120. Pavlova, M., et al., *Redesigning dehalogenase access tunnels as a strategy for degrading an anthropogenic substrate.* Nature Chem. Biol., 2009. **5**: p. 727-733.
121. Chaloupkova, R., et al., *Modification of activity and specificity of haloalkane dehalogenase from Sphingomonas paucimobilis UT26 by engineering of its entrance tunnel.* J. Biol. Chem., 2003. **278**: p. 52622-52628.
122. Carmichael, A.B. and L.L. Wong, *Protein engineering of Bacillus megaterium CYP102. The oxidation of polycyclic aromatic hydrocarbons.* Eur. J. Biochem., 2001. **268**: p. 3117-3125.
123. Lauble, H., et al., *Structure determinants of substrate specificity of hydroxynitrile lyase from Manihot esculenta.* Protein Sci., 2002. **11**: p. 65-71.

124. Fishman, A., et al., *Protein engineering of toluene 4-monooxygenase of Pseodomonas mendocina KR1 for synthesizing 4-nitrocatechol from nitrobenzene.* Biotechnol. Bioeng., 2004. **87**: p. 779-790.

125. Fedorov, R., et al., *Structures of nitric oxide synthase isoforms complexed with the inhibitor AR-R17477 suggest a rational basis for specificity and inhibitor design.* Proc. Natl. Acad. Sci. U.SA., 2004. **101**: p. 5892-5897.

126. Kotik, M., et al., *Cloning of an epoxide hydrolase-encoding gene from Aspergillus niger M200, overexpression in E. coli, and modification of activity and enantioselectivity of the enzyme by protein engineering.* J. Biotechnol., 2007. **132**: p. 8-15.

127. Feingersch, R., et al., *Protein engineering of toluene monooxygenases for synthesis of chiral sulfoxides.* Appl. Environ. Microbiol., 2008. **74**: p. 1555-1566.

128. Qian, Z. and S. Lutz, *Improving the catalytic activity of Candida antarctica lipase B by circular permutation.* J. Am. Chem. Soc., 2005. **127**: p. 13466-13467.

129. Qian, Z., et al., *Structural redesign of lipase B from Candida antarctica by circular permutation and incremental truncation.* J. Mol. Biol., 2009. **393**: p. 191-201.

130. Bordes, F., et al., *Improvement of Yarrowia lipolytica lipase enantioselectivity by using mutagenesis targeted to the substrate binding site.* ChemBioChem, 2009. **10**: p. 1705-1713.

131. Forró, E. and F. Fülöp, *Enzymatic method for the synthesis of blockbuster drug intermediates - synthesis of five-membered cyclic γ-amino acid and γ-lactam enantiomers.* Eur. J. Org. Chem., 2008: p. 5263-5268.

132. Evans, C.T. and S.M. Roberts, *Substantially pure enantiomers of 2-azabicyclo(2.2.1)hept-5-en-3-one*, **US5498625**, 1996

133. Wisdom, R.A., C.S. Lee, and R.C. Brown, *Microorganism lactamase enzyme obtained therefrom and their use*, **US6423522**, 2002

134. Bernegger-Egli, C., et al., *Method for producing (1R, 4S)-2-Azabicyclo[2.2.1]hept-5-en-3-on derivatives*, **WO/2000/003032**, 1999

135. Henke, E., *Untersuchungen zur Erweiterung der Substratspezifität von Carboxylester-Hydrolasen*. 2001, University of Greifswald.

136. Bradford, M.M., *A rapid and sensitive method for the quantification of micro-gram quantities of protein utilizing the principle of protein-dye binding* Anal. Biochem., 1976. **72**: p. 248-254.

137. Kudoh, T., et al., *Synthesis of stable and cell-type selective analogues of cyclic ADP-ribose, a Ca^{2+}-mobilizing second messenger. Structure-activity relationship of the N1-Ribose Moiety.* J. Am. Chem. Soc., 2005. **127**(24): p. 8846-8855.

8. Appendix

Nucleotide composition of each position of the spiked oligo for CAS3 used for the OSCARR library construction

1	1	2	3
G	5.3	4.3	61.0
A	7.0	7.4	0.0
T	9.7	84.2	39.0
C	78.0	4.1	

2	1	2	3
G	84.1	84.4	44.9
A	7.1	7.1	0.0
T	4.2	5.4	55.1
C	4.6	3.2	

3	1	2	3
G	84.4	4.0	48.7
A	6.5	7.4	0.0
T	5.0	5.1	51.3
C	4.1	83.5	

4	1	2	3
G	83.9	4.7	45.1
A	6.9	7.4	0.0
T	4.8	84.0	54.9
C	4.4	3.9	

5	1	2	3
G	5.4	4.4	47.7
A	85.4	7.5	0.0
T	4.7	5.3	52.3
C	4.5	82.7	

6	1	2	3
G	5.4	4.5	46.4
A	6.8	7.4	0.0
T	4.2	5.1	53.6
C	83.6	83.0	

7	1	2	3
G	5.5	4.5	61.9
A	6.5	7.4	0.0
T	9.7	84.0	38.1
C	78.4	4.1	

8	1	2	3
G	5.3	4.6	7.9
A	7.1	7.2	0.0
T	84.5	84.2	92.1
C	3.1	4.1	

9	1	2	3
G	84.7	84.1	43.2
A	7.2	7.3	0.0
T	3.7	5.4	56.8
C	4.4	3.2	

10	1	2	3
G	5.4	4.7	62.7
A	6.6	85.4	29.6
T	4.4	5.6	7.6
C	83.6	4.3	

Amino acid composition of each position in the spiked oligo for CAS3

	Ala(A)	Arg(R)	Asn(N)	Asp(D)	Cys(C)	Gln(Q)	Glu(E)	Gly(G)	His(H)	Ile(I)	Leu(L)
	Lys(K)	Met(M)	Phe(F)	Pro(P)	Ser(S)	Thr(T)	Trp(W)	Tyr(Y)	Val(V)		Stop
1	0.22	0.18	0.20	0.15	1.46	3.54	0.24	0.23	2.26	2.29	70.66
	0.32	3.59	3.19	3.18	0.51	0.28	0.25	0.28	4.48		0.44
2	2.66	2.70	0.28	3.30	4.07	0.15	2.69	70.96	0.18	0.21	0.35
	0.23	0.17	0.12	0.14	3.44	0.23	1.58	0.16	4.51		0.13
3	70.43	0.13	0.25	3.21	0.19	0.15	3.05	3.38	0.16	0.17	0.34
	0.23	0.16	0.13	3.45	4.30	5.42	0.10	0.19	4.31		0.18
4	3.28	0.15	0.28	3.39	0.24	0.14	2.78	3.97	0.18	3.18	5.49
	0.23	2.61	2.22	0.17	0.37	0.27	0.10	0.19	70.51		0.16
5	4.46	1.81	3.35	0.21	0.21	0.16	0.19	0.24	0.17	2.39	0.36
	3.05	2.17	0.13	3.69	5.90	70.67	0.10	0.19	0.29		0.17
6	4.47	0.14	0.27	0.21	2.10	2.89	0.19	0.24	3.33	0.19	4.41
	0.23	0.16	0.12	69.37	3.67	5.60	0.09	0.17	0.28		0.15
7	0.22	0.18	0.18	0.16	1.50	3.60	0.25	0.25	2.22	2.07	70.88
	0.30	3.36	3.09	3.18	0.50	0.26	0.27	0.27	4.63		0.44
8	0.22	0.03	0.47	0.35	3.68	0.02	0.03	0.24	0.21	5.52	8.22
	0.04	0.47	65.50	0.13	3.77	0.29	0.30	5.58	4.46		0.48
9	2.73	2.61	0.30	3.51	3.86	0.14	2.66	71.28	0.18	0.22	0.32
	0.23	0.17	0.11	0.14	3.56	0.23	1.34	0.15	4.54		0.12
10	0.23	0.29	0.43	0.35	0.32	65.93	4.25	0.26	5.46	0.14	4.88
	5.22	0.23	0.02	3.62	0.21	0.29	0.13	0.28	0.30		3.50

Distribution of number of mutations caused by the spiked oligo for CAS3

Muts.	Distrib.	LLM-prob.
0	2.79	
1	11.63	7.17E-06
2	22.76	2.02E-09
3	26.70	2.56E-12
4	20.45	3.54E-15
5	10.63	5.01E-18
6	3.91	7.32E-21
7	0.96	1.15E-23
8	0.16	2.01E-26
9	0.01	4.38E-29
10	0.00	9.62E-32

Average # of mutations: 3.04

Hiermit erkläre ich, dass diese Arbeit bisher von mir weder an der Mathematisch-Naturwissenschaftlichen Fakultät der Ernst-Moritz-Arndt-Universität Greifswald noch einer anderen wissenschaftlichen Einrichtung zum Zwecke der Promotion eingereicht wurde.
Ferner erkläre ich, dass ich diese Arbeit selbständig verfasst und keine anderen als die darin angegebenen Hilfsmittel benutzt habe.

Greifswald, den

Lebenslauf

Persönliche Daten

Name	Anna Schließmann
Geburtsdatum und –ort	01.03.1981 in Husum
Staatsangehörigkeit	deutsch

Ausbildung

1987 – 1991	Hans-Momsen-Schule Fahretoft
1991 – 2000	Friedrich-Paulsen-Schule Niebüll (Gymnasium)
06/2000	Abschluß: Abitur
10/2001 – 02/2007	Studium der Biochemie an der Universität Greifswald Diplomarbeit: „Developing methods for focused directed evolution“
05/2007-05/2010	Doktorandin am Institut für Biochemie, Abteilung Biotechnologie und Enzymkatalyse

Auslandsaufenthalte

08/1997 – 07/1998	Austauschjahr in Utah, USA
02/2001 – 07/2001	Sprachkurs und Praktikum im Krankenhauslabor in Argentinien
10/2003 – 02/2004	Auslandssemester an der Universität Oviedo, Spanien

Sonstiges

04/2004 – 01/2005	Studentische Hilfskraft im Praktikum für quantitative und qualitative anorganische Analytik
04/2005 – 07/2005	Studentische Hilfskraft bei Prof. Dr. Hecker (v.a. Auswertung von 2D Proteingelen)
Sommer 2005	Sechswöchiges Betriebspraktikum bei der Seramun Diagnostica GmbH

Danksagungen

Ich danke Prof. Uwe Bornscheuer für die Überlassung des interessanten Themas sowie für die produktive fachliche Betreuung während meiner Doktorarbeit, durch die ich viele Methoden anwenden und viel lernen konnte.

Besonders bedanke ich mich bei Dr. Aurelio Hidalgo, ohne dessen Vorarbeit, fachliche und moralische Unterstützung die Arbeit nicht möglich gewesen wäre – muchísimas gracias!

Bedanken möchte ich mich auch bei Ina Menyes für die Unterstützung bei der HPLC Analytik.

Der DBU danke ich für die Finanzierung meines Promotionsprojekts.

Beim Arbeitskreis Biotechnologie und Enzymkatalyse bedanke ich mich für die gute Zusammenarbeit und viele schöne Stunden, besonders natürlich bei denjenigen, die in den Jahren zu Freunden wurden und die mich oftmals nach missglückten Experimenten wieder aufbauten. Besonderer Dank gilt Kristian, der auch meine Doktorarbeit (wie schon meine Diplomarbeit) akribisch auf Rechtschreib- und Formatierungsfehler überprüft hat.

Für die vielen schönen Jahre in Greifswald bedanke ich mich bei meinen neu gewonnenen Freunden und Bekannten, ein herzlicher Gruß geht an das „Kollektiv“!

Von ganzem Herzen danke ich meiner Familie, die mich mein Leben lang finanziell, aber vor allem auch ideell unterstützt hat, und ohne die ich nie so weit gekommen wäre.

Zum Schluß möchte ich noch Basti für seine Liebe, Geduld und Motivation danken.